

VALIDATION OF AGE AND GROWTH USING MICROCONSTITUENT
ANALYSIS OF FISH HARDPARTS

by

Benjamin Alexander Frey

Thesis submitted to the Faculty of the Graduate School of the
University of Maryland, College Park, in partial fulfillment
of the requirements for the degree of
Master of Science
2022

Advisory Committee:

Professor Dr. David Secor, Chair

Professor Dr. Rosemary Jagus, UMCES IMET

Professor Dr. Michael Wilberg, UMCES CBL

NOAA Scientist Dr. Anne Richards, NEFSC

© Copyright by
Benjamin Alexander Frey
2022

Table of Contents

Table of Contents	ii
List of Tables	iv
List of Figures	v
List of Abbreviations	viii
Chapter 1: Introduction	1
References	4
Chapter 2: Annular periodicity of otolith microconstituents in black sea bass (<i>Centropristis striata</i>)	5
Introduction	5
Methods	13
Otolith Analysis	13
Time Series Analysis	16
DTW Analysis	16
Results	17
LA-ICP-MS Analysis	17
Lomb-Scargle Periodogram Analysis	19
DTW analysis	19
Discussion	20
Tables and Figures	25
References	40
Chapter 3: Annular periodicity of microconstituents in the illicia of Atlantic monkfish (<i>Lophius americanus</i>)	46
Introduction	46
Methods	50
Hardpart Analysis	50
Time Series Analysis	53
Expected Ages vs Chemical Assignments	54
Results	54
LA-ICP-MS Analysis	54
Lomb-Scargle Periodogram Analysis	55
Expected Ages vs Chemical Assignments	56
Discussion	56
Tables and Figures	62
References	75
Chapter 4: Broader Impacts	78
Appendix 1. Electron microprobe analysis of Sr:Ca oscillations in black sea bass otoliths	80
Tables and Figures	81
List of References	84

List of Tables

Chapter 2

Table 2.1 List of 17 species and stocks routinely aged by the NOAA Northeast Fisheries Science Center ageing methods and validation type. Length frequency analysis (LFA), marginal increment analysis (MIA).

Table 2.2 Average mean elemental concentrations (ppm) in black sea bass otolith profiles (N=41).

Table 2.3 Results of ANOVA on the effect of age-class on otolith profile clusters classified through Dynamic Time Warping (DTW) cluster for black sea bass.

Chapter 3

Table 3.1 Mean elemental concentrations (ppm) in Atlantic monkfish illicia profiles

List of Figures

Chapter 2

Figure 2.1 Example of realignment of time series into centroids (red line) based on dynamic time warping. The black line represents a single Mg time series otolith profile for black sea bass, which together with other profiles would be warped similarly to the fitted time series centroid.

Figure 2.2 Age annotations for a sectioned and whole black sea bass otolith. Red counts assign the first transparent zone within the core region according to the alternate approach. Blue counts do not according to the “NEFSC” approach.

Figure 2.3 Length frequency diagram of black sea bass captured for use in this study (n=125). Fitted line indicates the normal curve that was fit to the average distribution of black sea bass total length.

Figure 2.4 Location of black sea bass captured through hook and line on wreck and artificial reef sites (20-30 m depth) off Ocean City, Maryland US during the summer and fall months of 2016 and 2018 (n= 125).

Figure 2.5 Annuli annotations across the trench created by the LA-ICP-MS’s ablated area (black line) on the surface of a sectioned black sea bass otolith. Blue points along the white line depict annuli used in constructing elemental profiles. Image captured and overlay via Infinity Analyze and Capture (Teledyne Lumenera software).

Figure 2.6 2-Dimensional elemental maps and light micrograph (Raw) image for two black sea bass sectioned otoliths (top and lower panels). Concentration scales from blue (low) to red (high). Note that contrast is optimized and depicted through pseudocolor for each map and is not common across elements. Standard (NEFSC approach) optical annuli annotations are depicted in circles.

Figure 2.7 Standardized profiles (n=34) across microconstituents for black sea bass otoliths. Colored by individual.

Figure 2.8 Standardized profiles across otolith microconstituents for a single black sea bass.

Figure 2.9 Lomb-Scargle periodograms for elemental profiles (N=34) including the full series of otolith annuli for black sea bass. Significance (power=0.001) is shown by the horizontal dashed line. The vertical dashed line is hypothesized period frequency=1.0. Note the difference in scale between the top and bottom rows.

Figure 2.10 Lomb-Scargle periodograms for otolith elemental profiles (N=34) including only annuli >1.0 for black sea bass. Significance (power=0.001) is shown by the horizontal dashed line. The vertical dashed line is hypothesized period frequency=1.0. Note the difference in scale between the top and bottom rows.

Figure 2.11 Barium centroids estimated through Dynamic Time Warping for black sea bass otolith profiles.

Figure 2.12 Box and whisker plots of ages across clusters determined through Dynamic Time Warping analysis of black sea bass otolith profiles.

Chapter 3

Figure 3.1 Atlantic monkfish hardpart comparison. A.) Whole otolith. B.) Sectioned otolith. C.) Baked vertebra. D.) Sectioned illicium.

Figure 3.2 Location of monkfish captured during bottom trawl surveys conducted by the NOAA Northeast Fisheries Science Center along the Atlantic coast of the United States from Virginia to Georges Bank between June 2015 and September 2018.

Figure 3.3 Length frequency diagram of monkfish captured for use in this study from the 2015-year class captured between 2015 and 2018 during bottom trawl surveys conducted by the NOAA Northeast Fisheries Science Center. Fitted lines indicates the normal curve that were fit to the average distribution of monkfish total length.

Figure 3.4 A.) Light micrograph (Raw) image and B-H.) 2-D elemental maps for two Atlantic monkfish illicia cross sections (top two panels and lower two panels). Shading indicates element concentration, scales from blue (low) to red (high). Note the contrast in the pseudo color, which is optimized for each map and is not common across elements.

Figure 3.5 Annulus widths and distances from the core for Atlantic monkfish illicia comparing the 2-D assignments (n=14) to the new assignment conventions (those based upon chemical annuli, n=57).

Figure 3.6 (A) Current NEFSC expert assignment of Atlantic monkfish illicium annuli (see Sutherland and Richards 2021), (B) assignment of chemical annuli, and (C) assignment of annuli using chemical conventions. Note the contrast in the pseudo color, which is optimized for each map and is not common across elements. Annuli annotations are depicted in circles.

Figure 3.7 Standardized Atlantic monkfish illicia profiles (n=57) across microconstituents and organized by distance on illicia. Colors represent each individual.

Figure 3.8 Standardized Atlantic monkfish illicia profiles (n=57) across microconstituents using chemical annulus assignments. Colors represent each individual.

Figure 3.9 Lomb-Scargle periodograms for Atlantic monkfish elemental profiles (N=57) using distance from illicia core. Significance is shown by the horizontal dashed line. Note the difference in the response amplitude between each element.

Figure 3.10 Lomb-Scargle periodograms for Atlantic monkfish elemental profiles (N=57) using new chemical annuli conventions. Significance is shown by the horizontal dashed line. The vertical dashed line is hypothesized period frequency=1.0. Note the difference in response amplitude between each element.

Figure 3.11 Age assignment comparison of expected ages vs chemical age assignments for Atlantic monkfish, evaluated with a paired t-test (see Results).

Figure 3.12 von Bertalanffy growth model fits for Atlantic monkfish A.) expected ages vs B.) new chemical ages (blue). Points jittered for clarity.

Appendix

Figure A.1 Image of sectioned black seabass otolith. **A.)** reflected light microscopy image of otolith section with red dots marking the end of annuli. **B.)** Micrograph image of same otolith section. **C.)** Overlap of both images.

Figure A.2 Strontium/Calcium ratio of black sea bass otolith. **1** covers the core region of the otolith. **2-5** depict one transparent to opaque annuli. Vertical lines represent annuli transition at the start of each transparent zone — annuli 1-5.

Figure A.3 Lomb-Scargle periodogram of black sea bass otolith Sr:Ca time series data (N=30) from otolith transect showing no significant periodicities in the data. Significance is indicated by the dotted line.

Figure A.4 Lomb-Scargle periodogram of black sea bass otolith Sr:Ca time series data (N=30) with the first annulus after core removed data from otolith transects showing no significant periodicities in the data. Significance is indicated by the dotted line.

List of Abbreviations

2-D – Two dimensional

AMU – Atomic mass unit

ASMFC – Atlantic States Marine Fisheries Commission

Ba – Barium

BCS-CRM 393 – Limestone standard

Co – Cobalt

Cu – Copper

DTW – Dynamic Time Warping

ECRM-752-NP – Limestone nano-pellet standard

GeoREM - Geochemical Database for Reference Materials

LA-IC-PMS – Laser ablation inductively coupled plasma mass spectrometry

LFA – Length frequency analysis

MAPS-4 – Bone pellet standard

MIA - Marginal increment analysis

Mg - Magnesium

Mn - Manganese

NEFSC - Northeast Fisheries Science Center

NIST-612 - National Institute for Standards and Technology glass and quartz
standard

S:N - Signal to noise ratio

Sr - Strontium

USGS MACS-3 – United States Geological Survey coral standard

Zn – Zinc

Chapter 1: Introduction

Validation of age estimation methods are an essential step in ensuring the proper assessment of a species, yet age validation studies are rare. Without proper validation, there can be substantial uncertainty and risk in stock assessments and management, which typically require age information to inform recruitment, growth, mortality, and selectivity estimates. Interpretation of optical zones (i.e. “rings”) in fish hardparts is the conventional approach for age estimation in most resource finfish species, which is also referenced as direct ageing (Casselman 1983; Vitale et al. 2019). Nevertheless, it remains the task of the investigator to determine whether each ring forms at an annual rate and thus could be considered useful for determining fish age (Campana 2001). This task is referred to as validation, defined as a process of establishing the accuracy of an age estimation method (Casselman 1983; Beamish and McFarlane 1983; Vitale et al. 2019). The traditional approaches used to validate the annual formation of these rings in hardparts can be divided between direct or indirect forms of validation (Vitale et al. 2019). Direct validation methods track individuals over time as annular zones form over seasons and years, using temporal reference points (markers) on hardparts. Indirect validation methods analyze samples of hardparts, relating annular structures to changes in season, year-class strength, or size modes.

Traditional approaches to age validation are not universally applicable. When complications arise preventing the age estimation or validation of a species, a novel

approach is required. This new approach could be found using microchemistry. Microchemistry approaches for age validation compare the cyclical patterns in microconstituents and stable isotopes to the features of hardparts (i.e., rings/ annuli). This concept stems from the premise that optical banding patterns (annuli) in hard parts coincide with changes in chemical composition, both of which alias seasonal changes in organic content and temperature. Work done by (Secor and Piccoli 1996) on striped bass otoliths and (Stevenson and Secor 1999) in Atlantic sturgeon (*Acipenser oxyrinchus*) fin spines have shown that changes in chemical composition relate to alternating organic-rich (winter) and Ca-rich (spring-summer-fall) zones. This study will apply microchemical approaches pioneered by Sherwood (2011), Siskey et al. (2016), and Brophy et al. (2019, 2021) to attempt to validate age determination in two species. In Chapter 1, I will apply the microchemical approach to a species whose age determination has already been validated, black sea bass, in order to confirm that the periodicity of microconstituents is annual and aligns with annuli formation on hardparts. In Chapter 2, this same general approach will be applied to a species for which traditional age determination methods are in question, Atlantic monkfish, to attempt to validate age estimates. Chemical validation of the optical interpretations of annuli would support age-structured assessments and allow fisheries managers to make well-informed assessments of stock status on which to build sound management practices.

My thesis work had lots of blind alleys, related to an initial emphasis on wavelength dispersive electron microprobe analysis versus Laser Ablation Inductively Coupled Plasma Spectrometry, and selection of candidate hard parts

(Atlantic monkfish) and elements (both species). As such, a growing list of collaborators contributed to this study, including: Sandy Sutherland from the NEFSC who provided essential samples and guidance in traditional ageing approaches; Dr. Philip Piccoli guided the initial analysis via electron microprobe at the Nanoscale Imaging Spectroscopy and Properties Laboratory at The University of Maryland, College Park; Dr. Nathaniel Miller and Dr. Michelle Sluis trained me and conducted the LA-IC-PMS analyses at the University of Texas at Austin Department of Geosciences; Dr. Vyacheslav Lyubchich was integral in the development of the dynamic time warping approach. Two publications corresponding to each chapter are anticipated.

References

- Beamish, R. J., and G. A. McFarlane. 1983. The forgotten requirement for age validation in fisheries biology. *Transactions of the American Fisheries Society* 112(6):735–743.
- Brophy, D., D. P. De Pontual, K. Mahe, and C.-M. Villanueva. 2019. Validating age-determination of anglerfish and hake. Report (Scientific report), IRELAND.
- Brophy, D., S. Pérez-Mayol, R. Duncan, K. Hüssy, A. J. Geffen, H. D. Gerritsen, M. C. Villanueva, and B. Morales-Nin. 2021. Elemental composition of illicia and otoliths and their potential application to age validation in white anglerfish (*Lophius piscatorius* linnaeus, 1758). *Estuarine, Coastal and Shelf Science* 261:107557.
- Campana, S. E. 2001. Accuracy, precision and quality control in age determination, including a review of the use and abuse of age validation methods. *Journal of Fish Biology* 59(2):197–242.
- Casselman, J. M. 1983. Age and growth assessment of fish from their calcified structures—techniques and tools. NOAA Technical Report NMFS 8:1–17.
- Secor, D. H., and P. M. Piccoli. 1996. Age- and sex-dependent migrations of striped bass in the Hudson River as determined by chemical microanalysis of otoliths. *Estuaries* 19(4):778–793.
- Sherwood, G. 2011. Appendix 2 of monkfish project completion report, otolith microchemistry analysis results for age and growth. Northeast Fisheries Science Center.
- Siskey, M. R., V. Lyubchich, D. Liang, P. M. Piccoli, and D. H. Secor. 2016. Periodicity of strontium: Calcium across annuli further validates otolith-ageing for Atlantic bluefin tuna (*Thunnus thynnus*). *Fisheries Research* 177:13–17.
- Stevenson, J. T., and D. Secor. 1999. Life history characteristics of Hudson River Atlantic sturgeon (*Acipenser oxyrinchus*) and a model for management. *Journal of Applied Ichthyology* 15(4–5):304–304.
- Vitale, F., L. A. Worsøe Clausen, G. N. Chonchúir, and International Council for the Exploration of the Sea. 2019. Handbook of fish age estimation protocols and validation methods. Pages 1–180. International Council for the Exploration of the Sea, 346.

Chapter 2: Annular periodicity of otolith microconstituents in black sea bass (*Centropristis striata*)

Introduction

Age estimation supports complex stock assessments for our most important managed fishery species, yet we have not yet verified age determination methods for many stocks. Age and its relationships to size and abundance support the estimation of key parameters (growth, mortality, recruitment) that allow current and future stock status determinations. By assessing the fluctuations in age, growth, and survival in connection to fishing pressure, managers can optimize the exploitation of a species without harming the overall sustainability of the harvest. Interpretation of optical zones (aka annuli or “rings”) in fish hardparts is the conventional approach for age determination, needed in age-based assessments, which is also referenced as direct ageing (Casselman 1983; Vitale et al. 2019). Hardparts are calcified structures, which include otoliths, vertebrae, opercula, fin rays, and scales. They often show patterns of seasonal zonation, which can be optically distinguished through microscopy (transmitted light) as alternating light and dark (translucent and opaque) zones that vary in their organic concentrations. Opaque zones typically have higher protein content, are relatively narrow in comparison to translucent zones, and are interpreted as representing periods of lower seasonal growth such as temperate winters (Thomas 1983; Machias et al. 1998; Walker and Sutton 2016). The two zones together define an annulus, but it remains the task of the investigator to determine whether each ring

forms at an annual rate and thus could be considered valid for determining fish age (Campana 2001). This task is referred to as validation, defined as a process for establishing the accuracy of an age estimation method (Casselman 1983; Beamish and McFarlane 1983; Vitale et al. 2019).

The lack of validated age determination methods is of direct consequence to fishery assessment and management. The use of unvalidated ageing techniques can affect catch-, selectivity-, numbers-, maturity-, and weight-at age, which can cause major bias and error in age-based assessments (Bradford 1991; Wilhelm et al. 2008; Elvarsson et al. 2018). Error in ageing can result in overexploitation and the eventual collapse of the stock and associated fishery as occurred for important Lake Superior cisco (*Coregonus artedii*) and South African sparid fisheries (*Cymatoceps nasutus*) (Mills and Beamish 1980; Chale-Matsau et al. 2001; Yule et al. 2008). Despite the risks of assuming the reliability of age determination, validation studies on annulus formation are rare for many important commercial stocks, including the majority of New England and Mid-Atlantic harvested species (Table 2.1). This presents substantial uncertainty and risk in stock assessments and management, which typically require age information to inform recruitment, growth, mortality, and selectivity estimates. Among the 19 species routinely aged by the NOAA Northeast Fisheries Science Center (NEFSC), validation studies occur for only Acadian redfish (*Sebastes fasciatus*), American plaice (*Hippoglossoides platessoides*), Atlantic cod (*Gadus morhua*), black sea bass (*Centropristis striata*), haddock (*Melanogrammus aeglefinus*), pollock (*Pollachius virens*), red hake (*Urophycis chuss*), weakfish (*Cynoscion regalis*), and yellowtail flounder (*Limanda ferruginea*) (Table 2.1).

Efforts to validate age determination are sometimes hampered owing to the requirement to compare age interpretations to known-age fish. The set of approaches used to validate the annual formation of annuli in hardparts can be divided between direct or indirect forms of validation (Vitale et al. 2019). Direct validation methods track individuals over time as annular zones form over seasons and years, using temporal reference points (markers) on hardparts. Indirect validation methods analyze samples of hardparts, relating annular structures to changes in season, year-class strength, or size modes. Common direct ageing methods include tag-recapture, captive rearing, and bomb radiocarbon dating (Vitale et al. 2019). Tag-recapture is a common, yet difficult, method that relates the post-tagging time interval to the number of annuli. This method often employs a chemical marker (such as tetracycline) applied to a hard part or a tag applied at the time of capture as a time stamp. Difficulties in this method arise owing to low recapture rates (Rotella and Hines 2005; Oosthuizen et al. 2010; Bank et al. 2020). In contrast, long-term rearing studies utilize controlled laboratory settings to support the comparison of annular structures across seasons and years. Often, however, artificial conditions do not fully emulate those that result in the optical patterns observed in wild specimens since annulus formation is strongly influenced by the environment (Campana and Neilson 1982; Schramm 1989). Bomb radiocarbon dating is also a feasible validation approach, which utilizes a baseline of expected ambient radiocarbon levels to levels of radiocarbon in hardparts. The approach has been particularly useful in validating longevity estimates and is best used with long-lived species (Francis et al. 2010; Casselman et al. 2019; Daugherty et al. 2020).

Indirect validation methods include length frequency analysis, marginal increment analysis, and microchemistry (Vitale et al. 2019). Length frequency analysis (LFA) operates under the assumption that seasonal interruptions in growth result in discrete size modes that relate to age. Such seasonal length frequency modes can be observed in samples obtained from monitoring surveys and commercial landings. The method is best suited for young, fast-growing fish where the length modes for each age group are easily distinguished and not obscured by individual growth variation (Campana 2001; Sutherland and Richards 2021). Single dominant length modes associated with strong year-classes offer increased certainty in identifying age-classes and following them for increased years. Comparisons between modal length and age assignments thus provide an indirect means of age validation (e.g. LFA mode number vs. annulus number). Using this method, Mayo et al., (1981) classified size modes up to age 7 to estimate the size at age of Acadian redfish (*Sebastes fasciatus*). A second indirect approach, marginal increment analysis (MIA), measures the most peripheral annular zone over seasons of the year, with an expectation of cyclical growth of the increment (Okamura et al. 2013). Limitations of this method usually result from the difficulty in measuring small increments accurately; this and curtailed hardpart growth in older individuals make this method best suited for fast-growing and/or young fish (Campana 2001).

A promising new approach for age validation uses annular periodicity in hardpart microconstituents. Siskey et al. (2016) and Brophy et al. (2019) have recently shown that the periodicity of some elements in hardparts is annual and synchronizes with optical annuli patterns. Siskey et al. pioneered a quantitative

approach, Lomb-Scargle periodogram analysis, to evaluate dominant periods of oscillations from noisy time series data, testing the hypothesis that the dominant microconstituent cycle is annual. Brophy et al. (2019) adapted the Lomb-Scargle periodogram analysis in their work to detect peaks in chemical oscillations and identify trends that showed promise as indicators of age. A second time series analysis that can identify periodic behavior in time series in an unsupervised manner (i.e., without annulus assignments) is dynamic time warping (Maharaj et al. 2019; Hegg and Kennedy 2021). Dynamic time warping measures shape and oscillation similarity between multiple time series that are unequally measured in time, and support classifications of similar trends (Figure 2.1). This level of temporal adaptability is pertinent when comparing time series extracted from non-uniform otoliths or other hard parts.

The underlying premise of microconstituent validation is that optical banding patterns (annuli) in hard parts coincide with changes in chemical composition, both of which alias seasonal changes in organic content and temperature. Fish that reside or migrate through coastal and shelf environments are exposed to mixtures of terrestrial, anthropogenic, and marine sources of aqueous metals and isotopes. Higher abundance elements Sr, Mg, Mn, and Ba substitute within the crystalline lattice of aragonitic otoliths in proportional to environmental exposure but also modified by temperature and growth (Hüssy et al. 2020). Trace constituents such as P, Co, Cu, and Zn are bound in the otoliths protein matrix and hypothesized to be physiologically controlled (Hüssy et al. 2020), albeit some evidence indicates a role for environmental exposures (Arslan and Secor 2005). Thus, across candidate elements, the kinetics of tracer

incorporation are driven jointly by exposure, temperature, and physiology. In temperate shelf environments, candidate element concentrations do not vary as substantially as they would in freshwater, estuarine, and nearshore environments. Here, I hypothesize that exposure to seasonally changing temperatures drive variation in microconstituent concentrations.

For temperate species, composition changes are thought to relate to alternating organic-rich (winter) and Ca-rich (spring-summer-fall) zones as has been observed in striped bass otolith Sr (Secor and Piccoli 1996) and other species (Hüssy et al. 2020). These optical zones are also associated with seasonal changes in temperature with the translucent zone occurring during high growth seasons of summer and fall and the narrow opaque zone forming during winter and early spring (Zlokovitz et al. 2003). For example, strontium in hardparts can serve as a proxy for expected oscillations in temperature: in cooler temperatures, higher levels of Sr are substituted for calcium (Ca) in the lattice structure of the hardpart (Engstedt et al. 2012). For temperate fishes, such oscillations across hardpart optical zones have been observed for red emperor (Seyama et al. 1991) and Atlantic bluefin tuna otoliths (Siskey et al. 2016). Thus, the variations in microchemical composition across optical zones can validate the seasonal frequency of these zones (annuli). Otolith microconstituents can show marked seasonality, and in that way can be regarded as a “chemical calendar-clock” with time-keeping properties similar to the optical annuli on hardparts (Limburg et al. 2018).

My goal is to evaluate chemical ageing as a novel approach for a model species for which age determination has been validated previously. Black sea bass

(*Centropristis striata*) are a ubiquitous, structure-associated fish found in the Gulf of Mexico and along the Atlantic coast, from Florida to the Gulf of Maine. Black sea bass supports an important commercial fishery along the Atlantic coast and are valued as a recreational species, ranked first in the US as the most-landed recreational species (Musick and Mercer 1977; NEFSC 2019; ASMFC 2021). Black sea bass are most abundant as adults in temperate shelf environments, although their young (<2 years in age) often occur in estuarine and coastal habitats. The black sea bass assessment uses statistical catch-at-age models such that ageing errors will have direct impacts on the primary biological reference point, stock status, and stock projections.

Ageing methodology for black sea bass has been validated through marginal increment analysis (Dery and Mayo 1988; Penttila and Dery 1988; Robillard et al. 2016), but the zonation of the first annulus remains uncertain, as its optical properties can be variable and difficult to interpret (Figure 2.2). Most work suggests opaque material is deposited around the core of the otolith (assumed to be formed as age-0 juveniles, originating during winter) and the deposition of this material is complete by the following spring, forming the first annulus (Penttila and Dery 1988; Robillard et al. 2016). This annulus is then followed by a wide translucent zone that forms during the summer and autumn of the second year. However, inconsistencies between identification of the first annulus have been identified as a major source of error and an area of concern for stock assessment (ASMFC 2013; Robillard et al. 2016). Recent work by Koob et al. (2021) has validated the first annulus via marginal increment

analysis with results in line with the methodology used by the NEFSC and therefore used in this study.

I hypothesize that the two optical zones of each annulus will result in a chemical record of differentially deposited microconstituents. Cycles of microconstituents (aka chemical zonation) will reference age by aliasing the seasonal temperature changes with a periodicity of one cycle per annulus. By linking the optical interpretation to the chemical interpretation, the rate of periodicity can be tested through time series analysis, and in this way, interpretations of all annuli within a hard part can be verified to occur yearly or alternatively, at a different rate. The objectives of this chapter are,

1. Identify candidate microconstituents, which show annular patterns in their concentrations.
2. Construct microconstituent profiles and 2-dimensional (2-D) microconstituent maps, using Laser Inductive Coupled Mass Spectrometry (LA-ICP-MS) for a representative sample of black sea bass.
3. Align optical annuli and microconstituent profiles through image analysis.
4. Conduct Lomb-Scargle periodogram analysis on candidate microconstituent profiles to test the hypothesis that the dominant period = 1.0 optical annular cycle. Owing to anticipated difficulties in interpreting the first annulus two alternate periodogram analyses were conducted on datasets containing (1) all annuli, or (2) annuli >1.0 .
5. Conduct dynamic time warping cluster (DTW) analysis to evaluate whether clusters exhibit oscillating behaviors that are significantly related to age-class.

Methods

Otolith Analysis

Sagittal otoliths were collected from black sea bass (total length range 19.5 - 36.3 cm, Figure 2.3) captured through hook and line on wreck and artificial reef sites (20-30 m depth) off Ocean City, Maryland US (Figure 2.4) during the summer and fall months of 2016 and 2018 (n= 125). Annuli in whole and sectioned otoliths were defined as continuous opaque zones with no breaks (Figure 2.2). By convention, a birth date of January 1st was assumed (spring spawning) (Vanderkooy et al. 2020). Thus, fish collected before June 30 are assumed to have completed <0.5 of the most recent year of life and counts of opaque zones=estimated age. For those captured after June 30, the edge is counted as these fish have completed >0.5 years of life beyond the last opaque zone (Dery and Mayo 1988; Vanderkooy et al. 2020). Black sea bass whole otoliths were photographed under reflected light at 1.5x magnification using a camera-microscope system and Infinity Analyze and Capture (Teledyne Lumenera software). Following whole otolith assignments, otoliths were then embedded in Struers epoxy resin (Struers A/S, Ballerup, Denmark) for sectioning. A 2.0-mm thick section containing the core region (the inner-most portion of the otolith, pertaining to the first year of life) was cut along a transverse plane using a Buehler IsoMet saw (Beuhler, Lake Bluff, Illinois). The otolith section was then attached to a glass slide using Crystalbond 509 mounting adhesive (SPI Supplies, West Chester, Pennsylvania) in preparation for microchemical analysis and further annuli interpretations.

Microchemical analysis of elemental variations from the core region to the otolith's periphery was measured by LA-ICP-MS at the University of Texas at Austin Department of Geosciences. Initial trials using wavelength dispersive electron microprobe analysis of strontium levels were unsuccessful (Appendix 1), leading me to pursue the multi-elemental capabilities of LA-ICP-MS. Instrumentation was an ESI NWR193 excimer laser ablation system (193 nm, 4 ns pulse width) coupled to an Agilent 7500ce ICP-MS. The LA-ICP-MS system is equipped with a large format, two-volume, sample cell with fast washout (< 1s) that accommodated all samples and standards (USGS MACS-3, NIST-612) in three laser cell loadings. The system was optimized daily for sensitivity across the AMU mass range and low oxide production (ThO/Th: 0.58 ± 0.06) by tuning on a standard (NIST 612), and these parameters were checked from trial transects on representative specimens. Following pre-ablation (75 μ m spot, 50 μ m/s scan rate, 3.3 J cm⁻² fluence) to remove shallow surface contaminants, core-to-rim profiles were performed on each specimen, using a 25 μ m diameter spot, a 5 μ m s⁻¹ scan rate, 2.92 ± 0.15 J cm⁻² energy density (fluence), 15 Hz repetition rate, and carrier gas flows (L min⁻¹) of 0.8 for Ar and 0.80-0.85 for He. The quadrupole time-resolved method measured 12 masses with integration times of 10 ms (²⁴Mg, ⁴³⁻⁴⁴Ca, ⁸⁸Sr), 20ms (²⁵Mg, ³¹P, ⁵⁵Mn), and 25ms (⁵⁹Co, ⁶³Cu, ⁶⁶Zn, ¹³⁷⁻¹³⁸Ba). The quadrupole duty cycle of 0.3732 s corresponds to 94% measurement time, with a corresponding linear sampling rate of 1.867 μ m, equivalent to 13.4 measurements within the footprint of either aperture. Measured intensities were converted to elemental concentrations (ppm) using iolite software (Paton et al. 2011), with ⁴³Ca as the internal standard and a Ca index value of 38.3 wt% for unknowns.

For the otoliths, USGS MACS-3 (synthetic aragonite) was used as the primary calibration standard, and NIST 612 and ECRM-752-NP (nano-particulate pressed limestone powder pellet made from BCS-CRM 393 Limestone: www.basrid.co.uk) were used as external reference standards. Over the four days, the grand average of secondary standard (n=42) recovery fractions for all elements was typically within 5% of GeoREM preferred values (<http://georem.mpch-mainz.gwdg.de>).

Typical concentrations over specimen transects were $10\text{-}10^3$ times higher than the limits of detection for most elements (Table 2.2; elements with average concentrations less than three times the detection limits are shown in red italicized font). The derived elemental time-series (profiles) were smoothed by consecutive moving average filters using a 9-point boxcar width (13 and 26 μm equivalent distances), resulting in smooth, locally weighted, signals that were free from high-frequency outliers. Signals were converted to distance (μm) from the core based on the scan rate and duty cycle. Because signals for elements measured with multiple isotopes were identical, we use the higher abundance isotope (e.g., ^{24}Mg , ^{138}Ba) for plotting and statistical analysis.

For 2-D microconstituent maps, scanned areas involved contiguous line traverses using $17\times 17\ \mu\text{m}$ spaced by diameter of two otolith sections. The scan rate (105, 62, 31 $\mu\text{m s}^{-1}$) was set to provide one quadrupole measurement cycle per aperture footprint. The quadrupole method used for mapping surveyed nine elements (10 ms: $^{43-44}\text{Ca}$, ^{88}Sr ; 20 ms: ^{55}Mn , ^{138}Ba ; 25ms: ^{24}Mg , ^{65}Cu , ^{66}Zn) with a significantly shorter duty cycle of 0.1612s with 90% measurement time. Calibration and secondary standards were as described above. External reference standard recoveries were

typically within 10% of certified reference values. Image conversions were performed using iolite4 software (Paton et al. 2011).

Time Series Analysis

To determine if optical annuli coincide with the microconstituent profiles, LA-ICP-MS data was aligned with micrographs of transverse otolith sections through image analysis. Using Infinity Analyze and Capture (Teledyne Lumenera software), annuli were assigned and measured for each transparent and opaque zone cycle. Distances along the trench created by the LA-ICP-MS's ablated area on the surface of the otolith were measured according to optical annulus assignments (Figure 2.5). Opaque zones were considered the terminus of each annulus, and measurement points within a cycle (transparent > opaque) were converted to fractional ages within each annuli cycle, assuming linear otolith growth.

The elemental profiles of detrended (differenced regression model) and standardized (Z-score) time series for each individual and element were subjected to Lomb-Scargle periodogram analysis, a flexible approach that accounts for the unequally spaced measures across annuli (Lomb 1976; Scargle 1982; Ruf 1999). Normalized power was used to evaluate significant period frequencies. Owing to uncertainties in the first annulus assignment, alternate periodogram analyses were performed for the entire series of annuli and for annuli >1.0.

DTW Analysis

To see if common patterns in the set of profile time-series relate to age class, a dynamic time warp (DTW) analysis was applied. As opposed to the periodogram

analysis, this approach only uses time-series shape characteristics (e.g., number of oscillations and their relative alignment between profiles), rather than classifications that used annuli assignments. For a subset of microconstituents (Mg, Mn, Ba, and Sr), those which exhibited consistent annular patterns (see Results), profiles were subjected to DTW analysis to cluster time series into common centroids (Figure 2.1) under the hypothesis that differing age-classes would exhibit discrete oscillating patterns. Dynamic time warping can align time series based on their shape information and support classification through hierarchical cluster analysis.

Clustering was performed on the individual profiles using the `{dtwclust}` package (Sardá-Espinosa 2017) and agglomerative hierarchical clustering `{hclust}` method in R with Wards distance. Clusters were selected by comparing the average distances within and between clusters, evaluating cluster separation through the Dunn index (ratio of the smallest distance between observations not in the same cluster to the largest intra-cluster distance) and WB-index (sum-of-squares based index where a minimum value can be attained as the number of clusters) (Dunn 1974; Zhao et al. 2009). To determine if the resulting clusters aligned with age-classes, ages were contrasted between defined clusters using a one-way ANOVA and visualized using box and whisker plots.

Results

LA-ICP-MS Analysis

Elements Mg, Mn, Co, Cu, Zn, Sr, and Ba were all measured at detectable levels by LA-ICP-MS (Table 2.2). Several elements occurred below the signal: noise

threshold of 3.0 including P (S:N=2.7), Cu (S:N=0.3), and Zn (S:N=0.3).

Concentration amplitudes were within the range expected for marine teleost otoliths: <ppm for transition metals Mn, Co, Cu, and Zn; ppm levels for Mg, P, and Ba; and ppt levels for Sr (Campana 1999; Hüseyin et al. 2020).

Among measured elements, Ba exhibited the sharpest contrast across presumed annuli as revealed by 2-D elemental maps (Figure 2.6). Of the eight elements analyzed, Ba, Mg, Mn, and Sr all exhibited chemical zonation that aligned with conventional light microscopy. For Ba, chemical zonation was most apparent for annuli > 2, with weak contrast prior to annulus 3. Magnesium exhibited strong zonation for the entire series of annuli. Manganese exhibited elevated concentrations in the core region for both scanned otoliths and had faint but distinct chemical zonation across the series of annuli. Strontium exhibited inconsistent zonation between the two otoliths (Figure 2.6 G, upper and lower panels), one showing a faint series of annuli and the other with narrow chemical zonation for annuli >2. Copper and Zn exhibited uniform concentrations in both otolith sections with no apparent zonation. Calcium was homogeneous in both 2-D maps as expected.

Despite notable zonation in the 2-D maps, oscillating patterns in standardized elemental profiles were not aligned across individuals nor obviously associated with age (Figure 2.7). Note that the majority of profiles correspond to estimated age ≤ 4 with two profiles continuing to age 6. Profiles for transition metals Co, Cu, and Zn whose 2-D maps were especially noisy, which corresponds to the lack of patterning in the 2-D scans. For Ba, Mg, and Mn, peaks and nadirs of oscillations were giving

some indication of association with optical annuli, but visual classifications were deemed too subjective (Figure 2.8).

Lomb-Scargle Periodogram Analysis

Periodogram analysis of entire elemental profiles revealed significant periodicity in the microchemical transects, albeit at frequencies other than the expected 1.0 years (Figures 2.9). Only Mg exhibited significant annular periodicity at 1 year per cycle and a second frequency at about 2.5 years. Elements Ba and Mn showed evidence of significant periodicity but at a rate of ~1.5 years per cycle, each at a lower normalized power respectively (Figure 2.9). Strontium had no defined peak and therefore no determinable primary chemical cycle. The periodograms for P, Co, Cu, and Zn exhibited frequencies of 1.5, 1, .5, and 0.5 years per cycle respectively, albeit at low normalized power (i.e., reduced significance).

The alternate Lomb-Scargle periodogram analysis which removed ages <2.0, detected significant periodicity for Mg, Ba, Mn, and P at the hypothesized 1.0 annulus per cycle at high normalized power (Figure 2.10). Magnesium remained at 1 year per cycle after truncation. The periodogram for Sr again failed to exhibit a peak period. In truncated series, Co, Cu, and Zn exhibited multiple peaks, all of which deviated from the expected frequency of 1.0 years.

DTW analysis

Dynamic time warping analysis of the microconstituent timeseries classified profiles into 9-10 centroids (generalized time series) for Mg, Mn, Ba, and Sr profiles (example for Ba shown in Figure 2.11). Although several of these centroids exhibited

repeating oscillations, none were clearly associated with expected annular frequencies. Individuals classified as centroids did not significantly differ among age-classes (Table 2.3; Figure 2.12).

Discussion

Confirmation of the hypothesis of aligned optical and chemical oscillations across annuli was confirmed for all ages for Mg and for ages >1.0 for microconstituents Ba, Mg, P, and Mn through the Lomb-Scargle periodogram analysis. Further, 2-D maps showed chemical zonation that corresponded with optical zonation for all annuli (Mg), or for annuli >1 (Ba, P, and Mn). Other elements showed no zonation (Co, Cu, Zn) or patterns that were inconsistent with optical annuli (Sr). Strontium exhibited weak patterning in 2-D maps and standardized profiles. This lack of detected annual periodicity in Sr is consistent with why the initial microprobe analysis of Sr was inconclusive (Appendix A).

Here we tested two quantitative approaches to verify the periodicity of chemical annuli. Similar to past applications (Siskey et al. 2016; Brophy et al. 2019), the Lomb-Scargle periodogram approach was well suited to test expected frequency (1.0) for the unequally spaced time-series. The alternative DTW time series, even when employed on my best candidate element, Mg, failed to extract clusters that were related to age-class. Unlike the periodogram analysis, the DTW analysis evaluates time series without reference to chemical annulus assignments, which could cause centroids to reflect patterns unrelated to annuli or age-classes.

Both periodogram analysis and 2-D maps indicated issues in identifying the first annulus. The inclusion and removal of the first annulus in the periodogram

analysis had a large influence on the expected periodicity of Sr, Ba, and Mn. This could be explained by a period of rapid and variable growth in black sea bass in their first-year nursery habitat. Nursery habitats in estuarine and nearshore environments for black sea bass (ASMFC 2009) are heterogeneous in ambient concentrations of Sr, Ba, and Mn. Strontium conservatively mixes and is often positively associated with salinity (Kraus and Secor 2004), consistent with lower Sr during the first year of life (Figures 2.6, 2.7). Barium becomes less available in eutrophic waters of estuaries and coastal waters (Hüssy et al. 2020), which aligns with lower age-1 Ba. How Mn is associated with ambient exposure remains unsettled in the literature, but it has been associated definitively with hypoxic waters (Limburg and Casini 2018). Early elemental oscillations could also be reflective of black sea bass' change in reproductive state (maturation is achieved at age ≥ 2 years) or early habitat transitions (Steimle 1999). Understanding the lack of expected periodicity for age-1 black sea bass will require a deeper look into the otolith composition during the first year of life.

Another approach is to rely exclusively on 2-D maps. Optical annuli were well aligned with chemical annuli in the 2-D maps (Figure 2.6), especially Mg, suggesting age can be assigned through direct interpretation of the 2-D element maps. Such analysis of black sea bass otoliths could provide improved precision through high-contrast visualizations (Limburg et al. 2018; Heimbrand et al. 2020; Hüssy et al. 2020). Still, for even moderate-sized samples ($N > 50$), reliance on 2-D maps could be cost-prohibitive and demand many fold higher time investment than standard ageing

approaches. Further, 2-D map interpretations are subjective and not supported by objective time series analyses, such as the periodogram approach applied here.

To support the periodogram analysis, fractional ages were estimated based on linear interpretations under the assumption of constant seasonal otolith growth. Previous studies have validated the seasonal growth of black sea bass otolith annuli (Robillard et al. 2016), but little is known about the rate of formation of the first annulus. Recent work by Koob et al. (2021) supported our adoption of NEFSC conventions for first annulus assignments. Still, tests of the chemical ageing-periodogram approach should be pursued for other model species, particularly long-lived species, where seasonality of annulus formation is well known.

Seasonal changes in otolith composition in elements, Mg, Sr, and Mn conform to expectations of environmental and physiological influences (Grammer et al. 2017). Element Mg has exhibited strong periodicity supporting “chemical calendar clocks” in Baltic cod (Limburg and Casini 2018). Mg concentration in the otolith is known to be linked to growth (Grammer et al. 2017), which may explain the strength of the periodogram analysis and the visibility of chemical annuli in the 2-D maps. Recent work by (Brophy et al. 2021) has shown seasonal variation in otolith Sr is detectable in white anglerfish but in our analysis Sr oscillations were weak and no yearly periodic fluctuations were apparent. Otolith Ba, like Sr, may reflect seasonal temperature cycles (Barnes and Gillanders 2013; Reis-Santos et al. 2013; Stanley et al. 2015).

A central premise of aligning otolith microconstituent cycles with annulus zone formation is that black sea bass are exposed to seasonally changing

temperatures. Moser and Shepherd (2008) placed archival tags in black sea bass released off southern New England and the Mid-Atlantic Bight. These and conventionally tagged black sea bass showed offshore migrations during winter months, cued by cooling temperatures in near shelf regions. In the Mid-Atlantic Bight, black sea bass migrate to inner shelf regions in spring and reside in bottom waters that exhibit stable thermal conditions until fall, when fall turnover causes a rapid increase in water column temperatures (Wiernicki et al. 2020). These are then followed by late fall cooling, cueing offshore winter migrations (Moser and Shepherd 2008). For the Southern Mid-Atlantic Bight, where my samples originated this pattern of spring-fall residency and winter offshore migration would be associated with exposure to a 12-17 C seasonal amplitude, with most change occurring during August-November (based on observed bottom temperatures in near and mid-shelf waters off DelMarVa: Rothermel et al. 2020). For a single long-term (13 month) archival tag return, Moser and Shepherd (2008) observed experienced temperatures consistent with this seasonal cycle ranging between 6 C (winter) and 25 C (late summer-fall). As reviewed in the Introduction, seasonal temperature would be expected to influence Mg, Mn, Sr, and Ba – those elements that are incorporated into the otolith's aragonitic structure.

Validation of direct ageing through hardpart analysis provides the foundation for strong stock assessments. My study, testing a novel chemical ageing approach, supports recent marginal increment validation studies and optical annulus interpretations in general. Still, interpretations of the first annulus merit additional examination based on (1) varying results across candidate elements Mg, Ba, P, and

Mn (2) past uncertainty in first annulus assignment. Chemical validation of otolith annuli formation in black sea bass further strengthens the justification for age-structured black sea bass stock assessments. Although 2-D maps could be used for direct ageing, the analytical and time costs associated with high-resolution LA-ICP-MS analysis, suggest that chemical ageing is best used in validation studies. Further, as investigated in Chapter 3, the approach may provide a feasible means for validating ages in species where traditional validation approaches have failed.

Tables and Figures

Table 2.1 List of 17 species and stocks routinely aged by the NOAA Northeast Fisheries Science Center ageing methods and validation type. Length frequency analysis (LFA), marginal increment analysis (MIA).

Species	Scientific name	Hardpart	Validated	Method of Validation	Citation
Acadian redfish	<i>Sebastes fasciatus</i>	otolith section	Yes, Indirect	LFA vs. Annuli	Mayo 1981
American plaice	<i>Hippoglossoides platessoides</i>	otolith section	Yes	LFA vs. Annuli, Bomb radiocarbon	Powles 1966; Morin et al. 2013
Atlantic cod	<i>Gadus morhua</i>	otolith baked	Yes, Indirect	Microchemistry	Kohler 1964; Jensen 1970
Atlantic herring	<i>Clupea harengus</i>	otolith section	Limited	LFA vs. Annuli	Watson 1964; Dery and Chenoweth 1979
Atlantic mackerel	<i>Scomber scombrus</i>	otolith section	No		
Atlantic wolffish	<i>Anarhichas lupus</i>	scale, otolith	No		
Black sea bass	<i>Centropristis striata</i>	otolith whole	Yes, Direct	MIA, Tag-recapture	Robillard et al. 2016; Koob et al. 2021
Butterfish	<i>Peprilus triacanthus</i>	otolith whole	No		
Haddock	<i>Melanogrammus aeglefinus</i>	otolith, scale	Yes, Direct	Bomb radiocarbon	Jensen & Wise 1962; Campana 1997
Monkfish	<i>Lophious americanus</i>	vertebrae	No	Tag/recapture	Bank et al. 2020
Ocean pout	<i>Zoarces americanus</i>	otolith			
Pollock	<i>Pollachius virens</i>	otolith section	Yes, Direct	MIA, Tag/recapture	
Red hake	<i>Urophycis chuss</i>	otolith section	Yes, Indirect	LFA vs. Annuli	Dery 1988
Silver hake	<i>Merluccius bilinearis</i>	otolith section	Yes, Indirect	LFA vs. Annuli	Hunt 1980
Summer flounder	<i>Paralichthys dentatus</i>	scale	No	Cross-validated	
Weakfish	<i>Cynoscion regalis</i>	scale	Yes, Indirect	LFA vs. Annuli, MIA	Massmann 1963
Winter flounder	<i>Pseudopleuronectes americanus</i>	scale	No		
Witch Flounder	<i>Glyptocephalus cynoglossus</i>	otolith section	No	LFA vs. Annuli	
Yellowtail flounder	<i>Limanda ferruginea</i>	scale	Yes, Direct	Tag-recapture, Bomb radiocarbon	Lux and Nichy 1969; Dwyer et al. 2003

Table 2.2 Average mean elemental concentrations (ppm) in black sea bass otolith profiles (N=41).

	Mg	P	Mn	Co	Cu	Zn	Sr	Ba
Average	13.6	78.6	2.3	0.2	0.3	0.4	2,148.9	10.1
stdev	3.0	32.5	0.8	0.0	1.2	0.4	168.4	3.5
S:N*	23.7	2.7	4.6	3.2	<i>0.3</i>	<i>0.3</i>	45,555.2	370.2

*S:N, signal to noise ratio, is the mean transect concentration divided by the estimated mean detection limit among the population of analyzed specimens. Red italicized entries show elements with average concentrations <3x higher than detection limits.

Table 2.3 Results of ANOVA on the effect of age-class on otolith profile clusters classified through Dynamic Time Warping (DTW) cluster for black sea bass.

	Df	Sum Sq	Mean Sq	F value	Pr(>F)
Mg DTW Clusters	9	9.54	1.06	1.60	0.17
Ba DTW Clusters	9	8.47	0.94	1.33	0.27
Mn DTW Clusters	8	3.73	0.47	0.54	0.82
Sr DTW Clusters	9	6.11	0.68	0.85	0.58

Figure 2.1 Example of realignment of time series into centroids (red line) based on dynamic time warping. The black line represents a single Mg time series otolith profile for black sea bass, which together with other profiles would be warped similarly to the fitted time series centroid.

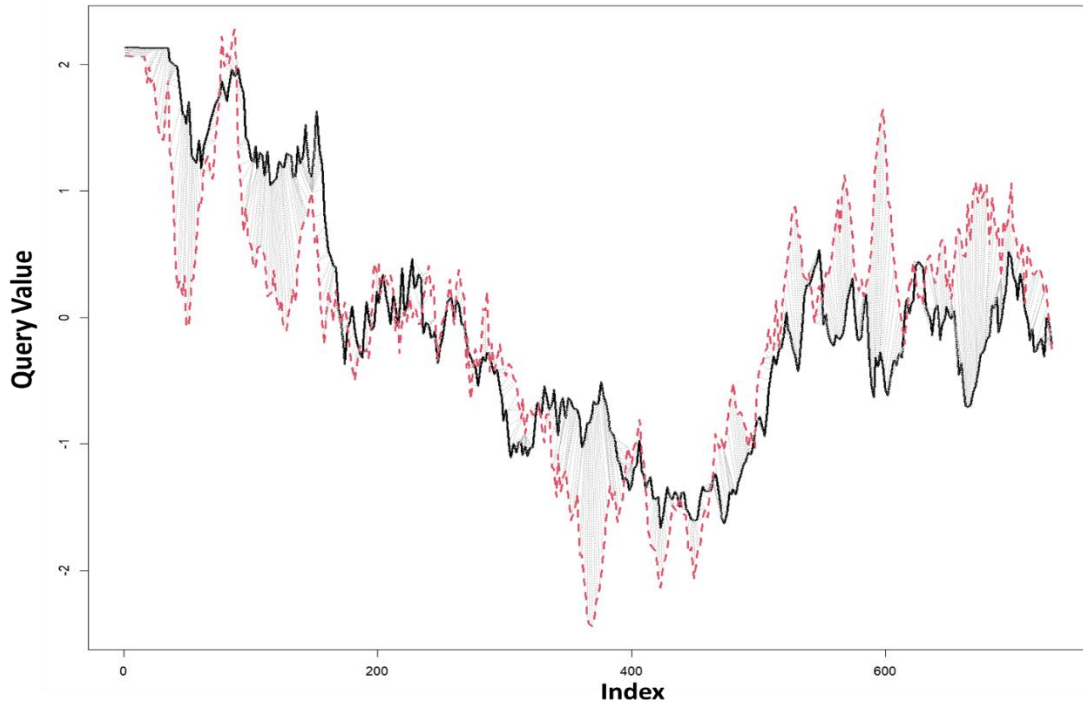


Figure 2.2 Age annotations for a sectioned and whole black sea bass otolith. Red counts assign the first transparent zone within the core region according to the alternate approach. Blue counts do not according to the “NEFSC” approach.

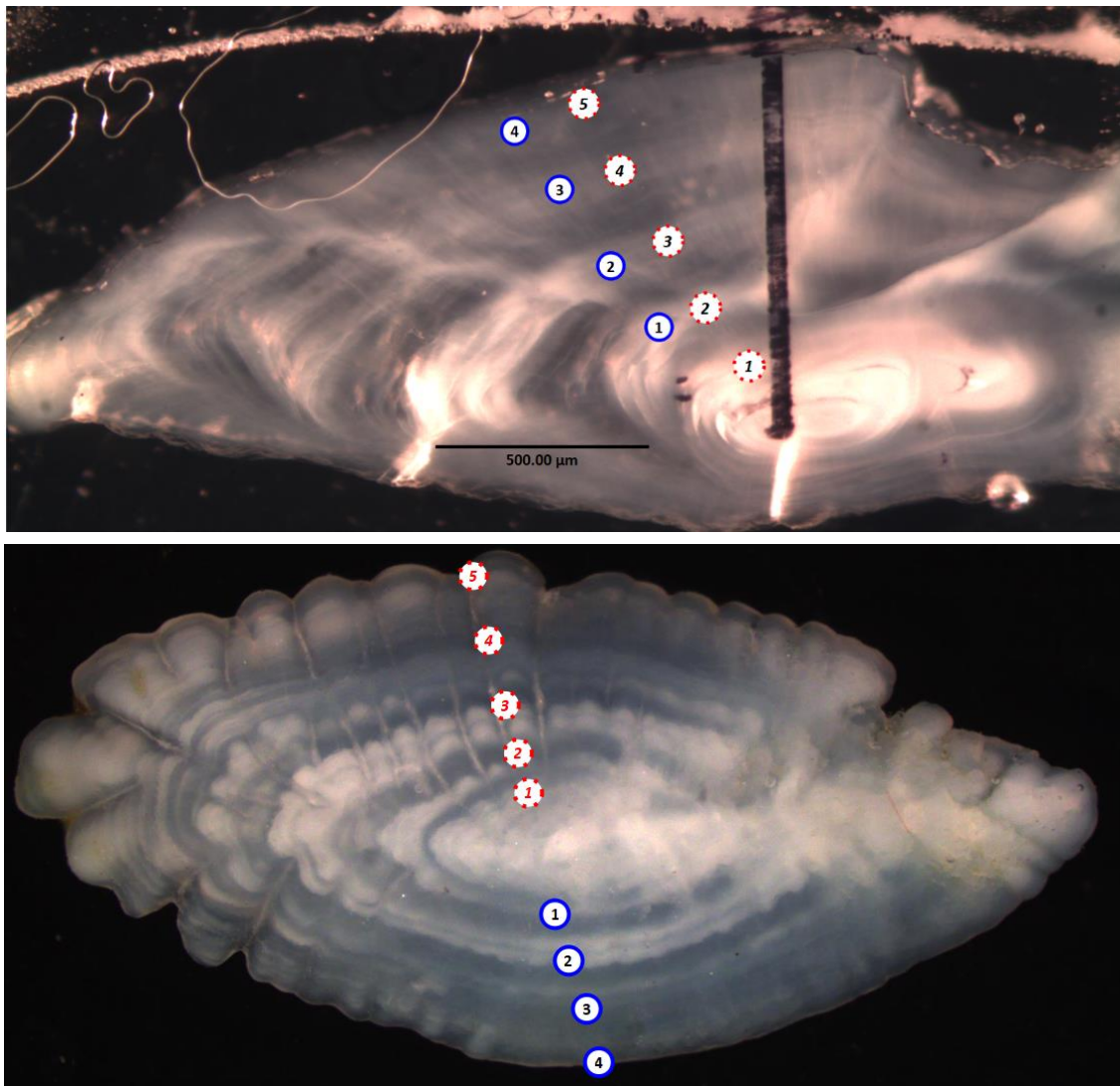


Figure 2.3 Length frequency diagram of black sea bass captured for use in this study (n=125). Line is a spline fit to the length frequency data.

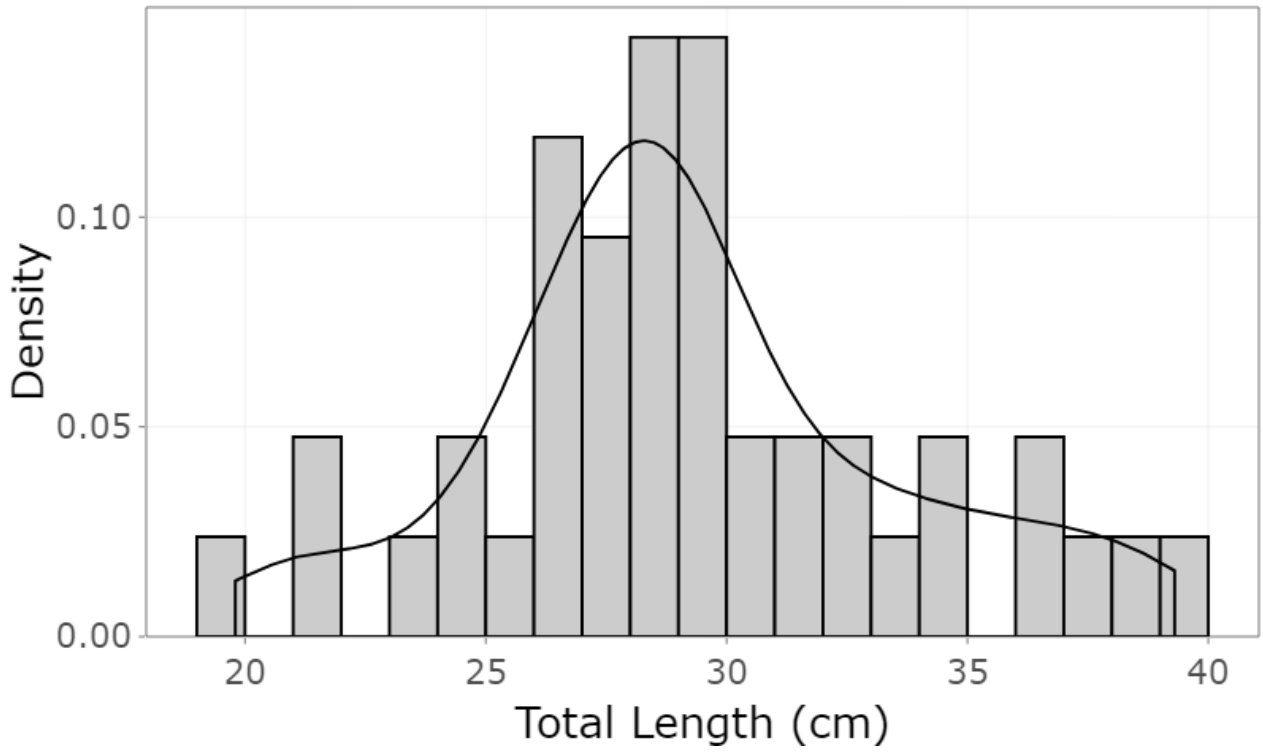


Figure 2.4 Location of black sea bass captured through hook and line on wreck and artificial reef sites (20-30 m depth) off Ocean City, Maryland US during the summer and fall months of 2016 and 2018 (n= 125).

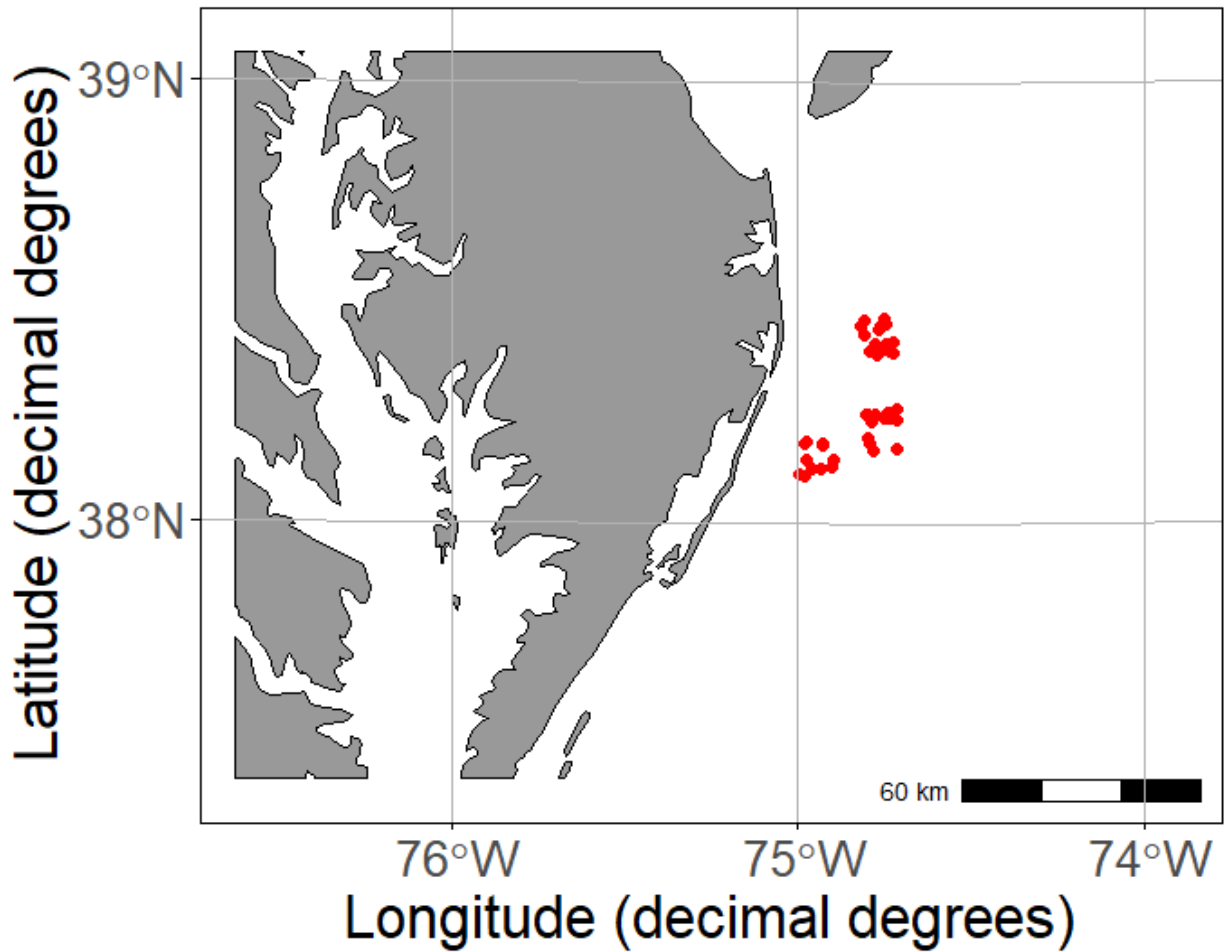


Figure 2.5 Annuli annotations across the trench created by the LA-ICP-MS's ablated area (black line) on the surface of a sectioned black sea bass otolith. Blue points along the white line depict annuli used in constructing elemental profiles. Image captured and overlay via Infinity Analyze and Capture (Teledyne Lumenera software).

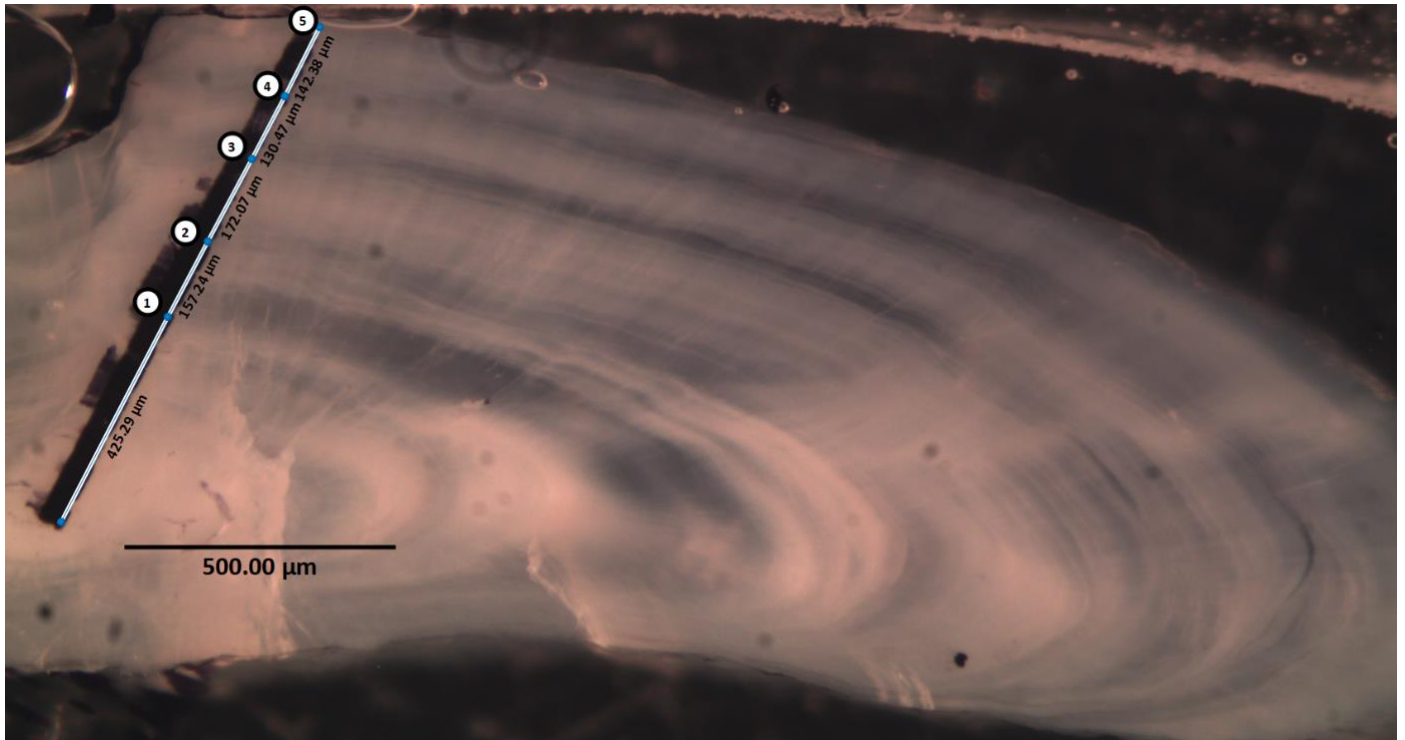


Figure 2.6 2-Dimensional elemental maps and light micrograph (Raw) image for two black sea bass sectioned otoliths (top and lower panels). Concentration scales from blue (low) to red (high). Note that contrast is optimized and depicted through pseudocolor for each map and is not common across elements. Standard (NEFSC approach) optical annuli annotations are depicted in circles.

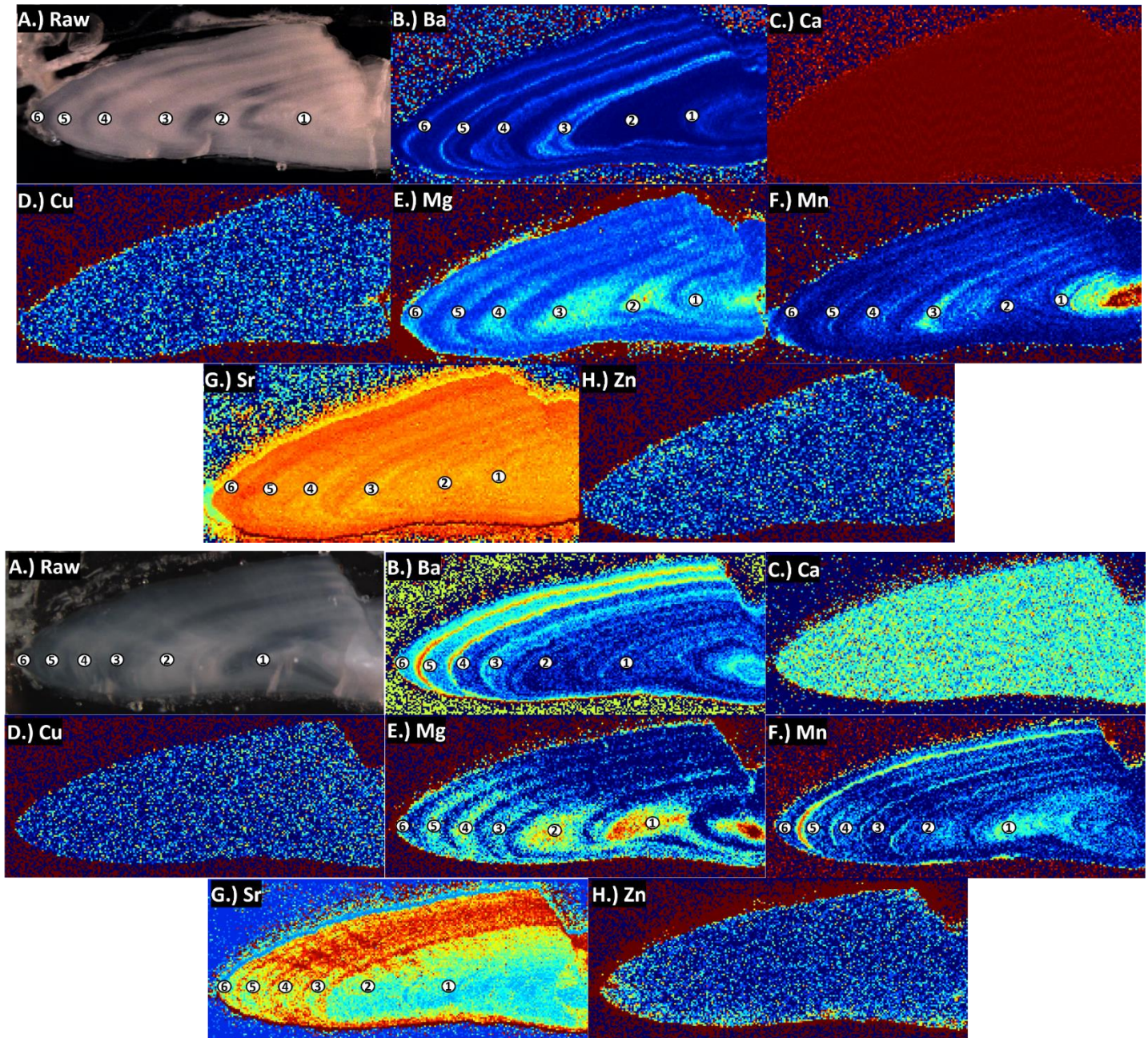


Figure 2.7 Standardized profiles (n=34) across microconstituents for black sea bass otoliths. Colored by individual.

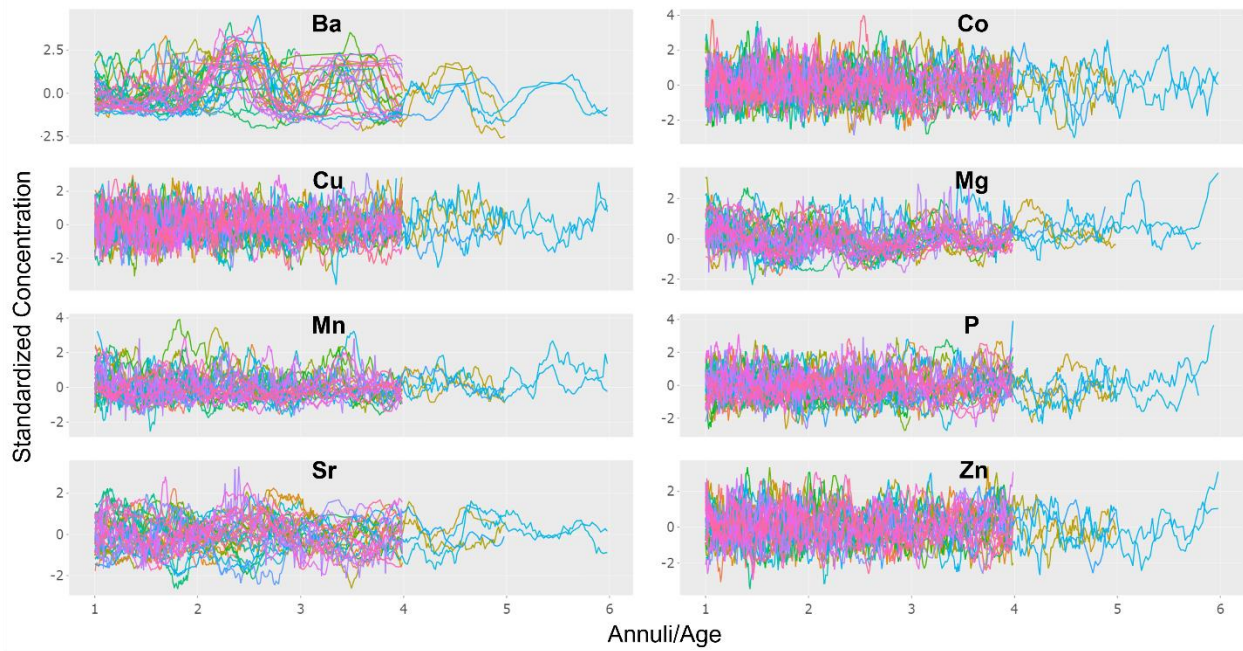


Figure 2.8 Standardized profiles across otolith microconstituents for a single black sea bass.

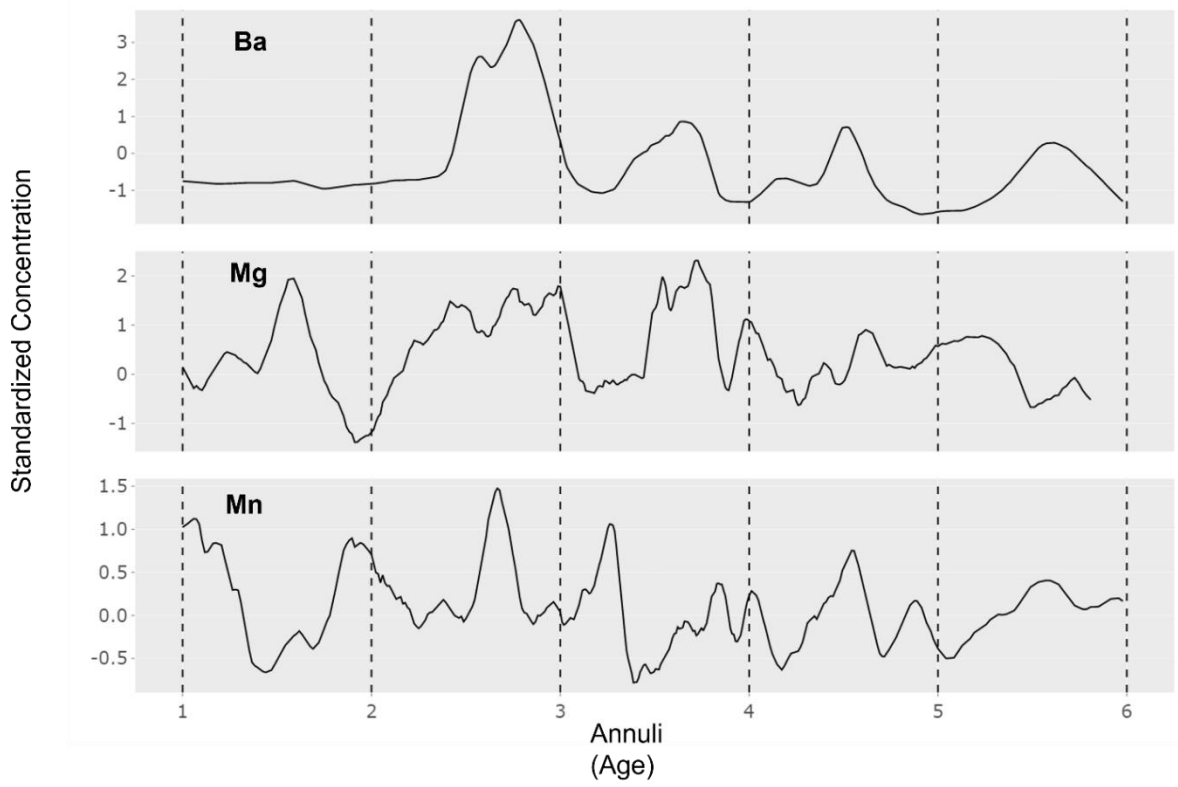


Figure 2.9 Lomb-Scargle periodograms for elemental profiles (N=34) including the full series of otolith annuli for black sea bass. Significance (power=0.001) is shown by the horizontal dashed line. The vertical dashed line is hypothesized period frequency=1.0. Note the difference in scale between the top and bottom rows.

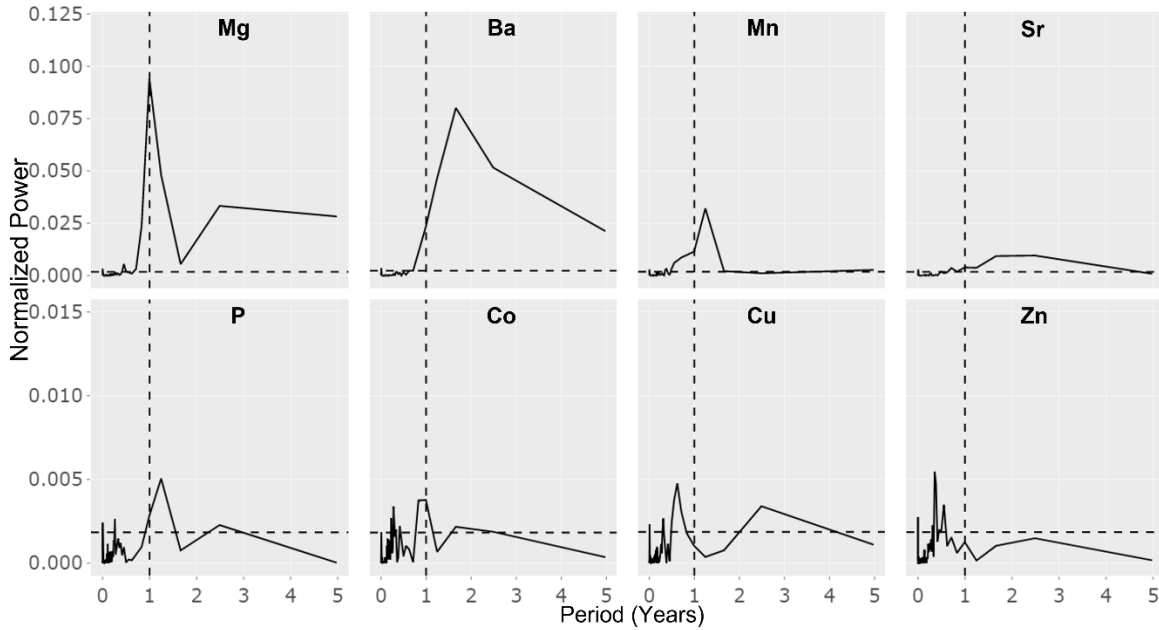


Figure 2.10 Lomb-Scargle periodograms for otolith elemental profiles (N=34) including only annuli >1.0 for black sea bass. Significance (power=0.001) is shown by the horizontal dashed line. The vertical dashed line is hypothesized period frequency=1.0. Note the difference in scale between the top and bottom rows.

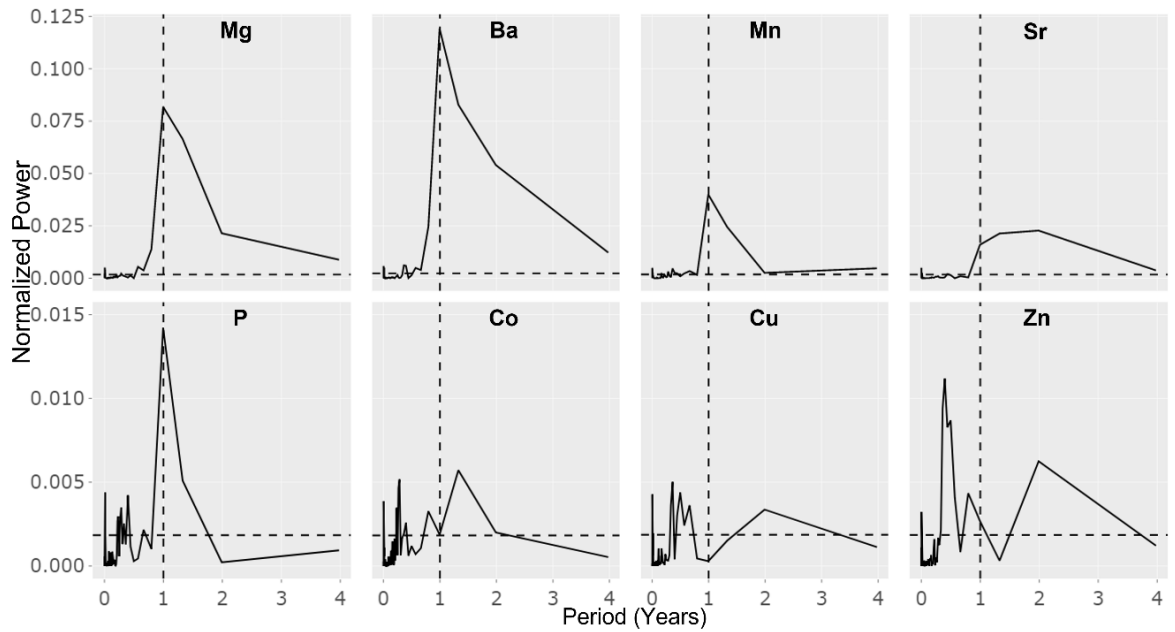


Figure 2.11 Barium centroids estimated through Dynamic Time Warping for black sea bass otolith profiles.

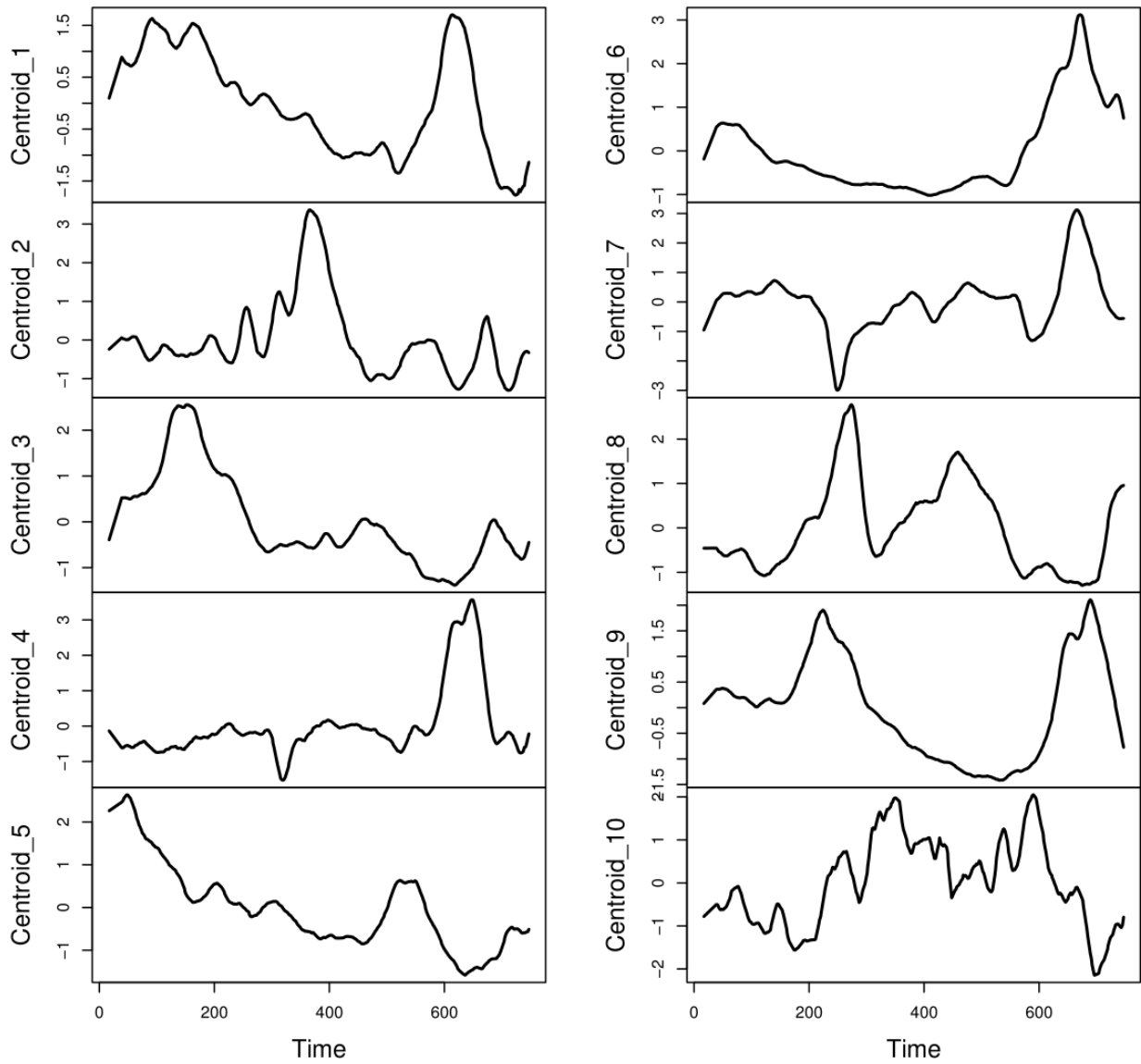
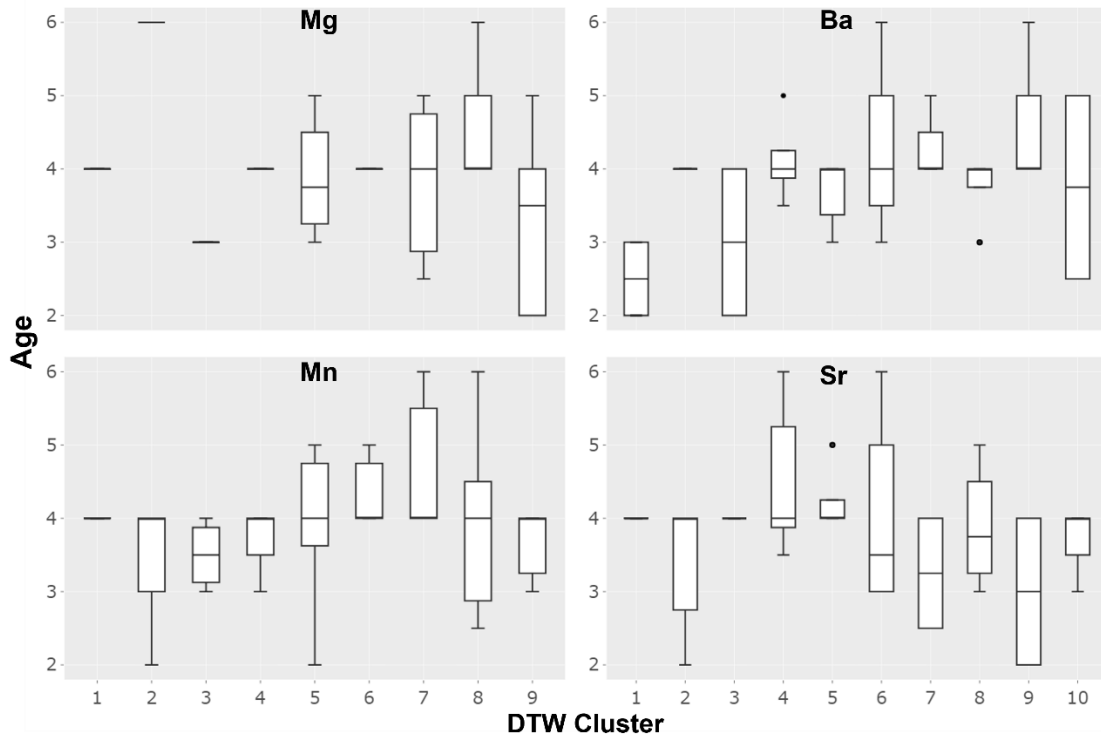


Figure 2.12 Box and whisker plots of ages across clusters determined through Dynamic Time Warping analysis of black sea bass otolith profiles.



References

- Arslan, Z., and D. H. Secor. 2005. Analysis of trace transition elements and heavy metals in fish otoliths as tracers of habitat use by American eels in the Hudson River estuary. *Estuaries* 28(3):382–393.
- ASMFC, (Atlantic States Marine Fisheries Commission). 2009. Species profile: Black sea bass. Joint management yields rebuilt status for popular mid-Atlantic fish. *ASMFC Fisheries Focus* 18(6):12.
- ASMFC, (Atlantic States Marine Fisheries Commission). 2013. Proceedings of the 2013 black sea bass ageing workshop. Pages 1–21. Atlantic States Marine Fisheries Commission.
- ASMFC, (Atlantic States Marine Fisheries Commission). 2021. Atlantic states marine fisheries commission review of the interstate fishery management plan:1–16.
- Bank, C. M., K. Oliveira, S. J. Sutherland, M. P. Armstrong, J. Landa, and S. X. Cadrin. 2020. Age validation for goosefish (*Lophius americanus*) in the northeastern United States. *Fishery Bulletin* 118(1):8–20.
- Barnes, T. C., and B. M. Gillanders. 2013. Combined effects of extrinsic and intrinsic factors on otolith chemistry: implications for environmental reconstructions. *Canadian Journal of Fisheries and Aquatic Sciences* 70(8):1159–1166.
- Beamish, R. J., and G. A. McFarlane. 1983. The forgotten requirement for age validation in fisheries biology. *Transactions of the American Fisheries Society* 112(6):735–743.
- Bradford, M. J. 1991. Effects of ageing errors on recruitment time series estimated from sequential population analysis. *Canadian Journal of Fisheries and Aquatic Sciences* 48(4):555–558.
- Brophy, D., D. P. De Pontual, K. Mahe, and C.-M. Villanueva. 2019. Validating age-determination of anglerfish and hake. Report (Scientific report), IRELAND.
- Brophy, D., S. Pérez-Mayol, R. Duncan, K. Hüsey, A. J. Geffen, H. D. Gerritsen, M. C. Villanueva, and B. Morales-Nin. 2021. Elemental composition of illicia and otoliths and their potential application to age validation in white anglerfish (*Lophius piscatorius* linnaeus, 1758). *Estuarine, Coastal and Shelf Science* 261:107557.
- Campana, S. E. 1997. Use of radiocarbon from nuclear fallout as a dated marker in the otoliths of haddock *Melanogrammus aeglefinus*. *Marine Ecology Progress Series* 150:49–56.
- Campana, S. E. 1999. Chemistry and composition of fish otoliths: pathways, mechanisms and applications. *Marine Ecology Progress Series* 188:263–297.
- Campana, S. E. 2001. Accuracy, precision and quality control in age determination, including a review of the use and abuse of age validation methods. *Journal of Fish Biology* 59(2):197–242.
- Campana, S. E., and J. D. Neilson. 1982. Daily growth increments in otoliths of starry flounder (*Platichthys stellatus*) and the influence of some environmental variables in their production. *Canadian Journal of Fisheries and Aquatic Sciences* 39(7):937–942.
- Casselman, J. M. 1983. Age and growth assessment of fish from their calcified structures—techniques and tools. NOAA Technical Report NMFS 8:1–17.

- Casselman, J. M., C. M. Jones, and S. E. Campana. 2019. Bomb radiocarbon age validation for the long-lived, unexploited Arctic fish species *Coregonus clupeaformis*. *Marine and Freshwater Research* 70(12):1781–1788.
- Chale-Matsau, J. R., A. Govender, and L. E. Beckley. 2001. Age, growth and retrospective stock assessment of an economically extinct sparid fish, *Polysteganus undulosus*, from South Africa. *Fisheries Research* 51(1):87–92.
- Daugherty, D. J., A. H. Andrews, and N. G. Smith. 2020. Otolith-based age estimates of alligator gar assessed using bomb radiocarbon dating to greater than 60 Years. *North American Journal of Fisheries Management* 40(3):613–621.
- Dery, L., and J. Chenoweth. 1979. Recent problems in ageing sea herring from the Gulf of Maine. NMFS, Northeast Fisheries Center.
- Dery, L. M. 1988. Red hake *Urophycis chuss*. Age Determination Methods for Northwest Atlantic Species. NOAA:49–57.
- Dery, L. M., and J. P. Mayo. 1988. Black sea bass *Centropristis striata*. NOAA Technical Report NMFS 72:59–70.
- Dunn, J. C. 1974. Well-separated clusters and optimal fuzzy partitions. *Journal of Cybernetics* 4(1):95–104.
- Dwyer, K. S., S. J. Walsh, and S. E. Campana. 2003. Age determination, validation and growth of Grand Bank yellowtail flounder (*Limanda ferruginea*). *ICES Journal of Marine Science* 60(5):1123–1138.
- Elvarsson, B. Þ., P. J. Woods, H. Björnsson, J. Lentin, and G. Thordarson. 2018. Pushing the limits of a data challenged stock: A size-and age-structured assessment of ling (*Molva molva*) in Icelandic waters using Gadget. *Fisheries Research* 207:95–109.
- Engstedt, O., P. Koch-Schmidt, and P. Larsson. 2012. Strontium (Sr) uptake from water and food in otoliths of juvenile pike (*Esox lucius L.*). *Journal of Experimental Marine Biology and Ecology* 418–419:69–74.
- Francis, C., H. Neil, and S. Campana. 2010. Validation of fish ageing methods should involve bias estimation rather than hypothesis testing: a proposed approach for bomb radiocarbon validations. *Canadian Journal of Fisheries and Aquatic Sciences* 67(9):1398–1408.
- Hegg, J. C., and B. P. Kennedy. 2021. Let's do the time warp again: non-linear time series matching as a tool for sequentially structured data in ecology. *Ecosphere* 12(9):e03742.
- Heimbrand, Y., K. E. Limburg, K. Hüsey, M. Casini, R. Sjöberg, A.-M. Palmén Bratt, S.-E. Levinsky, A. Karpushevskaya, K. Radtke, and J. Öhlund. 2020. Seeking the true time: Exploring otolith chemistry as an age-determination tool. *Journal of Fish Biology* 97(2):552–565.
- Hunt, J. J. 1980. Guidelines for age determination of silver hake, *Merluccius bilinearis*, using otoliths. NAFO Scientific Council Research 80.
- Hüsey, K., K. E. Limburg, H. de Pontual, O. R. B. Thomas, P. K. Cook, Y. Heimbrand, M. Blass, and A. M. Sturrock. 2020. Trace element patterns in otoliths: the role of biomineralization. *Reviews in Fisheries Science & Aquaculture*:1–33.
- Jensen, A. C. 1970. Validation of ages determined from otoliths of Gulf of Maine cod. *Transactions of the American Fisheries Society* 99(2):359–362.

- Jensen, A. C., and J. P. Wise. 1962. Determining age of young haddock from their scales. U.S. Fish and Wildlife Service, Washington.
- Kohler, A. C. 1964. Variations in the growth of Atlantic cod (*Gadus morhua* L.). *Journal of the Fisheries Board of Canada* 21(1):57–100.
- Koob, E. R., S. P. Elzey, J. W. Mandelman, and M. P. Armstrong. 2021. Age validation of the northern stock of black sea bass *Centropristis striata* in the Atlantic Ocean. *Fishery Bulletin* 119(4).
- Kraus, R. T., and D. H. Secor. 2004. Dynamics of white perch *Morone americana* population contingents in the Patuxent River estuary, Maryland, USA. *Marine Ecology Progress Series* 279:247–259.
- Limburg, K. E., and M. Casini. 2018. Effect of marine hypoxia on Baltic Sea cod *Gadus morhua*: evidence from otolith chemical proxies. *Frontiers in Marine Science* 5:482.
- Limburg, K. E., M. J. Wuenschel, K. Hüsey, Y. Heimbrand, and M. Samson. 2018. Making the otolith magnesium chemical calendar-clock tick: plausible mechanism and empirical evidence. *Reviews in Fisheries Science & Aquaculture* 26(4):479–493.
- Lomb, N. R. 1976. Least-squares frequency analysis of unequally spaced data. *Astrophysics and Space Science* 39(2):447–462.
- Lux, F. E., and F. E. Nichy. 1969. Growth of yellowtail flounder, *Limanda ferruginea* (Storer), on three New England fishing grounds. *ICNAF Res. Bull* 6:5–25.
- Machias, A., N. Tsimenides, L. Kokokiris, and P. Divanach. 1998. Ring formation on otoliths and scales of *Pagrus pagrus*: a comparative study. *Journal of Fish Biology* 52(2):350–361.
- Maharaj, E. A., P. D’Urso, and J. Caiado. 2019. Time series clustering and classification. Chapman and Hall/CRC.
- Massmann, W. H. 1963. Annulus formation on the scales of weakfish, *Cynoscion regalis*, of Chesapeake Bay. *Chesapeake Science* 4(1):54–56.
- Mayo, R. K. 1981. Age validation of redfish, *Sebastes marinus* (L.), from the Gulf of Maine-Georges Bank region. *Journal of Northwest Atlantic Fishery Science* 2:13–19.
- Mills, K. H., and R. J. Beamish. 1980. Comparison of fin-fay and scale age determinations for lake whitefish (*Coregonus clupeaformis*) and their implications for estimates of growth and annual survival. *Canadian Journal of Fisheries and Aquatic Sciences* 37(3):534–544.
- Morin, R., S. G. LeBlanc, and S. E. Campana. 2013. Bomb radiocarbon validates age and long-term growth declines in American plaice in the southern Gulf of St. Lawrence. *Transactions of the American Fisheries Society* 142(2):458–470.
- Moser, J., and G. R. Shepherd. 2008. Seasonal Distribution and Movement of Black Sea Bass (*Centropristis striata*) in the Northwest Atlantic as Determined from a Mark-Recapture Experiment. *Journal of Northwest Atlantic Fishery Science* 40.
- Musick, J. A., and L. P. Mercer. 1977. Seasonal distribution of black sea bass, *Centropristis striata*, in the Mid-Atlantic Bight with comments on the ecology and fisheries of the species. *Transactions of the American Fisheries Society* 106(1):12–25.

- NEFSC, (Northeast Fisheries Science Center). 2019. Operational assessment of the black sea bass, scup, bluefish, and monkfish Stocks, updated through 2018:164.
- Okamura, H., A. E. Punt, Y. Semba, and M. Ichinokawa. 2013. Marginal increment analysis: a new statistical approach of testing for temporal periodicity in fish age verification. *Journal of Fish Biology* 82(4):1239–1249.
- Oosthuizen, W. C., P. J. N. D. Bruyn, M. N. Bester, and M. Girondot. 2010. Cohort and tag-site-specific tag-loss rates in mark–recapture studies: a southern elephant seal cautionary case. *Marine Mammal Science* 26(2):350–369.
- Paton, C., J. Hellstrom, B. Paul, J. Woodhead, and J. Hergt. 2011. Iolite: Freeware for the visualisation and processing of mass spectrometric data. *Journal of Analytical Atomic Spectrometry* 26(12):2508–2518.
- Penttila, Judy., and L. M. Dery. 1988. Age determination methods for northwest Atlantic species. U.S. Dept. of Commerce, National Oceanic and Atmospheric Administration, National Marine Fisheries Service, [Silver Spring, Md.].
- Powles, P. M. 1966. Validity of ageing young American plaice from otoliths. *International Commission for the Northwest Atlantic Fisheries Research Bulletin* 3:103–105.
- Reis-Santos, P., S. E. Tanner, T. S. Elsdon, H. N. Cabral, and B. M. Gillanders. 2013. Effects of temperature, salinity and water composition on otolith elemental incorporation of *Dicentrarchus labrax*. *Journal of Experimental Marine Biology and Ecology* 446:245–252.
- Robillard, E., J. W. Gregg, J. Dayton, and J. Gartland. 2016. SARC 62 Working paper validation of black sea bass, *Centropristis striata*, ages using oxytetracycline marking and scale margin increments. Page 16.
- Rotella, J. J., and J. E. Hines. 2005. Effects of tag loss on direct estimates of population growth rate. *Ecology* 86(4):821–827.
- Rothermel, E. R., M. T. Balazik, J. E. Best, M. W. Breece, D. A. Fox, B. I. Gahagan, D. E. Haulsee, A. L. Higgs, M. H. O’Brien, and M. J. Oliver. 2020. Comparative migration ecology of striped bass and Atlantic sturgeon in the US Southern mid-Atlantic bight flyway. *PloS one* 15(6):e0234442.
- Ruf, T. 1999. The lomb-scargle periodogram in biological rhythm research: analysis of incomplete and unequally spaced time-series. *Biological Rhythm Research* 30(2):178–201.
- Sardá-Espinosa, A. 2017. Comparing time-series clustering algorithms in r using the dtwclust package. *R package vignette* 12:41.
- Scargle, J. D. 1982. Studies in astronomical time series analysis. II - Statistical aspects of spectral analysis of unevenly spaced data. *The Astrophysical Journal* 263:835–853.
- Schramm, H. L. 1989. Formation of annuli in otoliths of bluegills. *Transactions of the American Fisheries Society* 118(5):546–555.
- Secor, D. H., and P. M. Piccoli. 1996. Age- and sex-dependent migrations of striped bass in the Hudson River as determined by chemical microanalysis of otoliths. *Estuaries* 19(4):778–793.

- Seyama, H., J. S. Edmonds, M. J. Moran, Y. Shibata, M. Soma, and M. Morita. 1991. Periodicity in fish otolith Sr, Na, and K corresponds with visual banding. *Experientia* 47(11):1193–1196.
- Siskey, M. R., V. Lyubchich, D. Liang, P. M. Piccoli, and D. H. Secor. 2016. Periodicity of strontium: Calcium across annuli further validates otolith-ageing for Atlantic bluefin tuna (*Thunnus thynnus*). *Fisheries Research* 177:13–17.
- Stanley, R. R. E., I. R. Bradbury, C. DiBacco, P. V. R. Snelgrove, S. R. Thorrold, and S. S. Killen. 2015. Environmentally mediated trends in otolith composition of juvenile Atlantic cod (*Gadus morhua*). *ICES Journal of Marine Science* 72(8):2350–2363.
- Steimle, F. W. 1999. Essential fish habitat source document: Black sea bass, *Centropristis striata*, life history and habitat characteristics. DIANE Publishing.
- Sutherland, S. J., and R. A. Richards. 2021. Validation of methods for aging goosefish (*Lophius americanus*) based on length-mode progression of a strong cohort. *Fishery Bulletin* 120(1):13–25.
- Thomas, R. M. 1983. Back-calculation and time of hyaline ring formation in the otoliths of the pilchard off South West Africa. *South African Journal of Marine Science* 1(1):3–18.
- Vanderkooy, S., J. Carroll, S. Elzey, J. Gilmore, and J. Kipp. 2020. A Practical Handbook for Determining the Ages of Gulf of Mexico and Atlantic Coast Fishes - Third Edition.
- Vitale, F., L. A. Worsøe Clausen, G. N. Chonchúir, and International Council for the Exploration of the Sea. 2019. Handbook of fish age estimation protocols and validation methods. Pages 1–180. International Council for the Exploration of the Sea, 346.
- Walker, B. M., and T. M. Sutton. 2016. Growth-increment formation using otoliths and scales for age-0 Chinook salmon. *North American Journal of Fisheries Management* 36(5):995–999.
- Watson, J. E. 1964. Determining the age of young herring from their otoliths. *Transactions of the American Fisheries Society* 93(1):11–20.
- Wiernicki, C. J., M. H. O'Brien, F. Zhang, V. Lyubchich, M. Li, and D. H. Secor. 2020. The recurring impact of storm disturbance on black sea bass (*Centropristis striata*) movement behaviors in the Mid-Atlantic Bight. *PloS one* 15(12):e0239919.
- Wilhelm, M., M. Durholtz, and C. Kirchner. 2008. The effects of ageing biases on stock assessment and management advice: a case study on Namibian horse mackerel. *African Journal of Marine Science* 30(2):255–261.
- Yule, D. L., J. D. Stockwell, J. A. Black, K. I. Cullis, G. A. Cholwek, and J. T. Myers. 2008. How systematic age underestimation can impede understanding of fish population dynamics: lessons learned from a Lake Superior cisco stock. *Transactions of the American Fisheries Society* 137(2):481–495.
- Zhao, Q., M. Xu, and P. Fränti. 2009. Sum-of-squares based cluster validity index and significance analysis. Pages 313–322 International conference on adaptive and natural computing algorithms. Springer.

Zlokovitz, E. R., D. H. Secor, and P. M. Piccoli. 2003. Patterns of migration in Hudson River striped bass as determined by otolith microchemistry. *Fisheries Research* 63(2):245–259.

Chapter 3: Annular periodicity of microconstituents in the illicia of Atlantic monkfish (*Lophius americanus*)

Introduction

Atlantic monkfish (*Lophius americanus*), one of the most valuable finfish resources of the US Northeast Shelf, is incompletely assessed for its sustainability. The value of landings (\$26 million) far exceeds those of traditional groundfish species such as cod (\$19 million), haddock (\$14 million), and flatfish (\$600,000) (mean average values for 2001 to 2019; NMFS 2020). Measuring age structure is central to most fishery resource assessments, determined through the interpretation of optical zones (i.e., “rings” or annuli) on hardparts. Hardparts are calcified structures that often show patterns of seasonal zonation, which can be optically distinguished through microscopy as alternating light and dark zones that vary in their organic concentrations. Counts of these optical zones can support age determination but require careful verification studies. Several hardparts have been employed historically to determine the ages of Atlantic and other species of monkfish (Figure 3.1), including sagittal otoliths (Woodroffe et al. 2003; Duarte et al. 2005), vertebrae (Armstrong et al. 1992), and illicia—the long modified dorsal spine, which is a key characteristic of Lophiidae (Landa et al. 2013). Recent focus on illicia occurs in European stock assessments (Brophy et al. 2021) and research on Atlantic monkfish (Sutherland and Richards 2021). Optical zonation in illicia and other structures has not yet been related successfully to the season of deposition or age of an individual.

Despite recent directed research, annuli have yet to be validated for Atlantic monkfish hardparts. A previous study attempted to validate annuli using chemical marks on hardparts, applied through bodily injections of field-captured and laboratory fish (Bank et al. 2020). By counting annuli within vertebrae following the chemical mark, and knowing the interval following the injection, they showed that annuli counts were biased low for large monkfish (≥ 50 cm TL) and biased high for small monkfish (≤ 41 cm TL). (Vertebrae were the structure traditionally used for ageing in the Northeast U.S. (Armstrong et al. 1992)). Still, monkfish was difficult to rear resulting in low survival rates and possibly obscured annular zones. In addition, field recapture rates were quite low, resulting in a very low sample size to support inferences. Based on this recent research, previous age-structured stock assessments, which long informed the management of monkfish (Richards et al. 2008) are now viewed as highly uncertain (Richards 2016). Monkfish are now managed very conservatively, awaiting a valid ageing method, development of a growth model, and Biological Reference Points that are informed by age-dependent maturation, growth, and selectivity (NEFMC/MAFMC 2017).

Validation of the yearly rate of annulus formation in monkfish is an essential step to assessing stock status accurately. With monkfish proving to be resistant to traditional means of validation (i.e., tagging, lab rearing, etc.), a novel approach is required to validate monkfish annuli. One promising approach to age validation uses microchemistry with the understanding that the opaque zone in a hardpart is generally associated with a period of high growth rate (summer ring), while the translucent zone is viewed as a zone of reduced growth rate (winter ring) (Campana and Thorrold

2001). Microchemical approaches for age validation compare these features of hardparts (i.e., annuli/ growth-band pairs) to cyclical patterns in microconstituents and stable isotopes along these features. This concept stems from the premise that optical banding patterns (annuli) in hard parts coincide with changes in chemical composition, both of which alias seasonal changes in organic content and temperature. Compositional changes relate to alternating organic-rich (winter) and Ca-rich (spring-summer-fall) zones as has been observed in Atlantic sturgeon (*Acipenser oxyrinchus*) fin spines (Stevenson and Secor 1999). Microconstituents in hardparts can serve as a proxy for expected oscillations in temperature, particularly otoliths, where cooler temperatures cause higher levels of Sr and Ba to substituted for calcium (Ca) in the lattice structure of the hardpart (Clarke et al. 2011; Miller 2011; Barnes and Gillanders 2013; Reis-Santos et al. 2013). For temperate fishes, such oscillations across hardpart optical zones have been observed for red emperor (Seyama et al. 1991), Atlantic bluefin tuna (Siskey et al. 2016), European hake (Brophy et al. 2019), and white anglerfish hardparts (Brophy et al. 2021). Thus, the variations in microchemical composition across optical zones can validate the seasonal frequency of deposition (annuli). Hardpart microchemistry can show marked seasonality, and in that way can be regarded as a “chemical calendar-clock” with time-keeping properties similar to the traditional optical annuli on hardparts (Limburg et al. 2018).

I hypothesize that the optical annuli within monkfish illicia will comprise oscillating concentrations of candidate elements: Mg, P, Mn, Co, Cu, Zn, Sr, and Ba. As opposed to aragonitic otoliths, illicia are bony tissue composed of hydroxyapatite.

As divalent ions, all candidate elements can substitute for Ca and phosphorous is a major constituent as phosphate. Fish scales, also hydroxyapatite, show positive associations of Mg, Sr, Cd, and Ba concentrations with environmental exposure (Wells et al. 2000b, 2003). Fish scale Mn levels are substantially elevated in comparison to otoliths from the same individual (Wells et al. 2000a).

Because there is no established methodology to assign annuli in monkfish illicia, I developed one from chemical annuli within 2-dimensional (2-D) maps of Atlantic monkfish illicia, which was predicted to show characteristic radius dimensions that can guide improved optical annulus identification. For candidate elements, I conversely expected that dominant periods in profile amplitudes will show characteristic radius dimensions. I then tested whether dominant periods in profile amplitudes aligned with optical annulus assignments for candidate elements. With the use of a sub-sample of expected-age illicia, I hypothesized that chemical annuli will equal the expected age. I then examined size at estimated age for improved optical annulus assignments in comparison with a published relationship (Sutherland and Richards 2021) of size at known age. The objectives of this chapter are,

1. Measure concentrations of candidate elements through LA-ICP-MS profile analysis (radial distance from core). Examine profiles for regular oscillating patterns.
2. For a sub-sample, conduct 2-D mapping for candidate elements. Examine the maps for regular oscillating patterns. Assign chemical annuli and measure their annuli. Develop new annuli assignment conventions for each annulus.
3. Conduct Lomb-Scargle periodogram analysis on candidate microconstituent profiles to determine radii of regular cycles using distance from core of illicium.

4. Conduct Lomb-Scargle periodogram analysis on candidate microconstituent profiles using new annuli assignments (see Objective 2) to test the hypothesis that the dominant period = 1.0 optical annular cycle.
5. Conduct a paired t-test between expected and new assignment ages. Compare von Bertalanffy growth models derived from expected and chemical age estimates.

Methods

Hardpart Analysis

Sectioned and embedded Atlantic monkfish illicia were provided by the Northeast Fisheries Science Center (NEFSC) Fish Biology Program Reference Collection (total length range 25 - 46cm) captured during the NEFSC's annual fishery-independent bottom trawl surveys along the Atlantic coast of the United States from Virginia to Georges Bank (Politis et al. 2014) (Figure 3.2). Samples were drawn from the survey to allow comparison of estimated ages derived from chemical annuli to expected ages from an uncommonly strong year-class originating in 2015. The 2015-year class produced length-frequency modes that could be clearly distinguished from other modes during sampling years 2015-2018, corresponding to age-classes 0-3 (Figure 3.3). The results of Sutherland and Richards (2021) provide further details on subsampling the 2015 cohort. Note that for my subsample, there was overlap between presumed age-1 (2016 sample) and age-2 (2017 sample). Most samples (N=57) were associated with the 2015 year-class. Other samples included larger individuals outside of the 2015 cohort (n=12). The illicia were selected because they are used increasingly in European Union assessments (Brophy et al. 2021) and because initial microchemical analyses on otoliths and vertebrae did not show expected chemical profile oscillations.

At the NEFSC Population Biology Branch, illicia were sectioned 0.5 cm above the basal bulb at a thickness of 0.31 to 0.58 mm (Duarte et al. 1997). Sections were mounted in polystyrene resin with black pigment. Illicia were photographed under reflected and transmitted light at 100x magnification using a camera-microscope system and Infinity Analyze and Capture (Teledyne Lumenera software). At the Chesapeake Biological Laboratory, the illicia sections were attached to glass slides using Crystalbond 509 mounting adhesive (SPI Supplies, West Chester, Pennsylvania). Sections were polished with a Buehler microcloth on a lapping wheel to increase the visibility of annuli in preparation for microchemical analysis and annuli interpretations.

Microchemical profiles (n=57) and 2D maps (n=14) of Atlantic monkfish illicia were conducted by LA-ICP-MS at the University of Texas at Austin Department of Geosciences. Instrumentation was an ESI NWR193 excimer laser ablation system (193 nm, 4 ns pulse width) coupled to an Agilent 7500ce ICP-MS. The LA-ICP-MS system is equipped with a large format, two-volume, sample cell with fast washout (<1 s) that accommodated all samples and standards (USGS MACS-3, NIST-612) in three laser cell loadings. The system was optimized daily for sensitivity across the AMU mass range and low oxide production (ThO/Th: 0.58 ± 0.06) by tuning on a standard (NIST 612), and these parameters were checked from trial transects on representative specimens. Following pre-ablation (75 μ m spot, 50 μ m/s scan rate, 3.3 J cm⁻² fluence) to remove shallow surface contaminants, core-to-rim profiles were performed on each specimen, using a 25 μ m diameter spot, a 5 μ m s⁻¹ scan rate, 2.92 ± 0.15 J cm⁻² energy density (fluence), 15Hz repetition rate, and

carrier gas flows (L min^{-1}) of 0.8 for Ar and 0.80-0.85 for He. The quadrupole time-resolved method measured 12 masses with integration times of 10ms (^{24}Mg , $^{43-44}\text{Ca}$, ^{88}Sr), 20ms (^{25}Mg , ^{31}P , ^{55}Mn), and 25ms (^{59}Co , ^{63}Cu , ^{66}Zn , $^{137-138}\text{Ba}$). The quadrupole duty cycle of 0.3732s corresponds to 94% measurement time, with a corresponding linear sampling rate of $1.867 \mu\text{m}$, equivalent to 13.4 measurements within the footprint of either aperture. Measured intensities were converted to elemental concentrations (ppm) using iolite software (Paton et al. 2011), with ^{43}Ca as the internal standard and a Ca index value of 39.89 wt% for unknowns. For the illicia, MAPS-4 was used as the primary calibration standard. USGS MACS-3, NIST 612, and ECRM-752-NP (nano-particulate pressed limestone powder pellet made from BCS-CRM 393 Limestone: www.basrid.co.uk) were used as external reference standards. Over the four days, the grand average of secondary standard (n=42) recovery fractions for all elements was typically within 10% of GeoREM preferred values (<http://georem.mpch-mainz.gwdg.de>). Typical concentrations over specimen transects were $10-10^3$ times higher than the limits of detection for most elements (Table 3.1).

The derived elemental time-series (profiles) were smoothed by consecutive moving median and average filters using a 7-point boxcar width (13 and $26 \mu\text{m}$ equivalent distances), resulting in smooth, locally weighted, signals that excluded low-frequency outliers. Signals were converted to distance (μm) from the core based on the scan rate and duty cycle. Because signals for elements measured with multiple isotopes were identical, we use the higher abundance isotope (e.g., ^{24}Mg , ^{138}Ba) for plotting and statistical analysis.

For 2-D microconstituent maps, scanned areas involved contiguous line traverses using a 5 μm round (illicia) aperture spaced by diameter. The scan rate (105, 62, 31 $\mu\text{m s}^{-1}$) was set to provide one quadrupole measurement cycle per aperture footprint. The quadrupole method used for mapping surveyed 9 elements (10 ms: ^{43}Ca , ^{88}Sr ; 20ms: ^{55}Mn , ^{138}Ba ; 25ms: ^{24}Mg , ^{65}Cu , ^{66}Zn) with a significantly shorter duty cycle of 0.1612 s with 90% measurement time. Calibration and secondary standards were as described above. External reference standard recoveries were typically within 10% of certified reference values. Image conversions were performed using iolite4 software (Paton et al. 2011).

Time Series Analysis

To determine if the chemical cycles from the microconstituent profiles were associated with any of the optical annuli, LA-ICP-MS data was aligned with micrographs of illicia sections through image analysis. All line transects were taken from the core of the illicia to the edge of the hardpart. Using Infinity Analyze and Capture (Teledyne Lumenera software), the 2-D Mn elemental maps (n=14) were measured to determine the radii of chemical annuli (Figure 3.4F) and compared to radial dimensions among annuli to determine the average mean radii for each annulus (Figure 3.5). Then, the trenches created by the LA-ICP-MS's ablated area on the surface of the illicia were measured and annuli were assigned using the annuli assignment guide from the chemical annuli (see Results).

The elemental profiles of detrended (differenced regression model) and standardized (Z-score) time series for each individual illicium and element were subjected to Lomb-Scargle periodogram analysis, a flexible approach that accounts

for the un-equally spaced measures across annuli (Lomb 1976; Scargle 1982; Ruf 1999). Normalized power was used to evaluate significant period frequencies.

Expected Ages vs Chemical Assignments

The chemical annuli assignments guided by the LA-ICP-MS were compared to the expected ages for the 2015 year-class samples (based on length-mode thresholds: see Sutherland and Richards 2021) using a paired t-test under the hypothesis that the difference between assignment types would be zero. von Bertalanffy growth models were then compared between models fitted with chemical versus expected ages (Hilborn and Walters 1992). Average percent error was used to determine the precision of the new ageing method (Beamish and Fournier 1981).

Results

LA-ICP-MS Analysis

Elements Mg, P, Mn, Co, Cu, Zn, Sr, and Ba were all measured at detectable ranges by LA-IC-PMS (Table 3.1). Only Cu occurred below the signal:noise threshold of 3.0 (S:N=0.3). Concentration amplitudes were within the range expected for marine teleost hardparts: <ppm for transition metals Mn, Co, Cu, and Zn; ppm levels for Mg, P, and Ba; and ppt levels for Sr (Campana 1999; Arslan and Secor 2008; Hüseyin et al. 2020).

Element Mn exhibited the sharpest contrast across chemical annuli among measured elements, as revealed by two-dimensional elemental maps of illicia cross-sections (Figure 3.4). Of the seven elements analyzed, Mn, Ba, Sr, and Zn exhibited varying degrees of annular zonation. Manganese exhibited strong zonation across the entire illicium. Strontium also showed higher, although more complex patterns of contrast across annuli. In the 2-D pseudo-colored maps, Ba and Zn showed low levels

of contrast among annuli. Copper and Mg exhibited uniform concentrations in both illicia sections with no apparent zonation. Calcium was homogeneous as expected.

Radial distances associated with chemical zonation patterns in 2-D maps for Mn provided a “road map” for assigning new chemical ages. The average annular width for the n=14 2-D maps was 84.7 μm with annular increments showing a declining trend toward the edge of 104.9, 86.7, 78.8, and 68.5 μm for annulus 1, 2, 3, and 4 respectively (Figure 3.5). In combination with radial distance, this provided a reference to dimensions where annuli were likely deposited in illicia, which were used to guide the new age assignments used for the n= 57 illicia (Figure 3.6). These new ages tended to be less than the traditional age assignments for illicia (Figure 3.6). Further, annular widths were biased low for new age assignments, particularly for the annuli 2 and 3 (Figure 3.5).

Despite notable zonation in the 2-D maps (Figure 3.4), oscillating patterns in standardized elemental profiles, when indexed to radial illicia distance, were not obviously aligned across individuals (Figure 3.7). Profiles for Cu and Co had especially noisy profiles, which corresponds to the lack of patterning in the 2-D elemental maps. However, when profiles were aligned using new chemical annuli assignments (Figure 3.8), Mn displayed notable patterning corresponding with the hypothesized yearly cycle. Other elements did not exhibit expected oscillations.

Lomb-Scargle Periodogram Analysis

Periodogram analysis of elemental profiles using radial distance revealed significant periodicity in the microchemical transects at ~50 to 80 μm (Figure 3.9). The first major peak above the significance line is the primary peak of interest;

subsequent signals detected greater than $\sim 100 \mu\text{m}$ do not correspond to the true periodicity but represent a “reflection” of the first detected periodicity (VanderPlas 2018). Elements Ba, Mn, P, and most notably Sr showed significant periodicity with radial distance. Periodogram analysis of elemental profiles using new chemical annuli assignments revealed significant annular periodicity at or near the hypothesized 1.0 year per cycle rate for Ba, Mn, and Sr (Figure 3.10). Elements Co, Cu, and P displayed periodicity outside the hypothesized rate (Figures 3.10).

Expected Ages vs Chemical Assignments

Chemical ages significantly departed from expected ages by a mean of -0.21 ± 0.12 (paired t-test; H_0 : difference=0, $n=57$, $p<0.001$). Substantial overlap occurred between expected and new chemical ages (Figure 3.11), with an average percent error of 18.4%. The agreement between expected and chemical ages was 80.7%. Age-modes for age-classes 1 and 2 were the same between expected and chemical ages. In keeping with the positive bias in age estimation, a fitted von Bertalanffy growth model to chemical ages indicated lower growth than a model fitted to expected ages (Figure 3.12).

Discussion

My investigation confirmed the hypothesis that optical annuli within monkfish illicia were comprised of oscillating concentrations in the candidate elements Mn, Sr, and Ba. Prominent chemical annuli were revealed for these elements within the LA-ICP-MS 2-D maps, especially for Mn. Analysis via LA-ICP-MS trace element profiles in comparison to the 2-D maps revealed characteristic radii of the chemical

annuli, which were used to guide optical annuli assignments independent of LA-ICP-MS analysis. Chemically guided annulus assignments (new age assignments) were supported through the periodogram analysis not only for Mn (as expected) but also for Sr and Ba oscillations, which were not used to establish age determination criteria.

Despite confirmation of annular chemical periodicity of the new ages, significant departure occurred between these and the expected ages of the 2015 year-class sample. Chemically guided ages tended to overestimate ages with an average percent error of 18.4% which is reflected in the paired t-test. Still, deviations in all but one instance were 1 year, which will yield a high error rate for this sample of mostly 1 and 2 expected annuli. Sutherland and Richards (2021) optical annuli counts were also biased high in comparison to expected ages, but with much less agreement. Half (50%; also average percent agreement) of assigned annuli were 1 or 2 years higher than expected ages. Estimated ages by NEFSC procedures may have been biased high owing to checks associated with multiple spawning, migration, and habitat shifts (Sutherland and Richards 2021), which may not have been manifest by the elemental cycles observed here.

Annular widths measured here and by Sutherland and Richards (2021) support isometric growth of illicia and declining annular widths with fish length. Illicia radii at each chemical annulus were fairly discrete (Figure 3.5) supporting guiding criteria in annulus assignments. Still, for some unknown reason annular measures of the new age sample were lower than those derived from the 2-D maps, particularly at annuli 2 and 3. This deviation would be consistent with higher estimated ages in comparison to the expected age sample.

That both my study and Sutherland and Richards (2021) over-estimated expected age directs attention to possible errors in the expected age data set. In my study, there was large size overlap between expected ages 1 and 2 (2016 and 2017 samples; Figure 3.3.). Outliers in the comparison plot (Figure 3.11) for expected age 1 (N=8) were biased high in length (TL= 33-36 cm). Additionally, in both studies, expected ages were not corrected for ageing conventions associated with season of capture. Marginal increment analysis (Sutherland and Richards 2021) showed that the opaque zone formed during spring months with substantial variation. Thus, 2015 year-class fish collected during spring months may or may not exhibit an opaque zone. Although season and year of collection likely contributed to some error in the expected ages for the 2015 year-class cohort, a bias towards lower ages, consistent with my results, remains to be determined.

As with most ageing methods, these new assignments are subject to a combination of process and interpretation errors (Campana 2001), which would convey to assessment parameters. My reported error (18%) is greater than the conventional average percent error of 5%, albeit this error rate is amplified at younger ages (Beamish and Fournier 1981; Campana 2001). The von Bertalanffy growth plot exemplified the relevance of error associated with chemical age assignments yielding a much higher $L_{\infty} = 112.0$ and lower $K = 0.09$ vs. $L_{\infty} = 70.9$ and $K = 0.35$ in comparison to expected age assignments. In reference to L_{∞} , Atlantic monkfish can reach a max size of 138 cm (Richards et al. 2008).

Confirmation of chemical annuli via 2-D elemental map analysis was integral to defining the new age assignments. These maps, especially for Mn, revealed

complete annuli, rather than structural interruptions and checks, which might otherwise contribute error to age assignments. Past applications of 2-D map analysis have also revealed this to be a promising approach to revealing chemical banding patterns (Limburg and Elfman 2017; Hüseyin et al. 2020). These past applications used 2-D images to assign annuli subjectively, similar to conventional annulus ageing interpretations. This approach can be cost-prohibitive for even moderate samples and introduces subjective reader error. I used chemical annular widths, informed by 2-D mapping, as a cost-effective to develop new ageing assignments. Additionally, the approach was independently verified using a formal periodogram analysis.

Quantitative chemical profile analyses initially developed by Siskey et al. (2016) for Atlantic bluefin tuna, and then applied by Brophy et al. (2021) for hake and monkfish set the foundation for this work. Still, it was deemed risky meriting initial trials on a model species for which ages had been validated: black sea bass (see Chapter 2). Although the species differed in best candidate structure (otoliths in black sea bass and illicia in Atlantic monkfish) elements (Mg in black sea bass and Mn in Atlantic monkfish), the approaches sequence (2-D mapping, periodogram analysis of profiles, age assignments based on chemical annuli) was similar. Because the applications were similarly successful, the chemical annulus-periodogram approach could lend itself well to the large set of unvalidated assessed species (see Chapter 1, Table 2.1).

Of all the candidate elements, Mn had the clearest observable signals in 2-D maps with profiles of Sr and Ba showing similar signals. Elements Mn, Sr, and Ba are known to substitute for Ca in fish scales (Wells et al. 2000b), and I hypothesized that

these elements in illicia may be influenced by seasonal temperatures. Atlantic monkfish experience seasonal temperature ranges 4-17 °C (data from archival tags; Cadrin et al. 2014), ranging from cold offshore temperatures during late winter and early spring to warmer inshore waters during late spring to early winter, particularly during December when highest experienced temperatures (>15°C) occur. In a single study on juvenile spot scales, Wells et al. (2000a) showed no difference in uptake of Sr, Cd, or Ba between 20°C and 25°C, yet this temperature range is substantially less (5°C) than the seasonal variation experienced by monkfish (>10°C). Additional research on the influence of temperature on metal incorporation in fish bony structures is needed to support chemical ageing in monkfish illicia.

Illicia was used as the primary hard part in this study for multiple reasons. Although otoliths and vertebrae have been the preferred hardparts in other studies (Armstrong et al. 1992; Bank et al. 2020; Brophy et al. 2021), the relative size of illicia and symmetrical growth could support more consistent ageing conventions and improved precision. The illicia's small size relative to these other structures allows for quicker and more cost-effective microchemistry analysis at a higher resolution possible in comparison to the other hard parts. Having a more uniform growth in illicia allows the comparison of similar radii in annuli for our optical assignments (Figure 3.5). Uniform growth of illicia also avoids the problem that occurs in other parts such as otoliths whose irregular growth can prevent not only effective LA-ICP-MS analysis but confound optical age assignments (Figure 3.1A).

Additional studies are needed to develop chemical ageing approaches for monkfish. Future work would benefit from the analysis of larger/older monkfish to

provide more information not only for the growth analysis but also for much needed information on radii of age 4+ annuli for chemical assignments. Future studies should support precision trials and inter-lab collaborations to increase the number of experienced illicia age readers to develop best practices and fine-tune chemical annuli assignment criteria. With improved age estimation techniques, a validated growth model could be incorporated into stock assessments in the future to reduce scientific uncertainty and can lead to better management of monkfish.

Tables and Figures

Table 3.1 Mean elemental concentrations (ppm) in Atlantic monkfish illicia profiles (n=57).

	Mg	P	Mn	Co	Cu	Zn	Sr	Ba
mean	6,953.5	223,463.6	121.5	1.8	4.3	273.2	1,356.5	5.5
stdev	696.9	23,157.8	96.6	10.1	5.9	62.8	106	1.8
S:N*	12,273.4	6,527.2	263.4	30.9	3	245.2	30,513.1	231.4

*S:N, signal to noise ratio, is the mean transect concentration divided by the estimated mean detection limit among the population of analyzed specimens.

Figure 3.1 Atlantic monkfish hardpart comparison. A.) Whole otolith. B.) Sectioned otolith. C.) Baked vertebra. D.) Sectioned illicium.

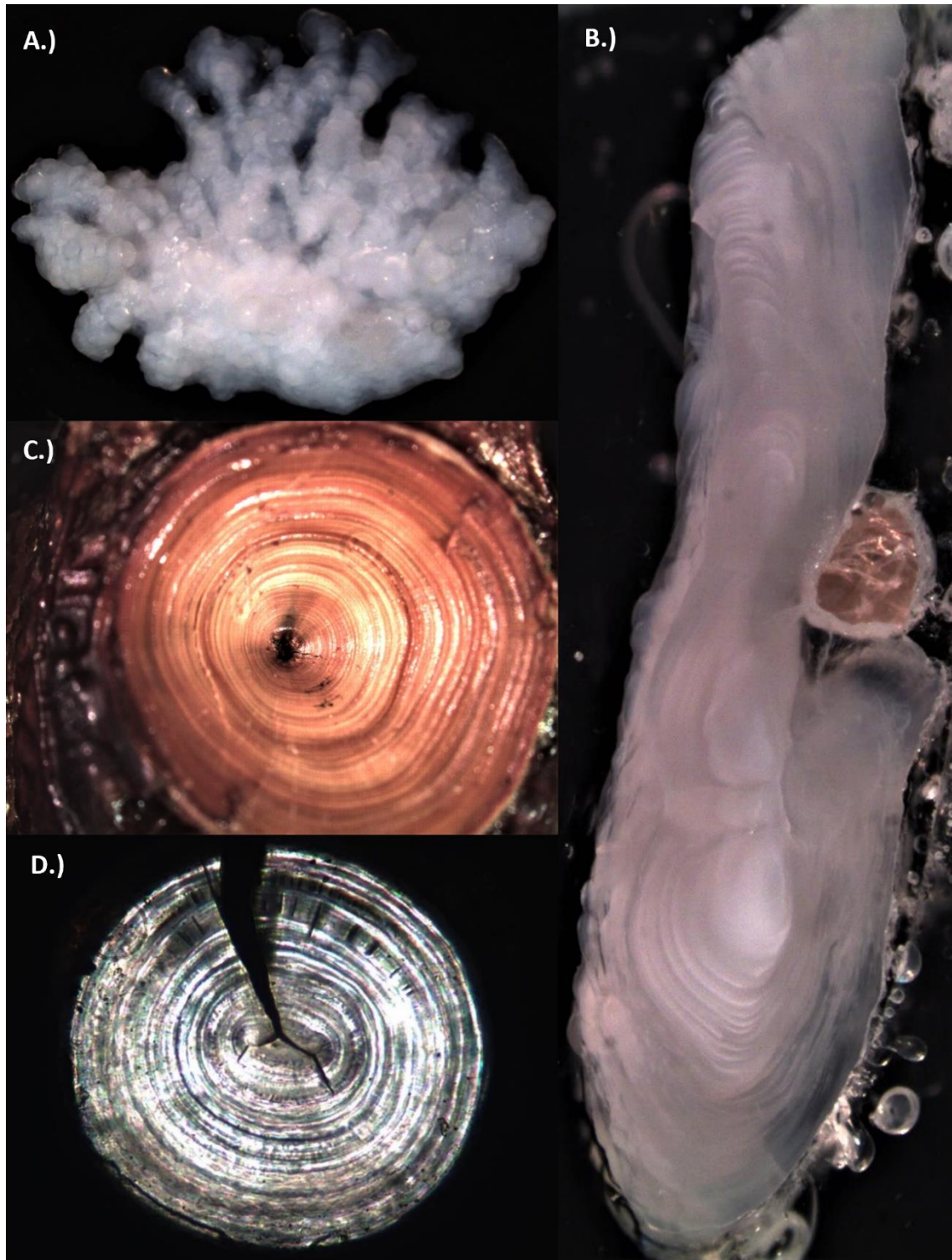
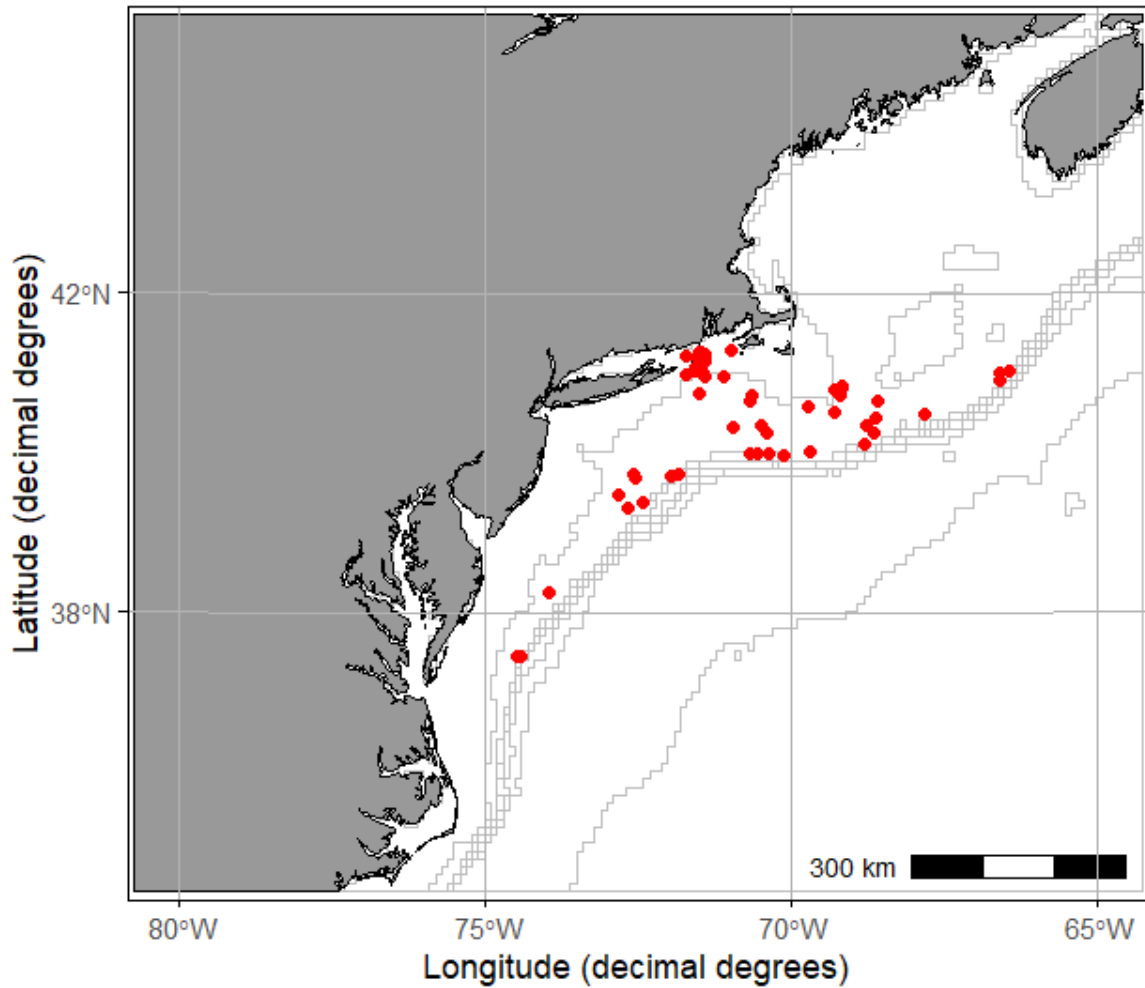


Figure 3.2 Location of Atlantic monkfish samples from which illicia were drawn. Monkfish were captured during bottom trawl surveys conducted by the NOAA Northeast Fisheries Science Center along the Atlantic coast of the United States from



Virginia to Georges Bank between June 2015 and September 2018.

Figure 3.3 Length frequency diagram of monkfish captured for use in this study from the 2015-year class captured between 2016 and 2017 during bottom trawl surveys conducted by the NOAA Northeast Fisheries Science Center. Fitted lines indicates a spline fit to the average distribution of monkfish total length.

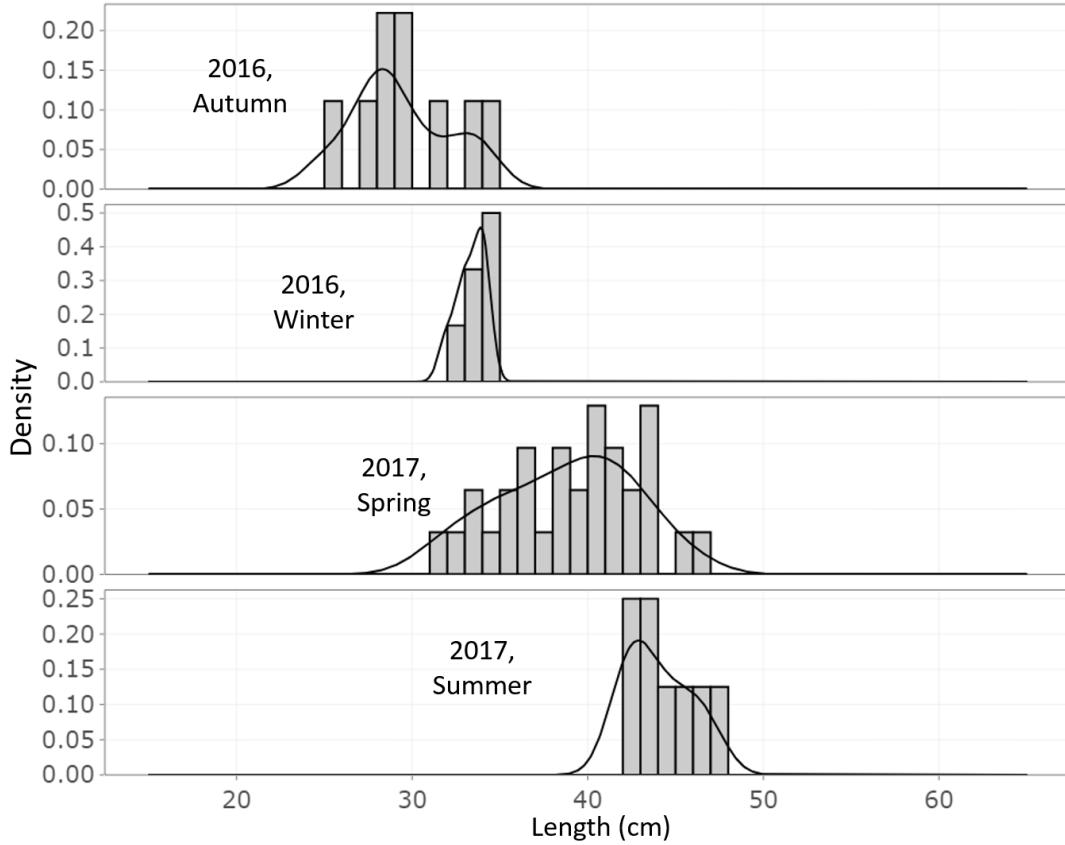
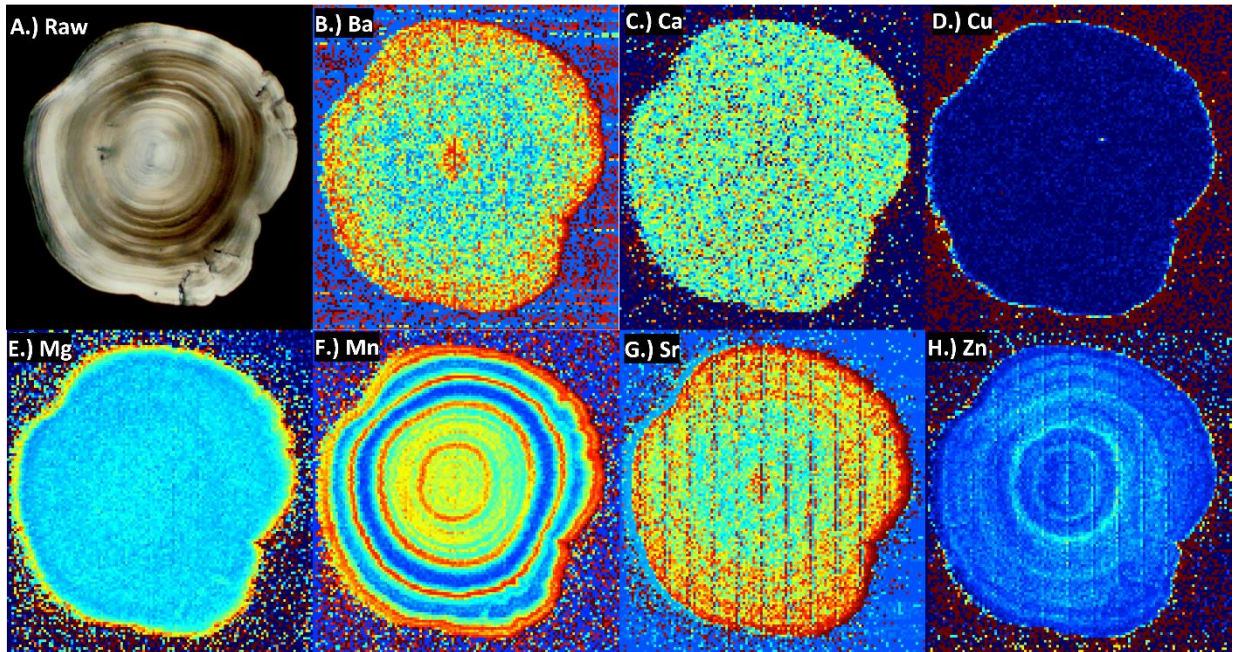


Figure 3.4 A.) Light micrograph (Raw) image and B-H.) 2-D elemental maps for two Atlantic monkfish illicia cross sections (top two panels and lower two panels). Hues indicate element concentration, scales from blue (low) to red (high). Note the contrast in the pseudo color, which is optimized for each map and is not common across elements.

Sample D05: TL 84.5 cm, Female



Sample D04: TL 56 cm, Male

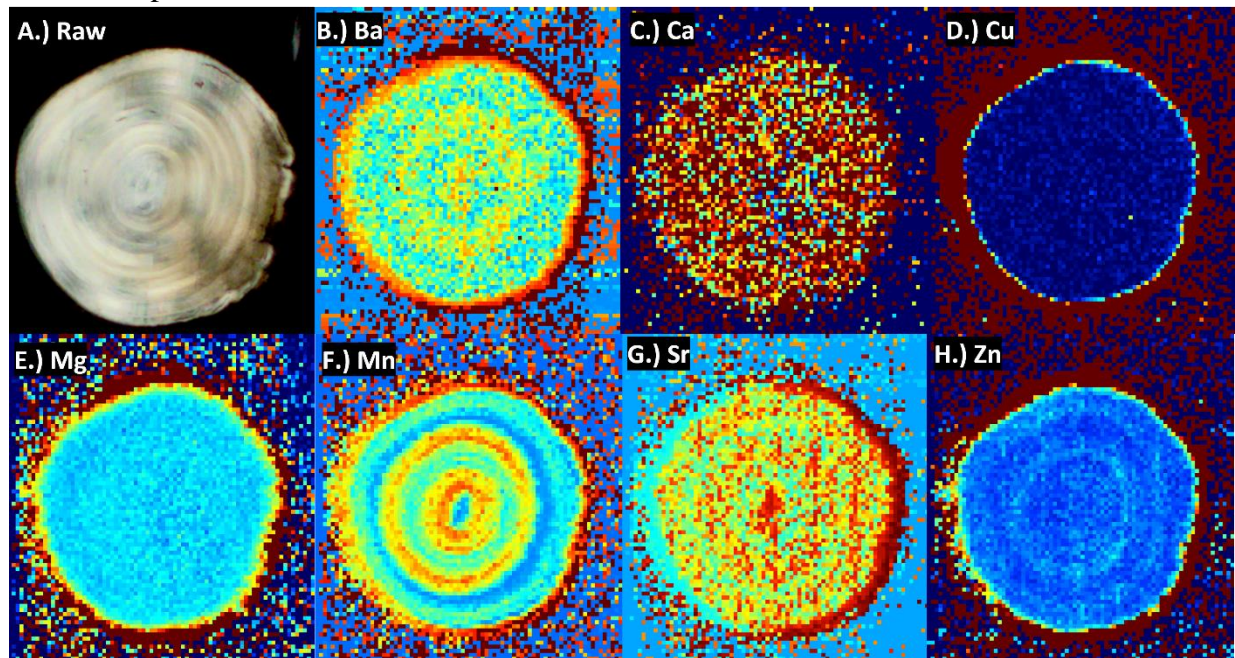


Figure 3.5 Annulus widths and distances from the core for Atlantic monkfish illicia comparing the 2-D assignments (n=14) to the new assignment conventions (those based upon chemical annuli, n=57).

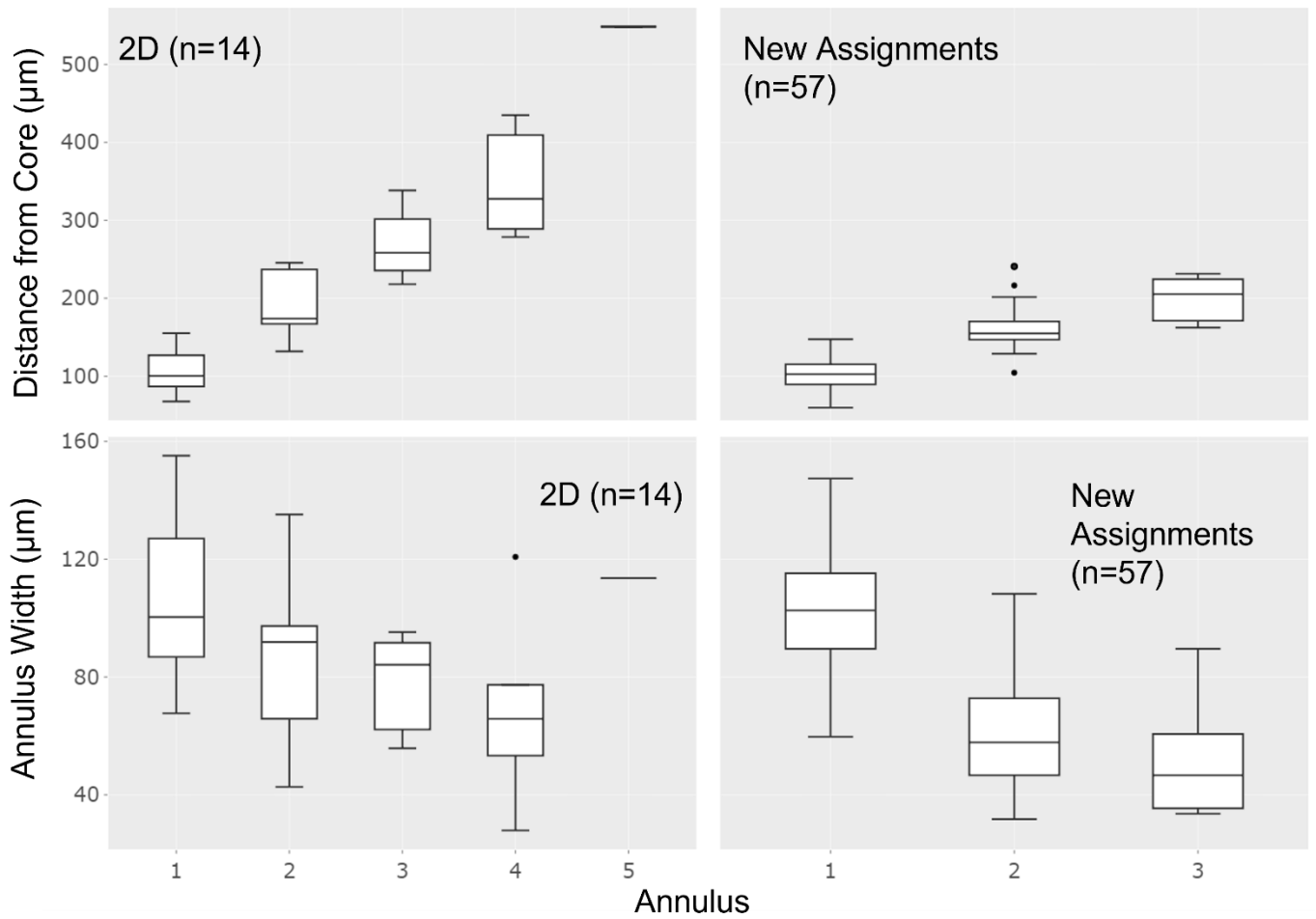


Figure 3.6 (A) Current NEFSC expert assignment of Atlantic monkfish illicium annuli (see Sutherland and Richards 2021), (B) assignment of chemical annuli, and (C) assignment of annuli using chemical conventions. Note the contrast in the pseudo color, which is optimized for each map and is not common across elements. Annuli annotations are depicted in circles.

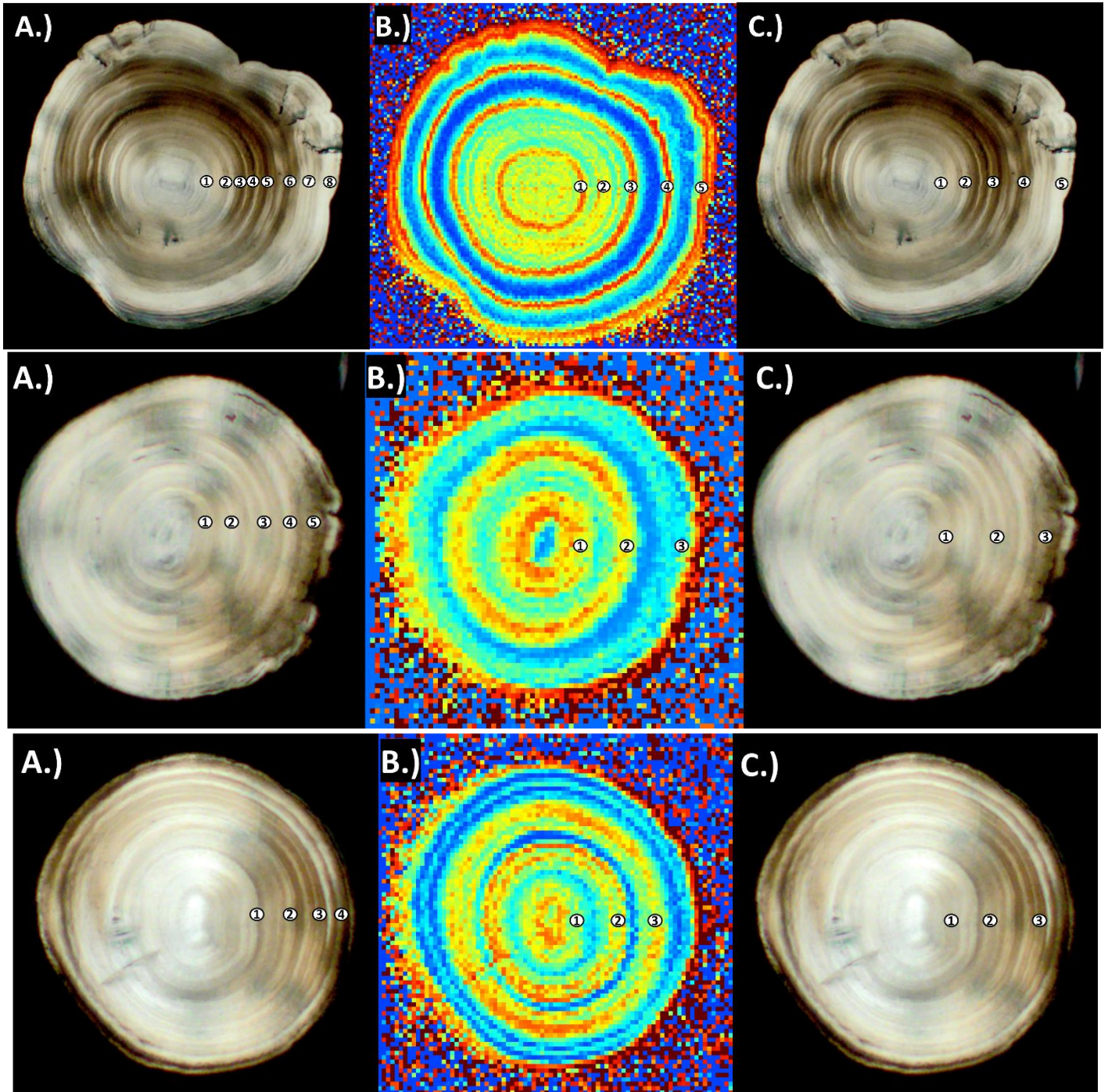


Figure 3.7 Standardized Atlantic monkfish illicia profiles (n=57) across microconstituents and organized by distance on illicia. Colors represent each individual.

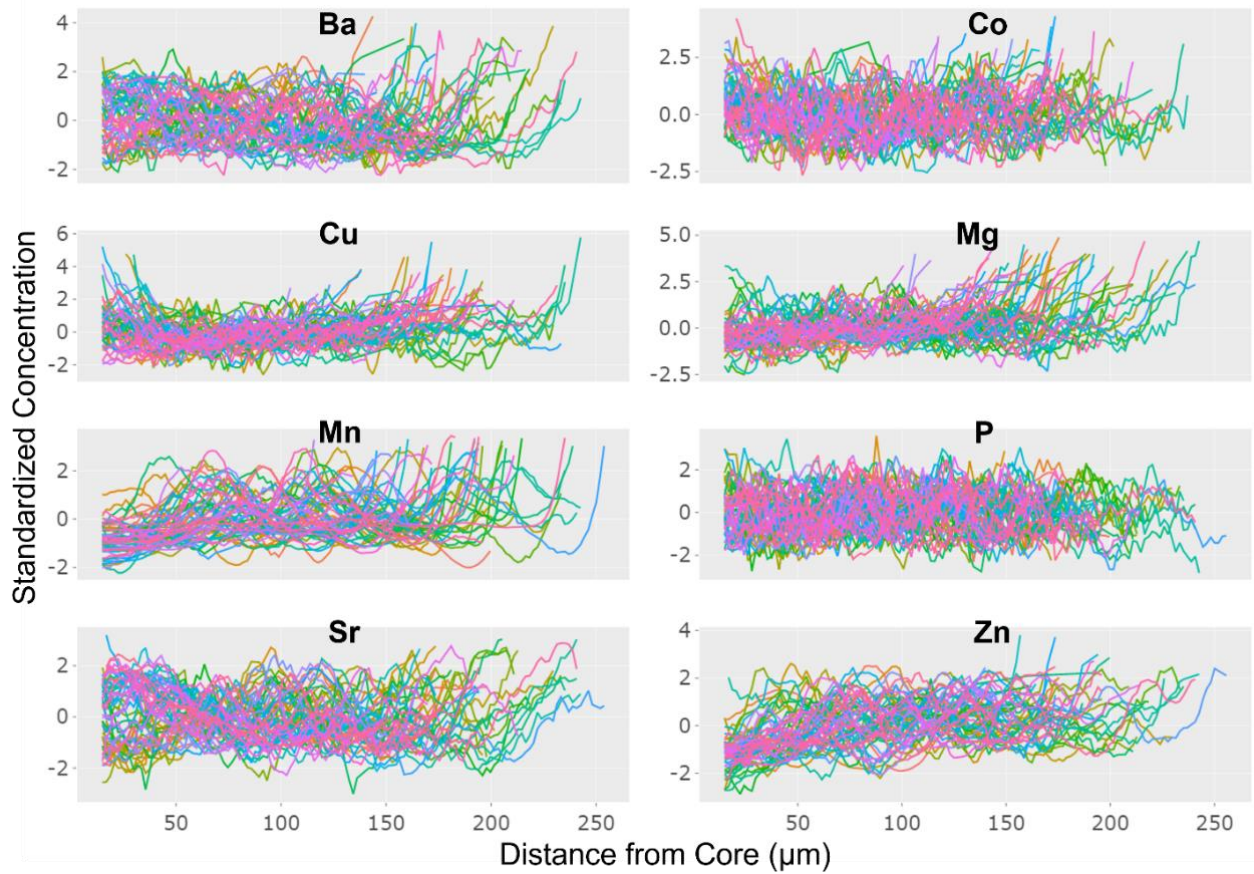


Figure 3.8 Standardized Atlantic monkfish illicia profiles (n=57) across microconstituents using chemical annulus assignments. Colors represent each individual.

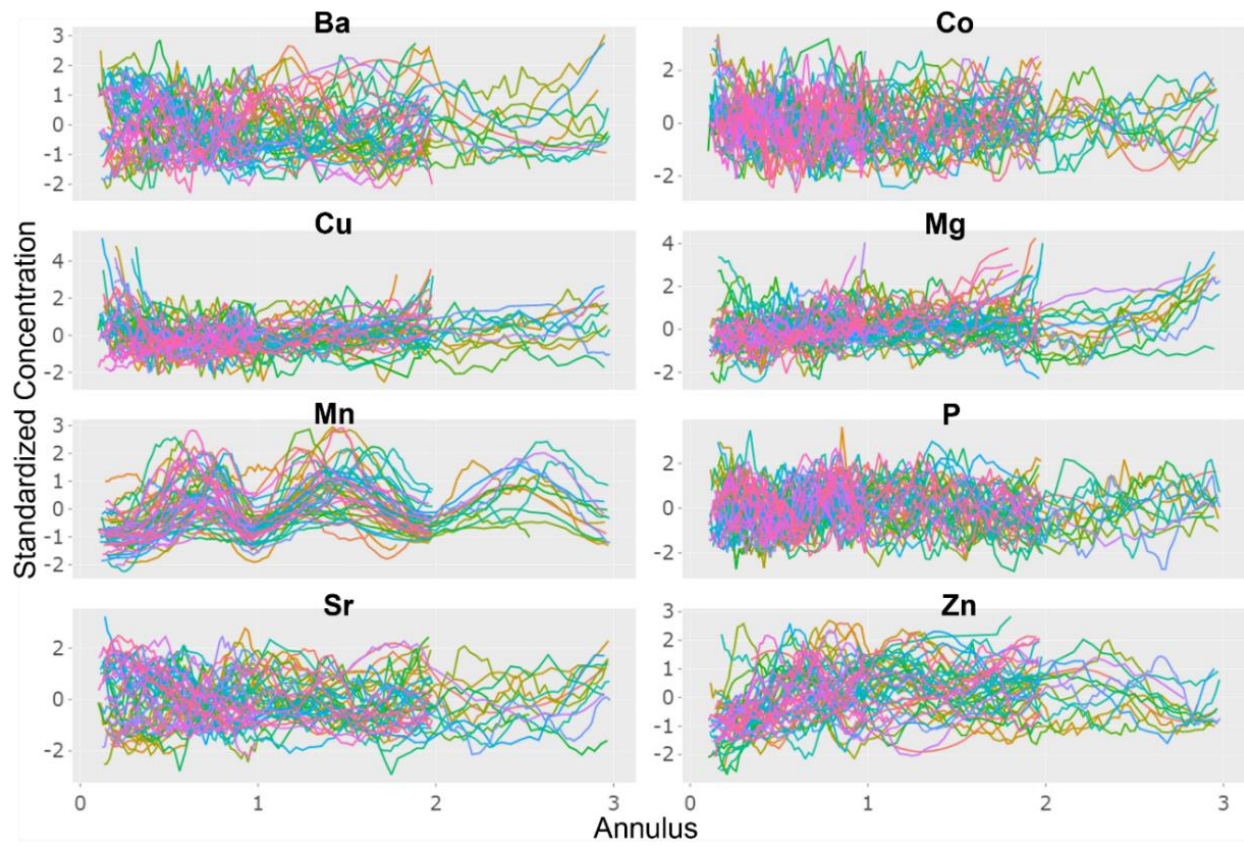


Figure 3.9 Lomb-Scargle periodograms for Atlantic monkfish elemental profiles (N=57) using distance from illicia core. Significance is shown by the horizontal dashed line. Note the difference in the response amplitude between each element.

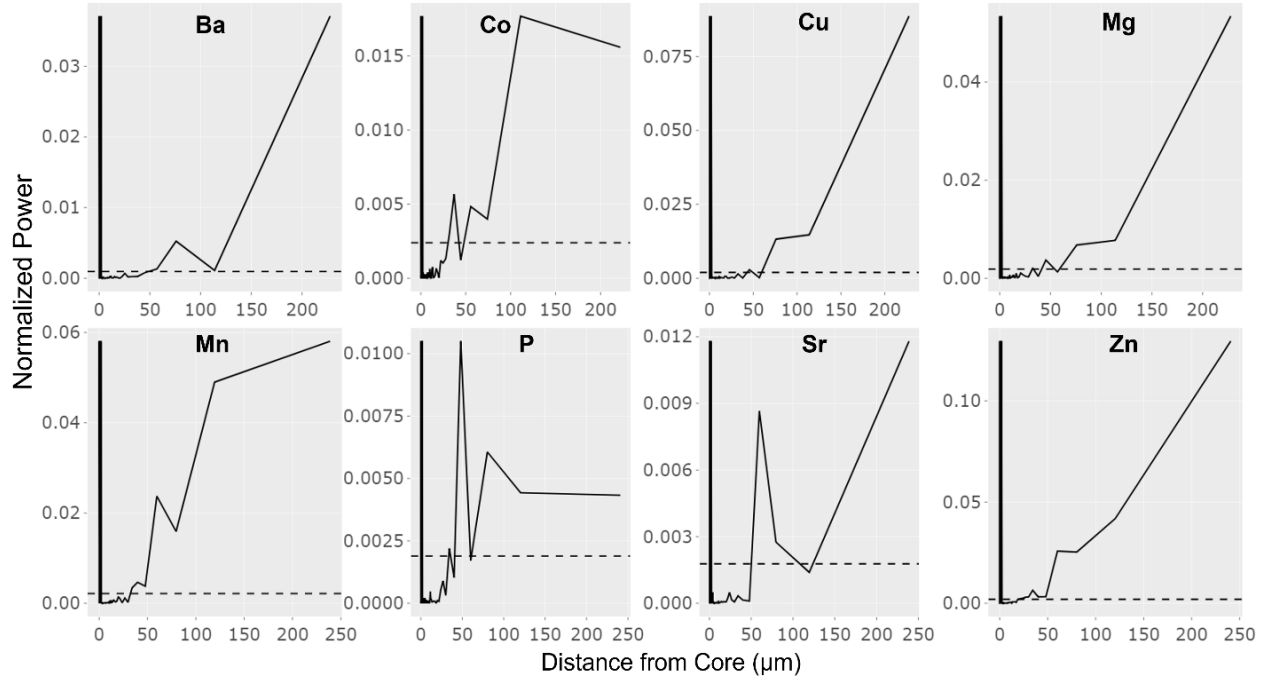


Figure 3.10 Lomb-Scargle periodograms for Atlantic monkfish elemental profiles (N=57) using new chemical annuli conventions. Significance is shown by the horizontal dashed line. The vertical dashed line is hypothesized period frequency=1.0. Note the difference in response amplitude between each element.

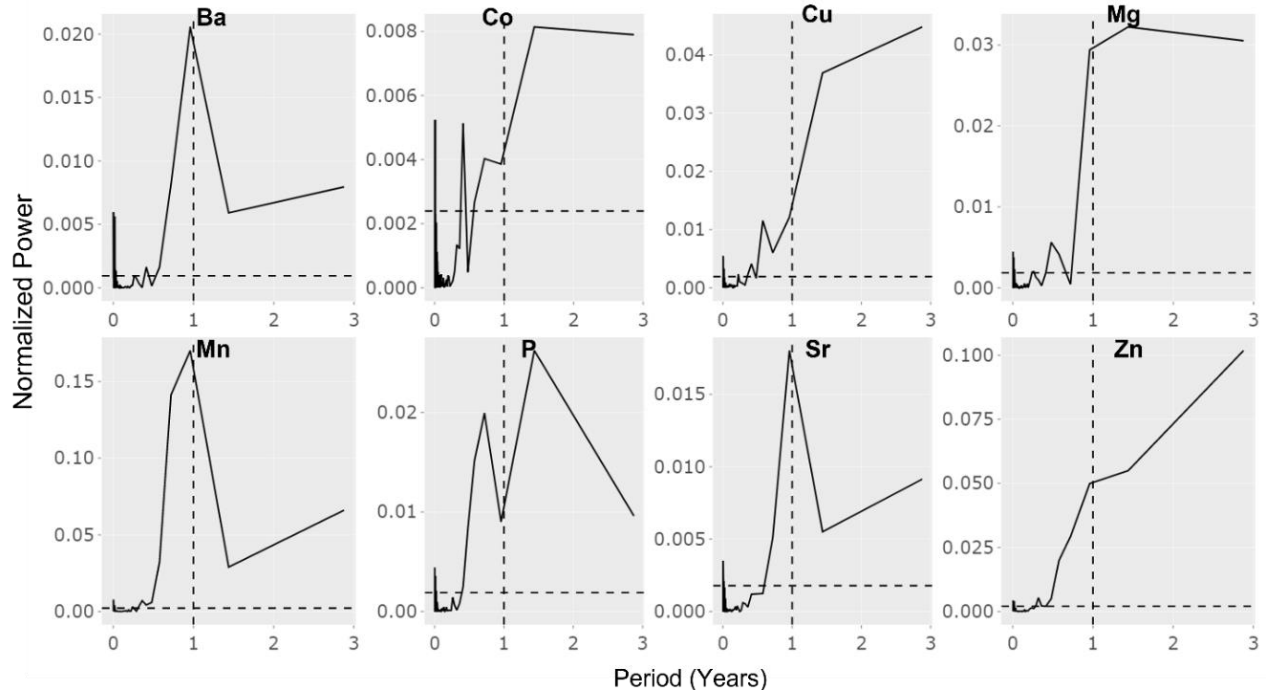


Figure 3.11 Age assignment comparison of expected ages vs chemical age assignments for Atlantic monkfish, evaluated with a paired t-test (see Results).

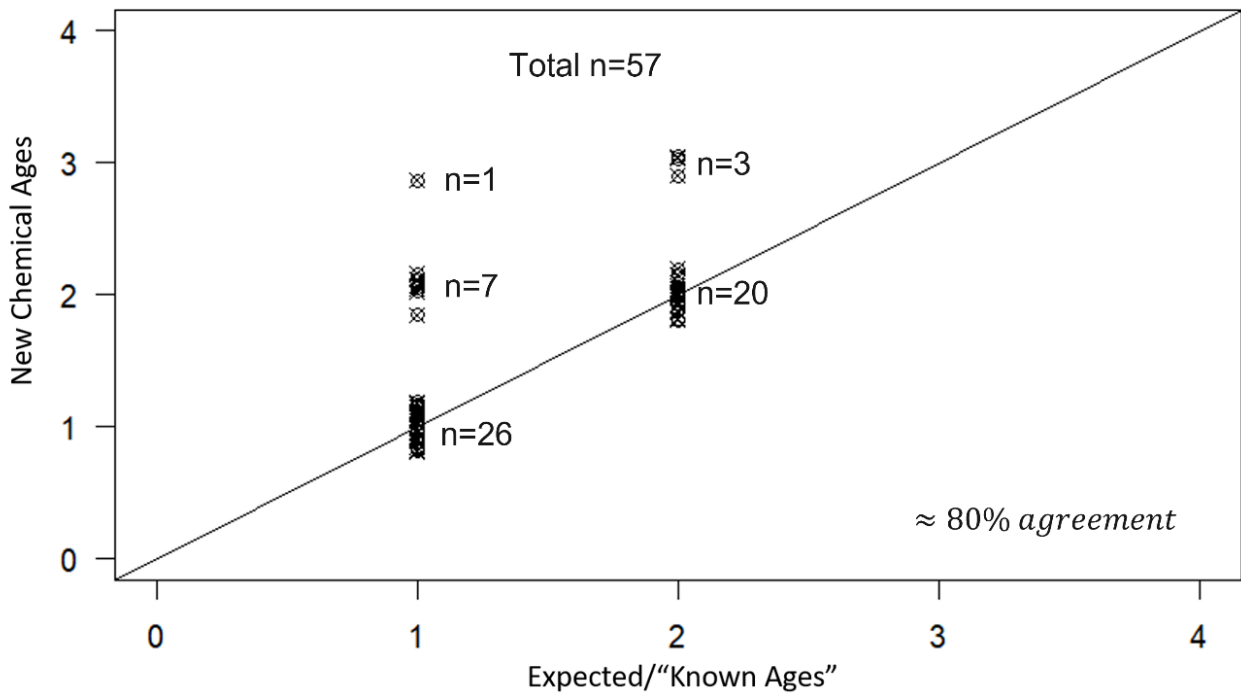
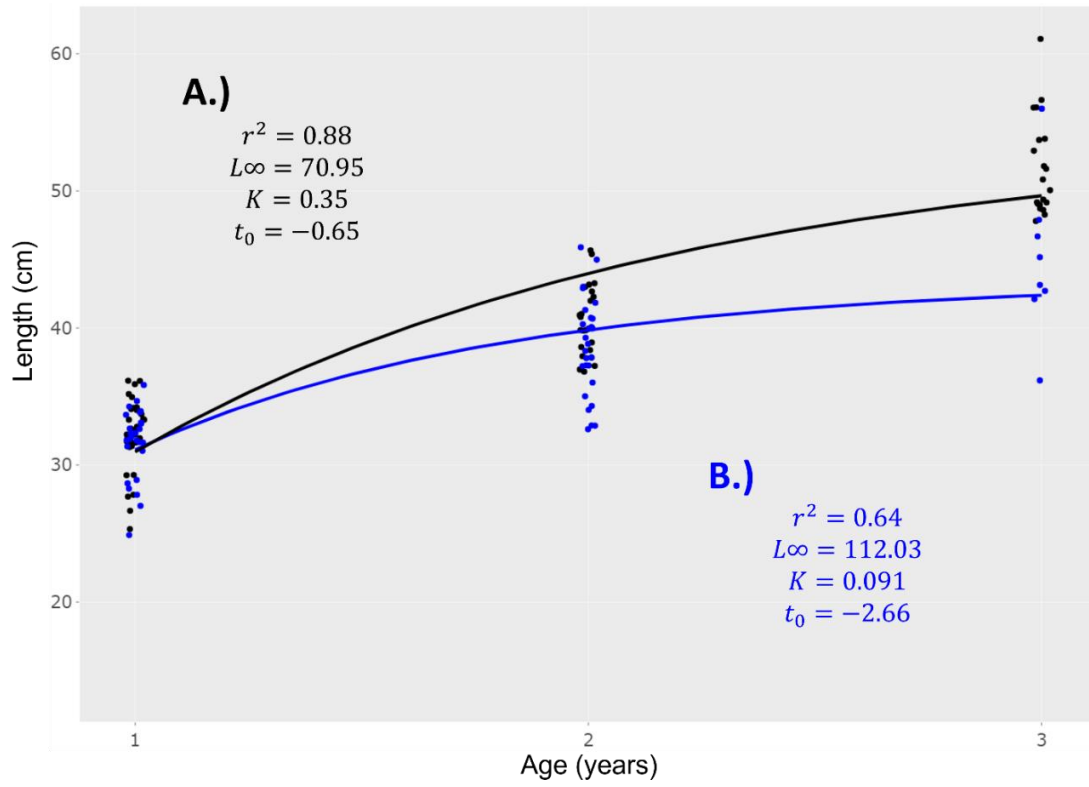


Figure 3.12 von Bertalanffy growth model fits for Atlantic monkfish A.) expected ages vs B.) new chemical ages (blue). Points jittered for clarity.



References

- Armstrong, M., J. Musick, and J. Colvocoresses. 1992. Age, growth, and reproduction of the goosefish *Lophius americanus* (Pisces, Lophiiformes). *Fishery Bulletin* 90(2):217–230.
- Arslan, Z., and D. H. Secor. 2008. High resolution micromill sampling for analysis of fish otoliths by ICP-MS: effects of sampling and specimen preparation on trace element fingerprints. *Marine environmental research* 66(3):364–371.
- Bank, C. M., K. Oliveira, S. J. Sutherland, M. P. Armstrong, J. Landa, and S. X. Cadrin. 2020. Age validation for goosefish (*Lophius americanus*) in the northeastern United States. *Fishery Bulletin* 118(1):8–20.
- Barnes, T. C., and B. M. Gillanders. 2013. Combined effects of extrinsic and intrinsic factors on otolith chemistry: implications for environmental reconstructions. *Canadian Journal of Fisheries and Aquatic Sciences* 70(8):1159–1166.
- Beamish, R. J., and D. A. Fournier. 1981. A method for comparing the precision of a set of age determinations. *Canadian Journal of Fisheries and Aquatic Sciences* 38(8):982–983.
- Brophy, D., D. P. De Pontual, K. Mahe, and C.-M. Villanueva. 2019. Validating age-determination of anglerfish and hake. Report (Scientific report), IRELAND.
- Brophy, D., S. Pérez-Mayol, R. Duncan, K. Hüsey, A. J. Geffen, H. D. Gerritsen, M. C. Villanueva, and B. Morales-Nin. 2021. Elemental composition of illicia and otoliths and their potential application to age validation in white anglerfish (*Lophius piscatorius* linnaeus, 1758). *Estuarine, Coastal and Shelf Science* 261:107557.
- Cadrin, S. X., C. Bank, J. H. Grabowski, and G. Sherwood. 2014. Archival tagging and age validation in the mid-Atlantic. *Northeast Fisheries Science Center*:51.
- Campana, S. E. 1999. Chemistry and composition of fish otoliths: pathways, mechanisms and applications. *Marine Ecology Progress Series* 188:263–297.
- Campana, S. E. 2001. Accuracy, precision and quality control in age determination, including a review of the use and abuse of age validation methods. *Journal of Fish Biology* 59(2):197–242.
- Campana, S. E., and S. R. Thorrold. 2001. Otoliths, increments, and elements: keys to a comprehensive understanding of fish populations? *Canadian Journal of Fisheries and Aquatic Sciences* 58(1):30–38.
- Clarke, L. M., S. R. Thorrold, and D. O. Conover. 2011. Population differences in otolith chemistry have a genetic basis in *Menidia menidia*. *Canadian Journal of Fisheries and Aquatic Sciences* 68(1):105–114.
- Duarte, R., M. Azevedo, and P. Pereda. 1997. Study of the growth of southern black and white monkfish stocks. *ICES Journal of Marine Science* 54(5):866–874.
- Duarte, R., J. Landa, C. Morgado, A. Marçal, S. Warne, E. Barcala, E. Bilbao, J. Dimeet, H. Djurhuus, and E. Jónsson. 2005. Report of the anglerfish Illicia/Otoliths ageing Workshop. IPIMAR, Lisbon.

- Hilborn, R., and C. J. Walters. 1992. Quantitative fisheries stock assessment: choice, dynamics and uncertainty. Springer Science & Business Media.
- Hüssy, K., K. E. Limburg, H. de Pontual, O. R. B. Thomas, P. K. Cook, Y. Heimbrand, M. Blass, and A. M. Sturrock. 2020. Trace element patterns in otoliths: the role of biomineralization. *Reviews in Fisheries Science & Aquaculture*:1–33.
- Landa, J., J. Barrado, and F. Velasco. 2013. Age and growth of anglerfish (*Lophius piscatorius*) on the Porcupine Bank (west of Ireland) based on illicia age estimation. *Fisheries Research* 137:30–40.
- Limburg, K. E., and M. Elfman. 2017. Insights from two-dimensional mapping of otolith chemistry. Pages 480–491 *Journal of Fish Biology*. Wiley Online Library.
- Limburg, K. E., M. J. Wuenschel, K. Hüssy, Y. Heimbrand, and M. Samson. 2018. Making the otolith magnesium chemical calendar-clock tick: plausible mechanism and empirical evidence. *Reviews in Fisheries Science & Aquaculture* 26(4):479–493.
- Lomb, N. R. 1976. Least-squares frequency analysis of unequally spaced data. *Astrophysics and Space Science* 39(2):447–462.
- Miller, J. A. 2011. Effects of water temperature and barium concentration on otolith composition along a salinity gradient: Implications for migratory reconstructions. *Journal of Experimental Marine Biology and Ecology* 405(1):42–52.
- NEFMC/MAFMC, (New England Fishery Management Council and Mid-Atlantic Fishery Management Council). 2017. Monkfish fishery management plan framework adjustment 10 including specifications for fishing years 2017-2019. Pages 1–218.
- NMFS, (National Marine Fisheries Service). 2020. Fisheries of the United States, 2018. <https://foss.nmfs.noaa.gov/apexfoss/f?p=215:8:9399893492877::NO::>
- Paton, C., J. Hellstrom, B. Paul, J. Woodhead, and J. Hergt. 2011. Iolite: Freeware for the visualisation and processing of mass spectrometric data. *Journal of Analytical Atomic Spectrometry* 26(12):2508–2518.
- Politis, P. J., J. K. Galbraith, P. Kostovick, and R. W. Brown. 2014. Northeast Fisheries Science Center bottom trawl survey protocols for the NOAA Ship Henry B. Bigelow.
- Reis-Santos, P., S. E. Tanner, T. S. Elsdon, H. N. Cabral, and B. M. Gillanders. 2013. Effects of temperature, salinity and water composition on otolith elemental incorporation of *Dicentrarchus labrax*. *Journal of Experimental Marine Biology and Ecology* 446:245–252.
- Richards, R. A. 2016. 2016 monkfish operational assessment. U.S. Department of Commerce, National Oceanic and Atmospheric Administration, National Marine Fisheries Service, Northeast Fisheries Science Center, Woods Hole, Mass.
- Richards, R. A., P. C. Nitschke, and K. A. Sosebee. 2008. Population biology of monkfish *Lophius americanus*. *ICES Journal of Marine Science* 65(7):1291–1305.

- Ruf, T. 1999. The lomb-scargle periodogram in biological rhythm research: analysis of incomplete and unequally spaced time-series. *Biological Rhythm Research* 30(2):178–201.
- Scargle, J. D. 1982. Studies in astronomical time series analysis. II - Statistical aspects of spectral analysis of unevenly spaced data. *The Astrophysical Journal* 263:835–853.
- Secor, D. H., and P. M. Piccoli. 1996. Age- and sex-dependent migrations of striped bass in the Hudson River as determined by chemical microanalysis of otoliths. *Estuaries* 19(4):778–793.
- Seyama, H., J. S. Edmonds, M. J. Moran, Y. Shibata, M. Soma, and M. Morita. 1991. Periodicity in fish otolith Sr, Na, and K corresponds with visual banding. *Experientia* 47(11):1193–1196.
- Sherwood, G. 2011. Appendix 2 of monkfish project completion report, otolith microchemistry analysis results for age and growth. Northeast Fisheries Science Center.
- Siskey, M. R., V. Lyubchich, D. Liang, P. M. Piccoli, and D. H. Secor. 2016. Periodicity of strontium: Calcium across annuli further validates otolith-ageing for Atlantic bluefin tuna (*Thunnus thynnus*). *Fisheries Research* 177:13–17.
- Stevenson, J. T., and D. Secor. 1999. Life history characteristics of Hudson River Atlantic sturgeon (*Acipenser oxyrinchus*) and a model for management. *Journal of Applied Ichthyology* 15(4–5):304–304.
- Sutherland, S. J., and R. A. Richards. 2021. Validation of methods for aging goosefish (*Lophius americanus*) based on length-mode progression of a strong cohort. *Fishery Bulletin* 120(1):13–25.
- VanderPlas, J. T. 2018. Understanding the Lomb–scargle periodogram. *The Astrophysical Journal Supplement Series* 236(1):16.
- Wells, B. K., G. E. Bath, S. R. Thorrold, and C. M. Jones. 2000a. Incorporation of strontium, cadmium, and barium in juvenile spot (*Leiostomus xanthurus*) scales reflects water chemistry. *Canadian Journal of Fisheries and Aquatic Sciences* 57(10):2122–2129.
- Wells, B. K., B. E. Rieman, J. L. Clayton, D. L. Horan, and C. M. Jones. 2003. Relationships between water, otolith, and scale chemistries of westslope cutthroat trout from the Coeur d’Alene River, Idaho: the potential application of hard-part chemistry to describe movements in freshwater. *Transactions of the American Fisheries Society* 132(3):409–424.
- Wells, B. K., S. R. Thorrold, and C. M. Jones. 2000b. Geographic variation in trace element composition of juvenile weakfish scales. *Transactions of the American Fisheries Society* 129(4):889–900.
- Woodroffe, D. A., P. J. Wright, and J. D. M. Gordon. 2003. Verification of annual increment formation in the white anglerfish, *Lophius piscatorius* using the illicia and sagitta otoliths. *Fisheries Research* 60(2–3):345–356.

Chapter 4: Broader Impacts

The motivating goal of my thesis was to develop a valid age determination procedure for Atlantic monkfish. Microchemical analysis of Mn in the illicia provides two ways forward: (1) development of ageing procedures for optical annuli; and (2) direct ageing of 2-D images of Mn. For the former objective, a few key steps need to be achieved. Firstly, agers should take advantage of the digital and easily shareable nature of the digitized 2-D Mn maps. Digitized images can permit inter-laboratory collaborations among experts and development of standardized ageing procedures. Costs limited the size of my reader set to 14 2-D maps of Mn (~\$2000 machine time). An expanded reader set of 100 2-D illicia maps (~7-10 illicia per age class) would support chemical annular measurements for an expected 5-6 annuli (e.g., 15-20 radial measurements per annuli). The sample should to the extent possible include larger fish (>75 cm TL). Chemical annuli and their associated radial dimensions should be assigned and measured in a single-blind manner among age determination experts. Precision in assignments and variance in associated radial measures will support standardized age determination procedures for optical annuli. Using these consensus guides, a test set of 100 sectioned illicia would then be subjected to a single-blind test for optical annulus assignments among multiple experienced readers. This test set should represent a range of sizes and ages. Samples must be completely randomized before examination, with no indication to the reader when the sample was collected. All assignments should be interpreted objectively, clearly annotating annuli

interpretations. The advantage of this approach is that it could support routine age assignments across laboratories based on optical annuli within illicia.

A second way forward is to directly age 2-D Mn elemental maps of illicia to support growth models and age-length keys. The clarity of chemical Mn annuli on 2-D maps provided via LA-ICP-MS could allow direct ageing. The von Bertalanffy growth plot suggest 7-10 fish per age-class may be adequate, while past assessments have employed a minimum sample of 50 hardparts per assessment year to construct age-structured models. Minimum sample size could be informed by a power analysis of size at age variance estimates. Creating 2-D Mn for 50 illicia with high resolution (5 μ m spatial resolution) LA-ICP-MS would be approximately \$5,000 in machine time alone, with each 2-D taking at least an hour of time to acquire. Another constraint of this approach is that it would have to be repeated or checked across assessments as growth may change, which would incur repeated costs.

Appendix 1. Electron microprobe analysis of Sr:Ca oscillations in black sea bass otoliths

Intra-annular oscillations in Sr:Ca were measured across opaque and translucent zones using an electron probe micro-analyzer (EPMA) (N=32; JXA-8900 Superprobe, JEOL USA, Inc., Peabody, Massachusetts, USA) located in the Nanoscale Imaging Spectroscopy and Properties Laboratory at the University of Maryland, College Park. This instrument is a wavelength-dispersive X-ray spectrometer that uses an electron beam to generate characteristic x-ray intensities of Sr and Ca. Efforts to measure levels of Mg and P were unsuccessful as concentrations were especially noisy, resulting in insignificant time series. Before analysis by EPMA, otolith samples were carbon-coated in a high-vacuum evaporator, and the instrument was calibrated using reference standards [calcite (CaCO_3) and strontianite (SrCO_3)]. Here, measurements of strontium and calcium for 30 black sea bass otoliths were at first taken over ~30 25- μm increments and then at ~50 15- μm increments to increase resolution. Measurements began proximal to the first annulus and ended distal to the final annulus Figure A.1A. Backscatter electron micrographs (Figure A.1B) were superimposed over light micrographs of the same sectioned otolith by matching landmarks apparent in both images (Figure A.1C). Opaque bands were considered the terminus of each annulus (Figure A.2), and measurement points within a cycle (transparent > opaque) were converted to fractional ages within each annuli cycle, assuming linear otolith growth. When subjected to Lomb-Scargle periodogram analysis, no significant periodicities were observed for Sr for the entire series of annuli or the truncated set (age>1.0 years) (Figure A.3, A.4).

Tables and Figures

Figure A.1 Image of sectioned black seabass otolith. **A.)** reflected light microscopy image of otolith section with red dots marking the end of annuli. **B.)** Micrograph image of same otolith section. **C.)** Overlap of both images.

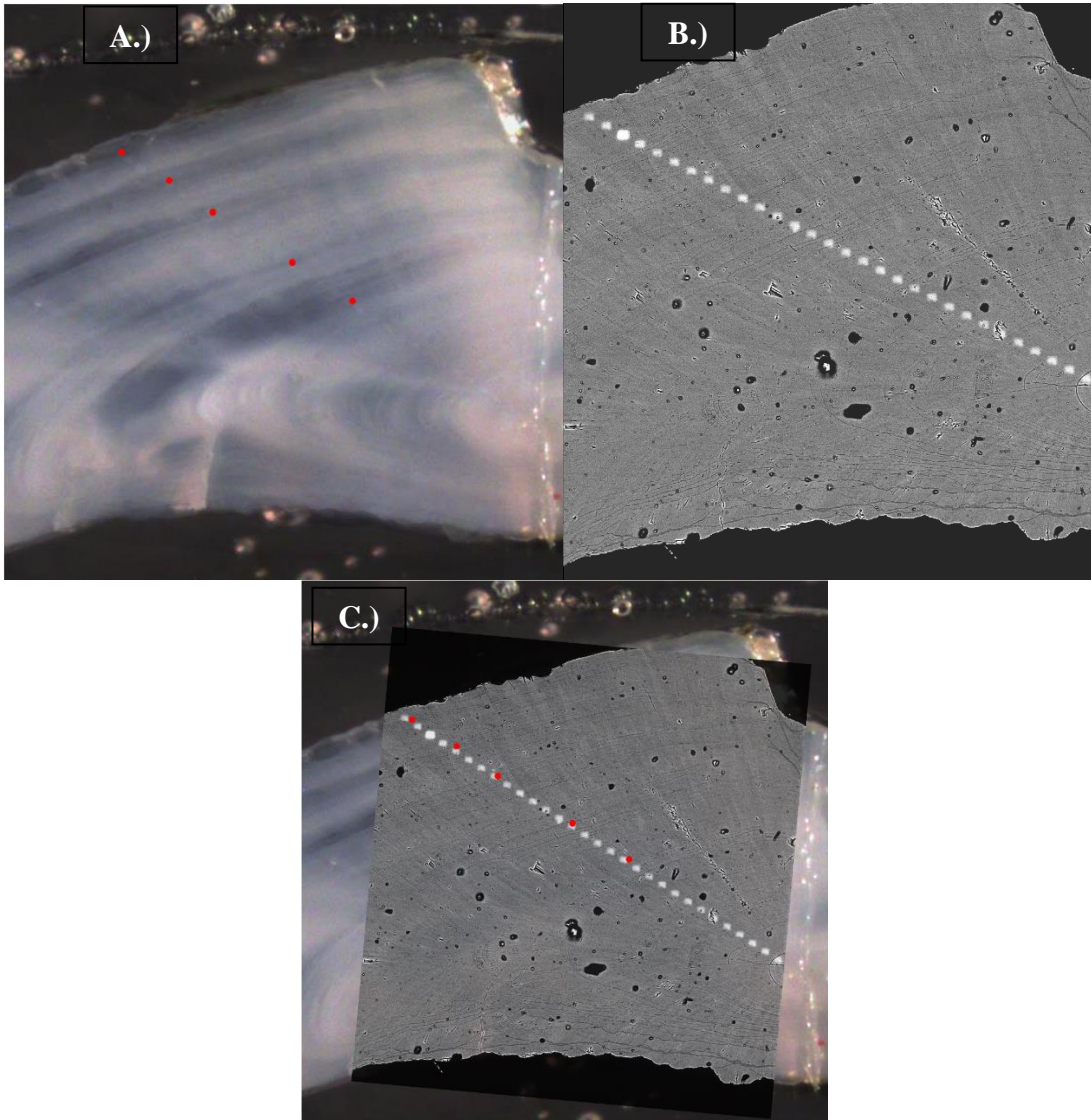


Figure A.2 Strontium/Calcium ratio of black sea bass otolith. **1** covers the core region of the otolith. **2-5** depict one transparent to opaque annuli. Vertical lines represent annuli transition at the start of each transparent zone — annuli 1-5.

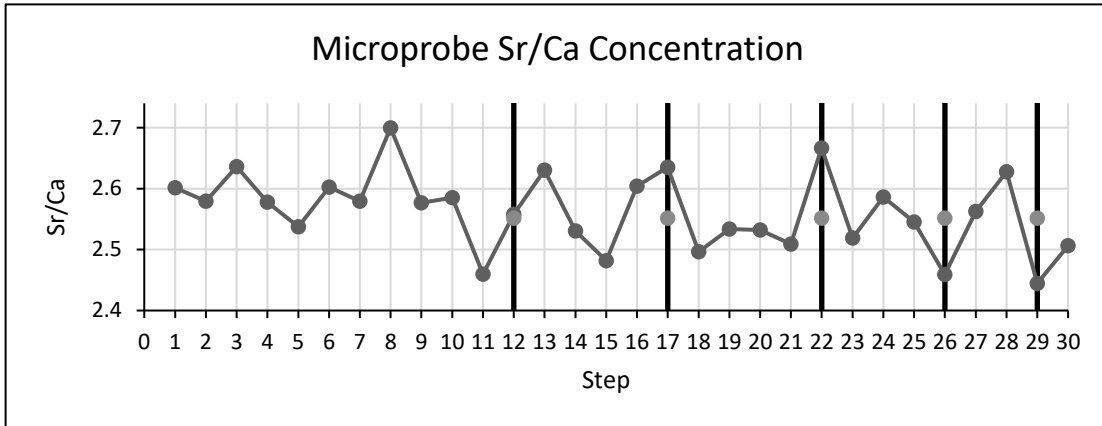


Figure A.3 Lomb-Scargle periodogram of black sea bass otolith Sr:Ca time series data (N=30) from otolith transect showing no significant periodicities in the data. Significance is indicated by the dotted line.

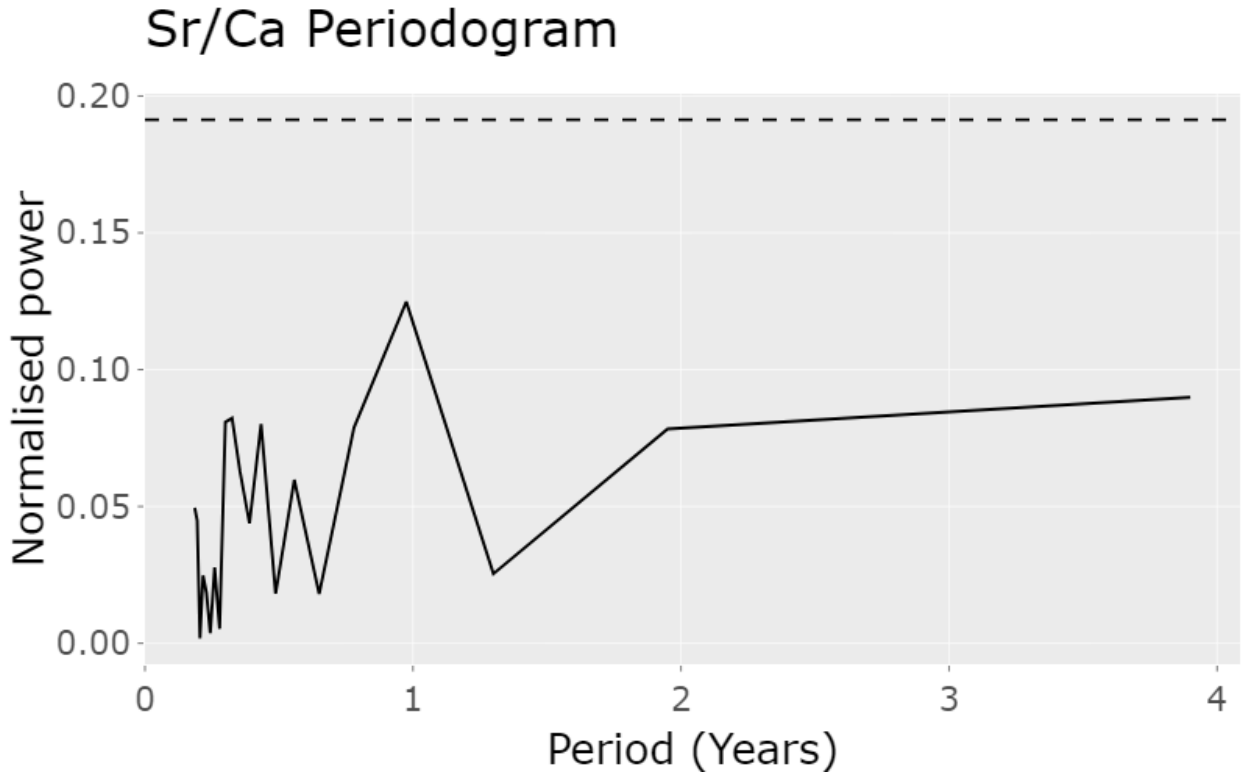
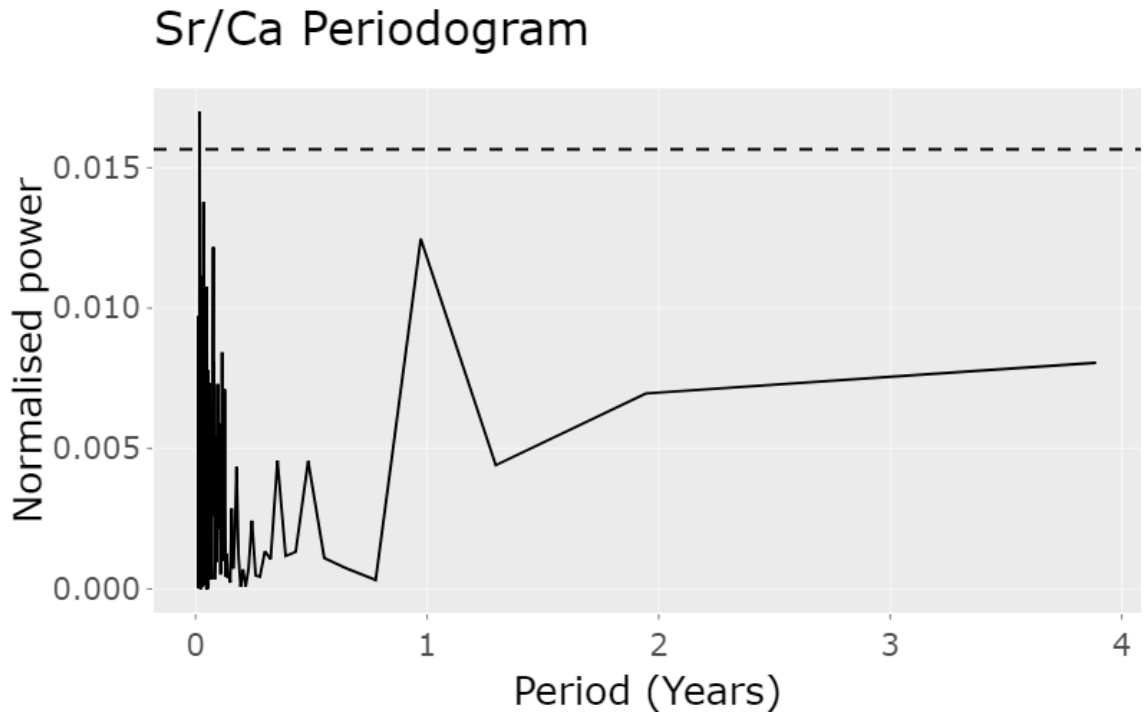


Figure A.4 Lomb-Scargle periodogram of black sea bass otolith Sr:Ca time series data (N=30) with the first annulus after core removed data from otolith transects showing no significant periodicities in the data. Significance is indicated by the dotted line.



List of References

- Armstrong, M., J. Musick, and J. Colvocoresses. 1992. Age, growth, and reproduction of the goosefish *Lophius americanus* (Pisces, Lophiiformes). *Fishery Bulletin* 90(2):217–230.
- Arslan, Z., and D. H. Secor. 2005. Analysis of trace transition elements and heavy metals in fish otoliths as tracers of habitat use by American eels in the Hudson River estuary. *Estuaries* 28(3):382–393.
- Arslan, Z., and D. H. Secor. 2008. High resolution micromill sampling for analysis of fish otoliths by ICP-MS: effects of sampling and specimen preparation on trace element fingerprints. *Marine environmental research* 66(3):364–371.
- ASMFC, (Atlantic States Marine Fisheries Commission). 2013. Proceedings of the 2013 black sea bass ageing workshop. Pages 1–21. Atlantic States Marine Fisheries Commission.
- ASMFC, (Atlantic States Marine Fisheries Commission). 2021. Atlantic states marine fisheries commission review of the interstate fishery management plan:1–16.
- Bank, C. M., K. Oliveira, S. J. Sutherland, M. P. Armstrong, J. Landa, and S. X. Cadrin. 2020. Age validation for goosefish (*Lophius americanus*) in the northeastern United States. *Fishery Bulletin* 118(1):8–20.
- Barnes, T. C., and B. M. Gillanders. 2013. Combined effects of extrinsic and intrinsic factors on otolith chemistry: implications for environmental reconstructions. *Canadian Journal of Fisheries and Aquatic Sciences* 70(8):1159–1166.
- Beamish, R. J., and D. A. Fournier. 1981. A method for comparing the precision of a set of age determinations. *Canadian Journal of Fisheries and Aquatic Sciences* 38(8):982–983.
- Beamish, R. J., and G. A. McFarlane. 1983. The forgotten requirement for age validation in fisheries biology. *Transactions of the American Fisheries Society* 112(6):735–743.
- Bradford, M. J. 1991. Effects of ageing errors on recruitment time series estimated from sequential population analysis. *Canadian Journal of Fisheries and Aquatic Sciences* 48(4):555–558.
- Brophy, D., D. P. De Pontual, K. Mahe, and C.-M. Villanueva. 2019. Validating age-determination of anglerfish and hake. Report (Scientific report), IRELAND.
- Brophy, D., S. Pérez-Mayol, R. Duncan, K. Hüsey, A. J. Geffen, H. D. Gerritsen, M. C. Villanueva, and B. Morales-Nin. 2021. Elemental composition of illicia and otoliths and their potential application to age validation in white anglerfish (*Lophius piscatorius* linnaeus, 1758). *Estuarine, Coastal and Shelf Science* 261:107557.
- Cadrin, S. X., C. Bank, J. H. Grabowski, and G. Sherwood. 2014. Archival tagging and age validation in the mid-Atlantic. *Northeast Fisheries Science Center*:51.
- Campana, S. E. 1999. Chemistry and composition of fish otoliths: pathways, mechanisms and applications. *Marine Ecology Progress Series* 188:263–297.
- Campana, S. E. 2001. Accuracy, precision and quality control in age determination, including a review of the use and abuse of age validation methods. *Journal of Fish Biology* 59(2):197–242.

- Campana, S. E., and J. D. Neilson. 1982. Daily growth increments in otoliths of starry flounder (*Platichthys stellatus*) and the influence of some environmental variables in their production. *Canadian Journal of Fisheries and Aquatic Sciences* 39(7):937–942.
- Campana, S. E., and S. R. Thorrold. 2001. Otoliths, increments, and elements: keys to a comprehensive understanding of fish populations? *Canadian Journal of Fisheries and Aquatic Sciences* 58(1):30–38.
- Casselman, J. M. 1983. Age and growth assessment of fish from their calcified structures—techniques and tools. NOAA Technical Report NMFS 8:1–17.
- Casselman, J. M., C. M. Jones, and S. E. Campana. 2019. Bomb radiocarbon age validation for the long-lived, unexploited Arctic fish species *Coregonus clupeaformis*. *Marine and Freshwater Research* 70(12):1781–1788.
- Chale-Matsau, J. R., A. Govender, and L. E. Beckley. 2001. Age, growth and retrospective stock assessment of an economically extinct sparid fish, *Polysteganus undulosus*, from South Africa. *Fisheries Research* 51(1):87–92.
- Clarke, L. M., S. R. Thorrold, and D. O. Conover. 2011. Population differences in otolith chemistry have a genetic basis in *Menidia menidia*. *Canadian Journal of Fisheries and Aquatic Sciences* 68(1):105–114.
- Daugherty, D. J., A. H. Andrews, and N. G. Smith. 2020. Otolith-based age estimates of alligator gar assessed using bomb radiocarbon dating to greater than 60 Years. *North American Journal of Fisheries Management* 40(3):613–621.
- Dery, L. M., and J. P. Mayo. 1988. Black sea bass *Centropristis striata*. NOAA Technical Report NMFS 72:59–70.
- Duarte, R., M. Azevedo, and P. Pereda. 1997. Study of the growth of southern black and white monkfish stocks. *ICES Journal of Marine Science* 54(5):866–874.
- Duarte, R., J. Landa, C. Morgado, A. Marçal, S. Warne, E. Barcala, E. Bilbao, J. Dimeet, H. Djurhuus, and E. Jónsson. 2005. Report of the anglerfish Illicia/Otoliths ageing Workshop. IPIMAR, Lisbon.
- Dunn, J. C. 1974. Well-separated clusters and optimal fuzzy partitions. *Journal of Cybernetics* 4(1):95–104.
- Elvarsson, B. Þ., P. J. Woods, H. Björnsson, J. Lentin, and G. Thordarson. 2018. Pushing the limits of a data challenged stock: A size-and age-structured assessment of ling (*Molva molva*) in Icelandic waters using Gadget. *Fisheries Research* 207:95–109.
- Engstedt, O., P. Koch-Schmidt, and P. Larsson. 2012. Strontium (Sr) uptake from water and food in otoliths of juvenile pike (*Esox lucius* L.). *Journal of Experimental Marine Biology and Ecology* 418–419:69–74.
- Francis, C., H. Neil, and S. Campana. 2010. Validation of fish ageing methods should involve bias estimation rather than hypothesis testing: a proposed approach for bomb radiocarbon validations. *Canadian Journal of Fisheries and Aquatic Sciences* 67(9):1398–1408.
- Hegg, J. C., and B. P. Kennedy. 2021. Let's do the time warp again: non-linear time series matching as a tool for sequentially structured data in ecology. *Ecosphere* 12(9):e03742.
- Heimbrand, Y., K. E. Limburg, K. Hüsey, M. Casini, R. Sjöberg, A.-M. Palmén Bratt, S.-E. Levinsky, A. Karpushevskaya, K. Radtke, and J. Öhlund. 2020. Seeking

- the true time: Exploring otolith chemistry as an age-determination tool. *Journal of Fish Biology* 97(2):552–565.
- Hilborn, R., and C. J. Walters. 1992. Quantitative fisheries stock assessment: choice, dynamics and uncertainty. Springer Science & Business Media.
- Hüssy, K., K. E. Limburg, H. de Pontual, O. R. B. Thomas, P. K. Cook, Y. Heimbrand, M. Blass, and A. M. Sturrock. 2020. Trace element patterns in otoliths: the role of biomineralization. *Reviews in Fisheries Science & Aquaculture*:1–33.
- Koob, E. R., S. P. Elzey, J. W. Mandelman, and M. P. Armstrong. 2021. Age validation of the northern stock of black sea bass *Centropristis striata* in the Atlantic Ocean. *Fishery Bulletin* 119(4).
- Kraus, R. T., and D. H. Secor. 2004. Dynamics of white perch *Morone americana* population contingents in the Patuxent River estuary, Maryland, USA. *Marine Ecology Progress Series* 279:247–259.
- Landa, J., J. Barrado, and F. Velasco. 2013. Age and growth of anglerfish (*Lophius piscatorius*) on the Porcupine Bank (west of Ireland) based on illicia age estimation. *Fisheries Research* 137:30–40.
- Limburg, K. E., and M. Casini. 2018. Effect of marine hypoxia on Baltic Sea cod *Gadus morhua*: evidence from otolith chemical proxies. *Frontiers in Marine Science* 5:482.
- Limburg, K. E., and M. Elfman. 2017. Insights from two-dimensional mapping of otolith chemistry. Pages 480–491 *Journal of Fish Biology*. Wiley Online Library.
- Limburg, K. E., M. J. Wuenschel, K. Hüssy, Y. Heimbrand, and M. Samson. 2018. Making the otolith magnesium chemical calendar-clock tick: plausible mechanism and empirical evidence. *Reviews in Fisheries Science & Aquaculture* 26(4):479–493.
- Lomb, N. R. 1976. Least-squares frequency analysis of unequally spaced data. *Astrophysics and Space Science* 39(2):447–462.
- Machias, A., N. Tsimenides, L. Kokokiris, and P. Divanach. 1998. Ring formation on otoliths and scales of *Pagrus pagrus*: a comparative study. *Journal of Fish Biology* 52(2):350–361.
- Maharaj, E. A., P. D’Urso, and J. Caiado. 2019. Time series clustering and classification. Chapman and Hall/CRC.
- Mayo, R. K. 1981. Age validation of redbfish, *Sebastes marinus* (L.), from the Gulf of Maine-Georges Bank region. *Journal of Northwest Atlantic Fishery Science* 2:13–19.
- Miller, J. A. 2011. Effects of water temperature and barium concentration on otolith composition along a salinity gradient: Implications for migratory reconstructions. *Journal of Experimental Marine Biology and Ecology* 405(1):42–52.
- Mills, K. H., and R. J. Beamish. 1980. Comparison of fin-fay and scale age determinations for lake whitefish (*Coregonus clupeaformis*) and their implications for estimates of growth and annual survival. *Canadian Journal of Fisheries and Aquatic Sciences* 37(3):534–544.

- Musick, J. A., and L. P. Mercer. 1977. Seasonal distribution of black sea bass, *Centropristis striata*, in the Mid-Atlantic Bight with comments on the ecology and fisheries of the species. *Transactions of the American Fisheries Society* 106(1):12–25.
- NEFMC/MAFMC, (New England Fishery Management Council and Mid-Atlantic Fishery Management Council). 2017. Monkfish fishery management plan framework adjustment 10 including specifications for fishing years 2017-2019. Pages 1–218.
- NEFSC, (Northeast Fisheries Science Center). 2019. Operational assessment of the black sea bass, scup, bluefish, and monkfish Stocks, updated through 2018:164.
- NMFS, (National Marine Fisheries Service). 2020. Fisheries of the United States, 2018. <https://foss.nmfs.noaa.gov/apexfoss/f?p=215:8:9399893492877::NO::>
- Okamura, H., A. E. Punt, Y. Semba, and M. Ichinokawa. 2013. Marginal increment analysis: a new statistical approach of testing for temporal periodicity in fish age verification. *Journal of Fish Biology* 82(4):1239–1249.
- Oosthuizen, W. C., P. J. N. D. Bruyn, M. N. Bester, and M. Girondot. 2010. Cohort and tag-site-specific tag-loss rates in mark–recapture studies: a southern elephant seal cautionary case. *Marine Mammal Science* 26(2):350–369.
- Paton, C., J. Hellstrom, B. Paul, J. Woodhead, and J. Hergt. 2011. Iolite: Freeware for the visualisation and processing of mass spectrometric data. *Journal of Analytical Atomic Spectrometry* 26(12):2508–2518.
- Penttila, Judy., and L. M. Dery. 1988. Age determination methods for northwest Atlantic species. U.S. Dept. of Commerce, National Oceanic and Atmospheric Administration, National Marine Fisheries Service, [Silver Spring, Md.].
- Politis, P. J., J. K. Galbraith, P. Kostovick, and R. W. Brown. 2014. Northeast Fisheries Science Center bottom trawl survey protocols for the NOAA Ship Henry B. Bigelow.
- Reis-Santos, P., S. E. Tanner, T. S. Elsdon, H. N. Cabral, and B. M. Gillanders. 2013. Effects of temperature, salinity and water composition on otolith elemental incorporation of *Dicentrarchus labrax*. *Journal of Experimental Marine Biology and Ecology* 446:245–252.
- Richards, R. A. 2016. 2016 monkfish operational assessment. U.S. Department of Commerce, National Oceanic and Atmospheric Administration, National Marine Fisheries Service, Northeast Fisheries Science Center, Woods Hole, Mass.
- Richards, R. A., P. C. Nitschke, and K. A. Sosebee. 2008. Population biology of monkfish *Lophius americanus*. *ICES Journal of Marine Science* 65(7):1291–1305.
- Robillard, E., J. W. Gregg, J. Dayton, and J. Gartland. 2016. SARC 62 Working paper validation of black sea bass, *Centropristis striata*, ages using oxytetracycline marking and scale margin increments. Page 16.
- Rotella, J. J., and J. E. Hines. 2005. Effects of tag loss on direct estimates of population growth rate. *Ecology* 86(4):821–827.

- Ruf, T. 1999. The lomb-scargle periodogram in biological rhythm research: analysis of incomplete and unequally spaced time-series. *Biological Rhythm Research* 30(2):178–201.
- Sardá-Espinosa, A. 2017. Comparing time-series clustering algorithms in r using the dtwclust package. *R package vignette* 12:41.
- Scargle, J. D. 1982. Studies in astronomical time series analysis. II - Statistical aspects of spectral analysis of unevenly spaced data. *The Astrophysical Journal* 263:835–853.
- Schramm, H. L. 1989. Formation of annuli in otoliths of bluegills. *Transactions of the American Fisheries Society* 118(5):546–555.
- Secor, D. H., and P. M. Piccoli. 1996. Age- and sex-dependent migrations of striped bass in the Hudson River as determined by chemical microanalysis of otoliths. *Estuaries* 19(4):778–793.
- Seyama, H., J. S. Edmonds, M. J. Moran, Y. Shibata, M. Soma, and M. Morita. 1991. Periodicity in fish otolith Sr, Na, and K corresponds with visual banding. *Experientia* 47(11):1193–1196.
- Sherwood, G. 2011. Appendix 2 of monkfish project completion report, otolith microchemistry analysis results for age and growth. Northeast Fisheries Science Center.
- Siskey, M. R., V. Lyubchich, D. Liang, P. M. Piccoli, and D. H. Secor. 2016. Periodicity of strontium: Calcium across annuli further validates otolith-ageing for Atlantic bluefin tuna (*Thunnus thynnus*). *Fisheries Research* 177:13–17.
- Stanley, R. R. E., I. R. Bradbury, C. DiBacco, P. V. R. Snelgrove, S. R. Thorrold, and S. S. Killen. 2015. Environmentally mediated trends in otolith composition of juvenile Atlantic cod (*Gadus morhua*). *ICES Journal of Marine Science* 72(8):2350–2363.
- Steimle, F. W. 1999. Essential fish habitat source document: Black sea bass, *Centropristis striata*, life history and habitat characteristics. DIANE Publishing.
- Stevenson, J. T., and D. Secor. 1999. Life history characteristics of Hudson River Atlantic sturgeon (*Acipenser oxyrinchus*) and a model for management. *Journal of Applied Ichthyology* 15(4–5):304–304.
- Sutherland, S. J., and R. A. Richards. 2021. Validation of methods for aging goosefish (*Lophius americanus*) based on length-mode progression of a strong cohort. *Fishery Bulletin* 120(1):13–25.
- Thomas, R. M. 1983. Back-calculation and time of hyaline ring formation in the otoliths of the pilchard off South West Africa. *South African Journal of Marine Science* 1(1):3–18.
- Vanderkooy, S., J. Carroll, S. Elzey, J. Gilmore, and J. Kipp. 2020. *A Practical Handbook for Determining the Ages of Gulf of Mexico and Atlantic Coast Fishes - Third Edition*.
- VanderPlas, J. T. 2018. Understanding the lomb–scargle periodogram. *The Astrophysical Journal Supplement Series* 236(1):16.
- Vitale, F., L. A. Worsøe Clausen, G. N. Chonchúir, and International Council for the Exploration of the Sea. 2019. *Handbook of fish age estimation protocols and*

- validation methods. Pages 1–180. International Council for the Exploration of the Sea, 346.
- Walker, B. M., and T. M. Sutton. 2016. Growth-increment formation using otoliths and scales for age-0 Chinook salmon. *North American Journal of Fisheries Management* 36(5):995–999.
- Wells, B. K., G. E. Bath, S. R. Thorrold, and C. M. Jones. 2000a. Incorporation of strontium, cadmium, and barium in juvenile spot (*Leiostomus xanthurus*) scales reflects water chemistry. *Canadian Journal of Fisheries and Aquatic Sciences* 57(10):2122–2129.
- Wells, B. K., B. E. Rieman, J. L. Clayton, D. L. Horan, and C. M. Jones. 2003. Relationships between water, otolith, and scale chemistries of westslope cutthroat trout from the Coeur d'Alene River, Idaho: the potential application of hard-part chemistry to describe movements in freshwater. *Transactions of the American Fisheries Society* 132(3):409–424.
- Wells, B. K., S. R. Thorrold, and C. M. Jones. 2000b. Geographic variation in trace element composition of juvenile weakfish scales. *Transactions of the American Fisheries Society* 129(4):889–900.
- Wilhelm, M., M. Durholtz, and C. Kirchner. 2008. The effects of ageing biases on stock assessment and management advice: a case study on Namibian horse mackerel. *African Journal of Marine Science* 30(2):255–261.
- Woodroffe, D. A., P. J. Wright, and J. D. M. Gordon. 2003. Verification of annual increment formation in the white anglerfish, *Lophius piscatorius* using the illicia and sagitta otoliths. *Fisheries Research* 60(2–3):345–356.
- Yule, D. L., J. D. Stockwell, J. A. Black, K. I. Cullis, G. A. Cholwek, and J. T. Myers. 2008. How systematic age underestimation can impede understanding of fish population dynamics: lessons learned from a Lake Superior cisco stock. *Transactions of the American Fisheries Society* 137(2):481–495.
- Zhao, Q., M. Xu, and P. Fränti. 2009. Sum-of-squares based cluster validity index and significance analysis. Pages 313–322 *International conference on adaptive and natural computing algorithms*. Springer.
- Zlokovitz, E. R., D. H. Secor, and P. M. Piccoli. 2003. Patterns of migration in Hudson River striped bass as determined by otolith microchemistry. *Fisheries Research* 63(2):245–259.